INTRODUCTION TO AEROSOL DYNAMICS

Andrew Maynard PhD

Andrew.maynard@asu.edu

Based on the Physical and Biological aspects of Aerosols graduate course, given at the University of Cincinnati in 2004. Note: This document does not reflect post-2004 advances in aerosol sampling and characterization.

CONTENTS

BASICS OF GAS BEHAVIOR

Suggested reading: [1]Baron and Willeke chapters 3, 4
[2]**Hinds chapters 1, 2**
[3]Vincent, chapters 1, 2.

Material Covered:

- Introduction to aerosols
- Microscopic Gas Properties - Concepts
  - Pressure
  - Mean Molecular Velocity
  - Mean Free Path
  - Diffusion
  - Viscosity
- Macroscopic Gas Properties – Concepts
  - Streamlines
  - Boundary Layers
  - Reynolds Number
  - Laminar and turbulent Flow

[1] Aerosol Measurement. Principles, Techniques and Applications. 2nd Ed. Baron, P A and Willeke, K (Eds.). Wiley Interscience, New York. 2001
[2] Aerosol Technology. 2nd Edition. Hinds, W C. Wiley Interscience, New York. 1999.
[3] Aerosol science for Industrial Hygienists. Vincent, J H. Elsevier Science, Bath, UK. 1995.

BACKGROUND NOTES

Background notes include supplemental material that is useful, but not essential, to the course.

1.1 Background

Aerosol: Collection of solid or liquid particles suspended in a gas. Note that the term 'Aerosol' refers to the two-phase system consisting of the **particles AND the gas**.

The term 'Aerosol' was coined around the 1920's as an analogy of Hydrosols – suspensions of solid particles in a liquid. Aerosols are also referred to as suspended particulate matter, aero-colloidal systems, and disperse systems.

Aerosols occur in many systems, either as a naturally occurring phenomenon, or as man-made (anthropogenic) products. They are responsible for influencing processes and phenomena as diverse as cloud formation, global warming and cooling, visibility, rainbows, microchip fabrication, pigment formation, nanoscale material production, global material transport, the application of pesticides, asthma attacks, plant propagation, drug delivery, and various pulmonary, cardiovascular and systemic diseases. Particle sizes range from the sub-nanometer (molecular clusters) to larger than several 100 μm. They may consist of biological material, including viruses and bacteria, solids, or liquids, and may be found in simple geometric forms such as spheres, or highly complex morphologies. Each particle may consist of a single substance, or may be a complex mixture of a number of substances.

The study of aerosols is therefore not only vital to the understanding of the environment in which we live and work, but it is a highly complex field that overlaps many other disciplines.

Aerosol science was at the forefront of physical science at the end of the 19th century and the beginning of the 20th century, as aerosol particles represented the smallest observable division of matter. Aerosols were central to the work of researchers like Tyndall and Rayleigh as they studied particle motion and light scattering. Aerosol science contributed to the early understanding of Brownian motion, the charge on an electron (in Millikan's oil droplet experiments), and the use of cloud chambers for studying ionizing radiation. This intense period of research into the physical aspects of aerosols resulted in the publication of The Mechanics of Aerosols by Nikolai Fuchs in 1955 – a seminal work on aerosols. Following the Second World War, aerosol research was dominated by growing realization of the impact of man-made air pollution on the environment and health. Over this period, many of the advances in aerosol science were associated with the characterization and control of undesirable aerosols within industry. The 1980's saw the increased use of aerosols in high-technology manufacturing processes – a trend which is still continuing. Aerosol research over the past decade has been dominated by the effect of aerosols on the global climate, the impact of environmental pollution on the health of the general population, and the development of new high-tech materials with structures on a nanometer scale. These trends are set to continue over the next decade, with aerosols continuing to play a significant role on the global scale.

Concept of 'good' and 'bad' aerosols. From the examples given, it is clear that some aerosols may be seen as beneficial in their effects and use ('good' aerosols), while some are harmful ('bad' aerosols). Occupational end Environmental health are generally concerned with the harmful effects of 'bad' aerosols. However it is important to bear in mind that not all aerosols are bad. At a very fundamental level, environmental cycles such as the water cycle depend on aerosols for the mass transport of material. A particularly interesting case is the delivery of drugs through inhalation – the very mechanisms that lead to some aerosols being more harmful than others may be harnessed to ensure inhaled drugs are administered most effectively. Many useful materials in today's' society involve the use of aerosols at some stage of the manufacturing process. In these cases, the aerosol may be seen to be 'good' for the process, but potentially 'bad' if allowed to enter the general workplace or environment. Finally, aerosols that are

generated as a by-product of a process (such as welding, grinding or mining) are generally thought of as 'bad'. However it is always possible that an aerosol generally thought of as 'bad' could be used as a positive asset – for instance the 'bad' aerosol formed while refining some metals may be useful for forming new materials, and thus be seen as a 'good' aerosol in some lights.

An idea of the complexity of measuring, characterizing and studying aerosols can be gained from comparing them to gases and vapors. At a first glance, measurement and characterization issues would seem to be similar: Gases and vapors are collections of large numbers of particles (atoms and molecules in this case), as are aerosols. However, a gas will typically contain many orders of magnitude more 'particles' than an aerosol, with each component 'particle' being identical. This allows a statistical approach to their analysis – looking at the 'average' properties of large numbers of molecules. Aerosols on the other hand are composed of relatively few particles, each one of which may be different from all the others (1 cm^3 of an aerosol may contain over 100,000 aerosol particles, and more than $2x10^{19}$ gas molecules). Ideally, complete characterization of an aerosol would require a description of each individual particle. In practice it is usually assumed that the particles have similar or identical characteristics, allowing the aerosol characteristics to be approximated by just a few parameters (as in the case of a gas). In this case, the quality, or nature of the aerosol that is of prime concern is measured (e.g. aerosol mass concentration is Industrial Hygiene, particle number and size in clean-room environmental control). However, it is important to remember that any practical aerosol analysis is only an **approximation** of the true nature of the aerosol.

Most industrial processes produce aerosols, which in the absence of adequate control measures are released into the workplace, and the environment. All of these aerosols have the potential to cause ill health if inhaled in sufficient quantities. However, health effects depend on more than the mass of material inhaled - particle size, composition and shape also play an important role. For instance, pneumoconiosis, a disease of the lower lung regions (the alveolar region) has been associated with fine, relatively insoluble mineral dusts. Silicosis – a specific form of pneumoconiosis - is associated with fine

crystalline silica particles. Asbestosis and mesothelioma are associated with the inhalation of fibrous asbestos particles. Nasal cancer has been linked to relatively large hardwood aerosol particles generated the furniture industry. Other occupational illnesses are associated with specific aspects of aerosols encountered in the workplace.

The first step to understanding the association between aerosols and their effect on health (or their behavior in other systems) is to be able to characterize them appropriately. Likewise, the interpretation of aerosol measurements is dependant on an understanding of the assumptions and simplifications being made in the measurement process. Much of this course is aimed at developing a sufficient understanding of aerosol behavior and measurement methods to allow the correct methods to be selected for specific needs, and to allow a clear understanding of the limitations and simplifications associated with any method used.

1.2 Properties of Gases

As an aerosol is a two-phase system consisting of particles and gas, to fully understand aerosol behavior it is also necessary to have a good understanding of how the gase behaves. Note that with most aerosol concentrations you will encounter, the aerosol mass is sufficiently low to make the assumption that the presence of the particulate phase does not unduly influence the gas behavior. However, *it is important to bear in mind that at high mass concentrations (typically where the aerosol density is greater than 1% different from the density of the gas alone), the presence of particles has a significant influence on gas properties.*

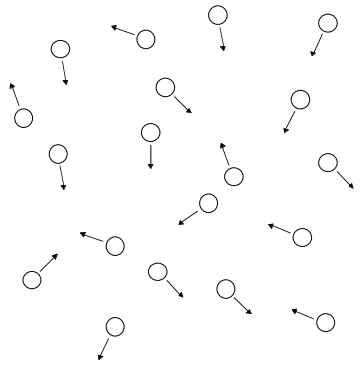

Fig 1.1. Kinetic model of an ideal gas

1.2.1 Kinetic theory of gases

A good understanding of how gases behave can be gained from a very simple physical model that treats individual molecules as rigid spheres analogous to billiard balls. It's referred to as the kinetic theory of gases, as it is based on the exchange of kinetic energy between molecules during collisions. Qualitatively understanding gas behavior using this model provides a good foundation to understanding aerosol particle motion later on.

Assumptions

- The gas consists of a great number of identical molecules.
- The physical dimensions of the molecules are much smaller than the distances between them
- The molecules are rigid. Collisions between molecules are elastic (no energy is lost), and they travel in straight lines between collisions.

Staring from these assumptions, it is possible to describe properties such as temperature, pressure, viscosity, mean free path, diffusion and thermal conductivity in terms of then number of molecules per unit volume n, the mass of individual molecules m, molecular diameter d_m and mean molecule velocity c.

Pressure

Imagine a kinetic gas molecule enclosed in a cubic box. Each time the molecule collides with a wall of the box, it 'pushes' the box away from it as it rebounds. As no energy is lost to the box wall, the molecule bounces back and forth between opposite walls indefinitely, giving the walls a little push with each collision. 'Pressure' simply describes how much of the molecule's effort goes into pushing the walls each second (i.e. the force) for each unit area of wall

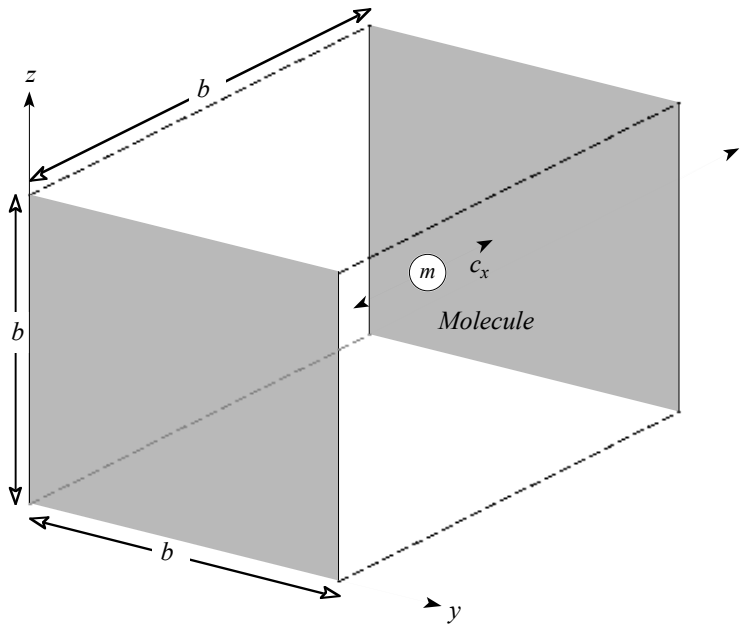

Fig. 1.2 derivation of expression for pressure from kinetic gas theory

The impulse of the molecule pushing against the wall is equal to the change in its momentum. Momentum is given by mass times velocity. We can assume that as the box is much more massive than the molecule, the molecule rebounds with an equal but opposite velocity to that with which it hit the wall. Thus if the mean molecule velocity is c_x, the change in momentum is $2mc_x$. We use c_x to show that the molecule is bouncing back and forth in just one direction at the moment.

The force applied to the box wall is simply the rate of change of momentum with time (Newton's second law), which is given by the change in momentum for one collision, divided by the time between collisions. In our one-molecule in a box model, the molecule has to travel from one side of the box to the other between collisions (note that we're looking at collisions with both of the end walls). Thus if the length of the box is *b*, the time between collisions is simply distance divided by velocity, or *b/c*. Therefore the force exerted per collision is

$$F = \frac{2mc_x}{b/c_x} = \frac{2mc_x^2}{b} \qquad 1.1$$

The force per unit area, or pressure, is simply *F* divided by the area of the box wall we're interested in. At this point the molecule is just bouncing back and forth between two opposite walls, and so the area we use is the area of these two walls – $2b^2$.

$$P = \frac{F}{2b^2} = \frac{c_x^2 m}{b^3} = \frac{c_x^2 m}{V} \qquad 1.2$$

where *V* is the volume of the box.

This is the pressure resulting from just one molecule in a box. To extend this to a box containing *N* molecules we must do two things. First, if we assume that collisions between molecules within the box don't really affect things (and it can be shown that they don't), then equation 1.2 can be multiplied by the total number of molecules (*N)* to get the resulting pressure from all molecules. However these molecules will now be traveling in all directions, not just back and forth between the two opposite walls of the box. It can be shown that the mean square molecule velocity (c_x^2) in each direction (*x*, *y* and *z*) is the same, and that the overall mean square velocity of the particles is given by

$$c^2 = c_x^2 + c_y^2 + c_z^2 \qquad 1.3$$

Thus c_x^2 in equation 1.2 can be replaced by $c^2/3$.

From a set of simple assumptions about a solid molecule trapped in a box, we therefore end up with pressure being defined as

$$P = \frac{mNc^2}{3V} \qquad 1.4$$

or

$$PV = \frac{mNc^2}{3} \qquad 1.5$$

This is simply a statement of Boyle's law, which states that for an ideal gas PV=constant for a fixed amount of gas at constant temperature. Equation 1.5 is the microscopic form of the ideal gas law. It is more usually used in its macroscopic form of

$$PV = nRT \qquad 1.6$$

where n is the number of moles of gas, R is the gas constant and T is the gas temperature in Kelvin For pressure in Newtons per square meter, or Pascals, and volume in m^3 (SI units), R=8.31 Pa m^3/K mol.

Mean Velocity.

As you can see from the above, kinetic theory is powerful in that by starting from very simple beginnings, a real understanding of gas behavior can be reached. For instance, equations 1.5 and 1.6 can be used without much further work to derive an expression for the mean square velocity of particles in a gas. For one mole of gas,

$$PV = RT = \frac{mN_a c^2}{3}$$
$$c^2 = \frac{3RT}{mN_a} \qquad 1.7$$

where N_a is Avogadro's number – the number of molecules in one mole of a substance [$N_a = 6.022 \times 10^{23}$ molecules per mole]. A more useful quantity is the root of the mean square velocity, c_{rms}.

$$c_{rms} = \sqrt{\left(c^2\right)} = \sqrt{\frac{3RT}{mN_a}} \qquad 1.8$$

This represents the mean velocity with which molecules are traveling in the gas. While this may not seem immediately applicable to aerosol particles, hang in there – the same derivation can be used to look at particle velocities within the gas (as we shall see later).

For a given gas, c_{rms} is just dependent on the gas' temperature. By taking an alternative look at molecule velocity, we can see that it tells us something about the temperature of the gas. As the molecule velocity rises, so does the gas temperature, and vice versa. Remembering that the kinetic energy of the molecules is a function of their velocity, equation 1.8 shows us that the temperature of the gas is related to the kinetic energy being carried around by the individual molecules.

In practice molecules in a gas will have a broad range of velocities. Unfortunately this means that a number of different ways of calculating the mean velocity exist, each leading to a slightly different result. The root mean square velocity is one methods of calculating a mean velocity. A commonly used alternative is to calculate the arithmetic mean of particle velocity – this is denoted by $\bar{c}$ and is calculated using

$$\bar{c} = \left(\frac{8RT}{\pi m N_a} \right)^{\frac{1}{2}} = \left(\frac{8RT}{\pi M} \right)^{\frac{1}{2}} \qquad 1.9$$

where M is the molecular weight of the gas.

Mean Free Path

Recall that one of the assumptions we started with was that molecules travel in straight lines between collisions. This distance is important as it indicates whether our assumptions about the molecule diameter being small compared to the distance traveled between collisions is correct. However it becomes much more important when we place particles in the gas. As we shall see later, a particle that is much smaller than this collision distance will behave differently within the gas to one that is much larger.

The distance between collisions is referred to as the free path, and as there will be some variation in these distances in a gas, the quantity most usually used is the ***mean free path***.

The molecule mean free path of a molecule λ, is simply calculated by dividing the mean velocity by the average number of collisions it encounters each second (n_c):

$$\lambda = \frac{\bar{c}}{n_c} \qquad 1.10$$

n_c is calculated by making assumptions on the area that each molecule presents to others (the collision cross section), and the number of molecules per unit volume in the gas n.

$$n_c = \sqrt{2} n \pi d_m^2 \bar{c} \qquad 1.11$$

where d_m is defined as the collision diameter of the molecule – essentially the distance between molecule centers at the point of collision. For air, the approximate collision diameter is 3.7×10^{-10} m. Combining equations 1.10 and 1.11 gives

$$\lambda = \frac{1}{\sqrt{2} n \pi d_m^2} \qquad 1.12$$

The mean free path for air at 101 kPa [1 atm] and 293K is 0.066 μm. Again, we will use similar arguments later to examine the mean free path of aerosol particles.

Diffusion.

As the molecules in a gas are constantly moving, they will move from one place to another (migrate) within an enclosed space even in the absence of a net flow of gas. If you were able to tag a single molecule and watch its progress with time, you would see it follow a series of jumps in random directions (associated with collisions with other molecules), gradually taking it further and further away from its original position – the molecules are said to take random walks. If all the molecules in an enclosure are identical, as one molecule moves away from its staring position, another one, indistinguishable from the first, takes its place. Thus it is not apparent that there is continual movement within the gas. However, if you started with an enclosed volume with, say, red molecules on one side and green on the other, the red molecules would follow random walks that would take some of them over to the green side, and likewise the green ones would follow random walks resulting in some ending up on the red

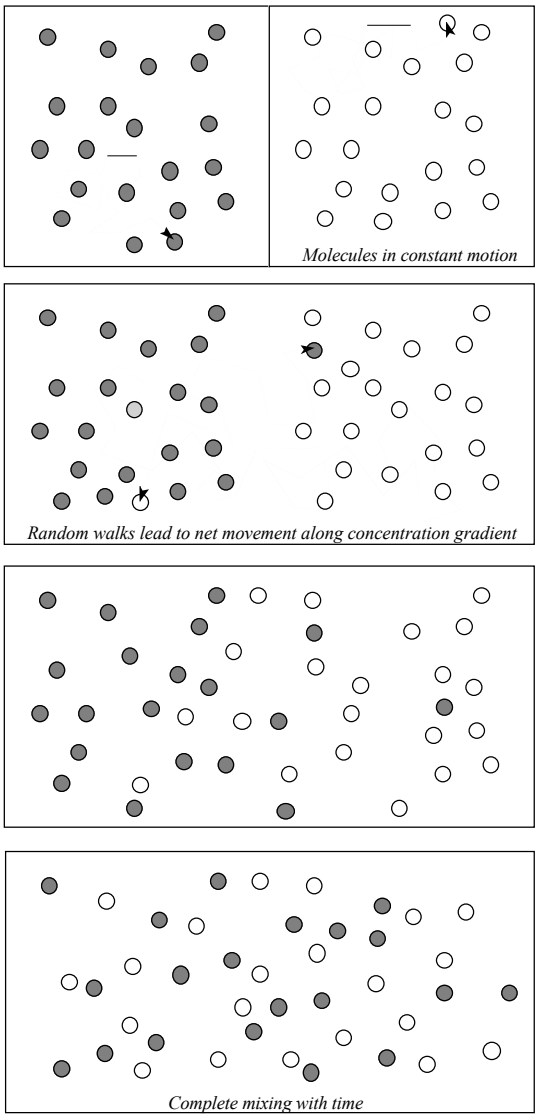

Fig. 1.3 Molecular diffusion

side. The end result would be a uniform mixture of red and green molecules. This process of molecule migration is referred to as diffusion, and is seen wherever there is a concentration gradient of a particular molecule type. The derivation of the equations determining diffusion are beyond this course. However, it is useful to be aware of the expression describing the quantity of a material diffusing per unit time through a unit area perpendicular to the direction of diffusion, J (Fick's first law of diffusion):

$$J = -D\frac{dC}{dx} \qquad 1.13$$

J is the flux of material moving along the concentration gradient dC/dx. D is a constant of proportionality called the diffusion coefficient.

Viscosity

The final gas property that it is useful to conceptualize in terms of kinetic theory is dynamic viscosity (usually just referred to as viscosity). If two parallel plates with a gas between them move relative to each other, there will be a resisting force resulting from the intervening gas. From Newton's law of viscosity, the force which must be applied to overcome this resisting force is proportional to the plate area A and the relative velocity U, and inversely proportional to the separation distance y. The constant of proportionality is the viscosity η, giving

$$F = \frac{\eta AU}{y} \qquad 1.14$$

On a microscopic scale, molecules at the surface of either plate will have a net velocity in the same direction as the plate. A molecule traveling from one plate to the other through thermal motion will effectively remove a small amount of energy from the first plate, and impart it to the other. The tendency in the absence of an external force will therefore be to reduce the relative motion between the plates. This is the source of the gas' viscosity. Using kinetic theory, it can be shown that η *is a function of gas constants and*

temperature alone, and that it increases with increasing temperature. It is independent of pressure.

2.2 Macroscopic properties of gases.

While kinetic theory provides a simple basis for understanding gas behavior, understanding the bulk motion and behavior of gases is not so straight forward. There are however fundamental properties of gas flow that need to be appreciated for an understanding of how aerosols behave. Bulk gas motion can be described using basic equations of motion and conservation – known collectively as the Navier Stokes Equations. While the underlying bases of these equations are relatively straight forward, solutions to the equations themselves are not! For simplicity therefore, the main concepts and properties of gas flow will be introduced with little derivation of the underlying physics.

Streamlines

One important set of solutions to the Navier Stokes equations results in streamlines – patterns which graphically characterize flow. In simple terms, streamlines show the path that a tagged parcel of gas would take through a flow system. Introducing a thin stream of smoke into a flow is one common method of visualizing streamlines. The more densely packed the streamlines, the higher the gas velocity.

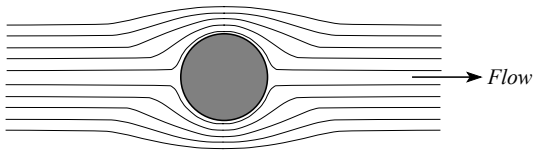

Fig. 1.4 Streamlines

Boundary Layers.

One physical constraint applicable to real fluids (including gases) is that the velocity of the fluid must be zero everywhere at solid boundaries to the flow. This means that there

must exist a steep velocity gradient next to a surface across which a gas is moving. The boundary layer defines the layer within which the gas velocity differs significantly from the bulk gas velocity. Figure 1.5 illustrates the nature of typical boundary layers across a flat sheet, and between a pair of plates. As can be seen, the boundary layer takes some time to fully develop. When the boundary layer is fully developed in a tube, the flow velocity has a parabolic profile across the tube diameter, with the velocity on the center-line being twice the average flow velocity ("Poiseuille flow"). *A common rule of thumb is that it takes approximately 10 diameters for this equilibrium flow to be fully established*.

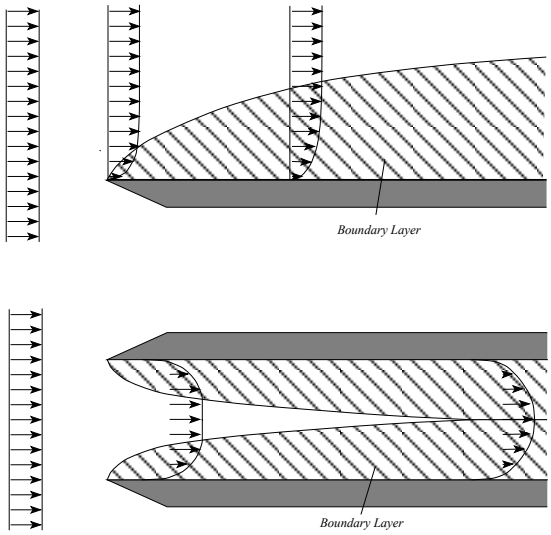

Fig. 1.5 Boundary layer formation

Two other characteristic of flow through a tube are worth noting as they are influential in how particles are transported: A constriction in the flow will force the gas to increase in velocity and be focused towards the center of the tube, leading to an effective tube diameter that is smaller than the actual diameter. The contraction region is termed the 'vena contracta'. Established tube flow round a bend in the tubing will result in secondary flow circulation within the tube. In each case the 10-diameters rule is a good rule of thumb for estimating the distance required to regain equilibrium flow after the disturbance.

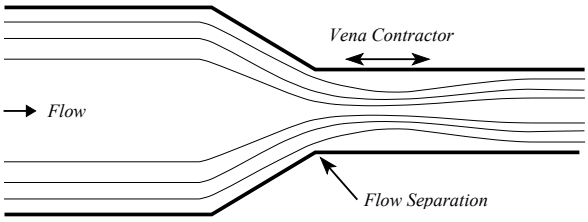

Fig. 1.6 Vena Contracta (an example of flow separation)

Reynolds Number

A key to understanding the flow of gases and the aerodynamic properties of aerosol particles is the Reynolds number (*Re*), a dimensionless number that characterizes fluid flow through a pipe or around an object. Dimensionless numbers are independent of scale and units system, and are widely used in engineering to characterize systems that exhibit similar properties at different scales. (Aspect ratio is perhaps the simplest dimensionless number to understand. It has no dimension of its own, and may be used to describe similarly shaped objects of any physical size). The Reynolds number has the following properties;

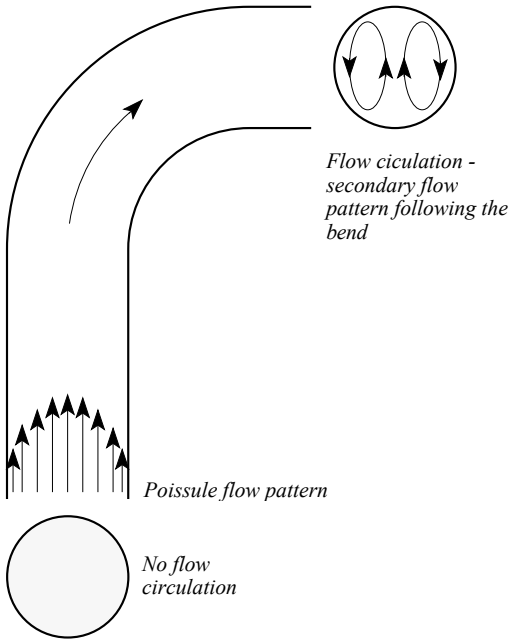

Fig. 1.7 Flow Circulation around a 90° bend

1. It provides a benchmark to determine whether flow is laminar or turbulent.
2. ***It is proportional to the ratio of inertial forces to frictional forces*** acting on each element of the fluid.
3. Geometrically similar flow will occur around geometrically similar objects at the same Reynolds number. Thus for a given *Re*, the streamlines will be the same around objects of different size, or flow of different fluids (or gas).

$$\mathrm{Re} = \frac{\rho V L}{\eta} \qquad 1.15$$

where ρ is the gas density, *V* the gas velocity, η the gas viscosity and *L* a characteristic dimension. For instance, or flow through a tube, *L*=tube diameter, and for flow around a

particle, L=particle diameter. *Re* is dimensionless in any unit system, but obviously all quantities need to be in the same system.

Re depends only on the relative velocity between an object and the gas flow. *Note that it is aerodynamically equivalent for air to flow past a stationary object, or for the object to move in stationary air.*

Laminar flow around a particle occurs when $Re<1$. Within this region, viscous forces are much greater than inertial forces. This type of flow is characterized by a smooth pattern of streamlines that are symmetrical on the upstream and downstream sides of the object. At $Re>>1$ eddies form in the flow downstream of the object, breaking the smooth pattern of the streamlines and leading to random fluctuations in flow and velocity for small packets of gas. Flow within this regime is classed as **turbulent flow**. Turbulence is a complete topic in itself, and perhaps one of the least understood aspects of fluid flow. However, its influence on flow systems is highly significant. Generally, turbulence occurs when an obstruction or change in flow system leads to high localized flow velocities, and inertial forces dominating viscous forces. The result is randomly-fluctuating gas motion superimposed on the mean flow. *Two consequences are an increase in apparent viscosity, and a sharp rise in the mixing properties of the gas.*

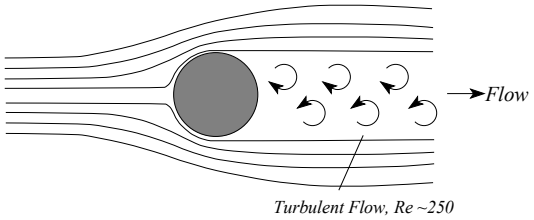

Fig. 1.8 Turbulent Flow

Flow through pipes is laminar for *Re*<2000, and turbulent for *Re*>4000.

Whether the flow around a particle or through a flow channel is laminar or turbulent has a significant influence on particle motion and behavior within the flow.

Flow Stagnation.

Where a streamline intercepts an object, the flow velocity falls to zero, resulting in a stagnation point. Stagnation points are particularly important when considering aerosol particle transportation, as particles approaching a stagnation point run the risk of being trapped in a zone of very little air movement.

Flow Separation

For idealized inviscid frictionless flow, all streamlines impinging on an object would move around the object and continue in the object's wake. However in the real world, where there is friction due to viscosity, some streamlines will loose sufficient energy to be 'lost'. The result is boundary layer separation – the fluid in the boundary layer close to the surface of the downstream side of the body comes to rest prematurely. When and where this occurs, the flow breaks away from the body, enclosing a negative-pressure recirculating region (this may or may not be turbulent). Formation of the vena contractor (fig. 1.6) at a sharp change in flow channel is an example of flow separation. In a rapidly expanding flow channel, flow will separate from the channel walls. *In general, the angle between the wall and the flow axis needs to be less than 7° to prevent separation.* As in the case of stagnation points, aerosol particles run the risk of being trapped in regions of separated flow. The mechanisms that determine whether a particle will enter such regions or not will be covered in a later lecture.

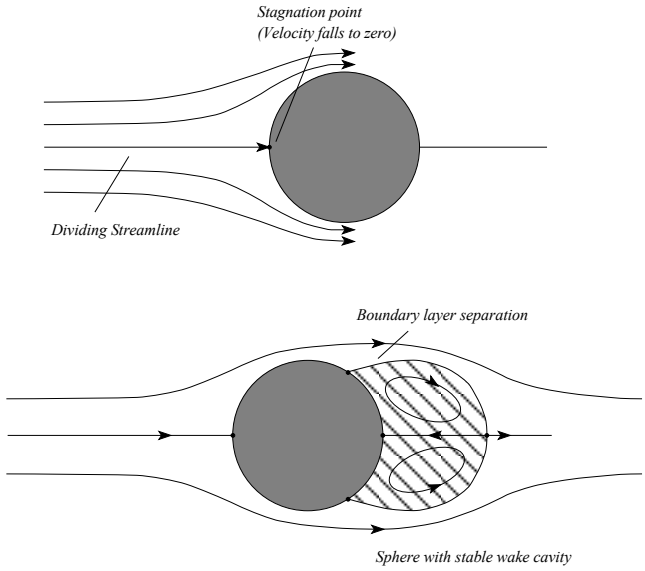

Fig. 1.9 Stagnation and Separation

PARTICLE MOTION IN AIR I

Suggested reading: [1]Baron and Willeke chapter 4
[2]**Hinds chapters 3, 5**
[3]Vincent, chapter 4.

Material Covered:

- Particle steady-state motion (settling velocity, terminal velocity)
  - Drag
  - Stokes Law
  - Particle Mobility – concept
  - Settling Velocity
  - Slip Correction
  - Particle shape and velocity
  - Tranquil and stirred settling
  - Aerodynamic Diameter
- Particle acceleration
  - Relaxation time
  - Stopping Distance
  - Stokes number

[1] Aerosol Measurement. Principles, Techniques and Applications. 2nd Ed. Baron, P A and Willeke, K (Eds.). Wiley Interscience, New York. 2001
[2] Aerosol Technology. 2nd Edition. Hinds, W C. Wiley Interscience, New York. 1999.
[3] Aerosol science for Industrial Hygienists. Vincent, J H. Elsevier Science, Bath, UK. 1995.

BACKGROUND NOTES

Background notes include supplemental material that is useful, but not essential, to the course.

1 Background

An understanding of how aerosol particles react in response to an applied force is fundamental to understanding many of the factors affecting their sampling, measurement and characterization. As the particles are suspended in a gas, any external force applied to them will be resisted as they move with respect to the gas. A steady state will eventually be reached where the resistive forces equal the applied forces, leading to particles moving at a constant velocity (with respect to the gas). The resulting steady state motion is often attained very rapidly, and an understanding of the relationship between an applied force (such as gravity, or an electrical field) and the resulting steady-state motion is a very useful tool. Once there is an understanding of the steady-state motion of aerosol particles, the basic concepts of motion under an applied force can be developed for the case where particles are under acceleration. *An understanding of both states is needed to understand many of the mechanisms leading to particle deposition, and particle sampling.*

2. Drag

Drag: Force that opposes particle motion relative to the surrounding gas. Drag results from a number of mechanisms, including gas viscosity (friction) and the energy required by the particle to displace gas as it moves (inertia). The applied force leading to

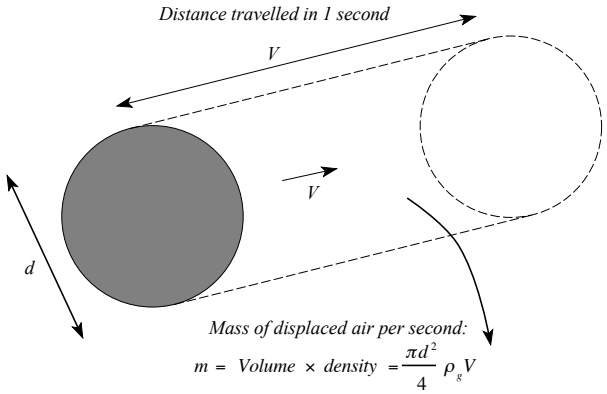

Fig. 2.1. Motion of a sphere in air

particle motion with respect to the gas can be any force that acts differentially on the particles and the gas in an aerosol – e.g. an electrostatic field will lead to a resultant force on charged particles, but not on the carrier gas. Gravity will lead to a net force on suspended particles.

Newtonian Drag

Intuitively, drag is proportional to the area of a particle, and its velocity with respect to the gas. Newton derived the general equation for the drag force on a sphere while considering the motion of cannon balls through the air. He reasoned that the drag experienced by a cannon ball results from the force required to remove the air from its path as it travels. The mass of air that has to be pushed aside each second by a sphere of diameter d is simply the projected area ($\pi d^2/4$) times the sphere's relative velocity (V) and the air's density (ρ_g). The force required to achieve this equals the change in momentum of the gas per unit time, which is simply equal to the *mass of gas displaced* times the *relative velocity between the sphere and the gas*. Drag force F_D is therefore given by

$$F_D = \frac{\text{change of momentum}}{\text{unit time}} \propto \rho_g \frac{\pi}{4} d^2 V^2$$

$$F_D = \frac{C_D}{2} \rho_g \frac{\pi}{4} d^2 V^2 \qquad 2.1$$

where C_D is the drag coefficient. This is the general form of Newton's resistance equation, and is valid for all sub-sonic particle motion, including that of aerosol particles! For situations where inertial forces dominate (Re > 1000) C_D is constant, and is ~ 0.44 (for spheres). However, as viscous forces become significant at lower Re, C_D no longer remains constant, but becomes dependant on Re. Below Re = 1, C_D =24/Re, and in the transition region, C_D can be approximated by an empirical expression:

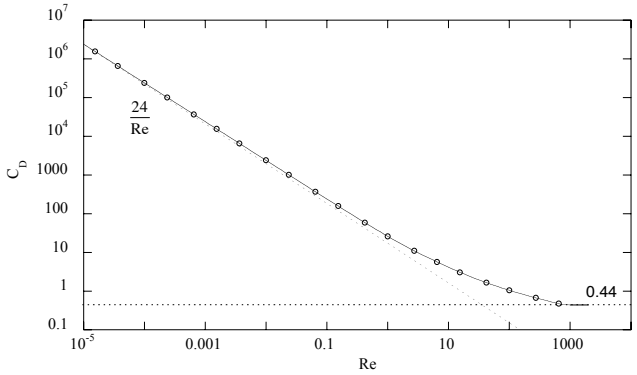

Fig. 2.2. Particle drag coefficient versus Reynolds number

$$C_D = \frac{24}{\mathrm{Re}}\left(1 + 0.15\mathrm{Re}^{0.687}\right) \qquad 2.2$$

Stokes Law

For aerosol particle motion, $Re < 1$ for much of the time, and drag forces are dominated by viscous forces. The expression for the drag force on a particle in this regime was derived by Stokes in 1851. Derivation of Stokes law is beyond this course, and so the law is simply stated:

$$F_D = 3\pi\eta V d \qquad 2.3$$

where η is the gas viscosity, V the particle's relative motion, and d the particle diameter (spherical particles). Note that in this regime, perhaps contrary to intuition, F_D is proportional to d and NOT d^2.

Note that comparing Stokes law to Newton's law gives

$$C_D = \frac{24\eta}{\rho_g V d} = \frac{24}{\mathrm{Re}} \qquad 2.4$$

Particle Mobility

The drag on a particle is a function of its velocity, and therefore if a constant force is applied to a particle, it will eventually reach a velocity where the applied force matches the drag force. This is the maximum velocity attainable with the applied force, and is referred to as the terminal velocity (settling velocity when the force is gravity).

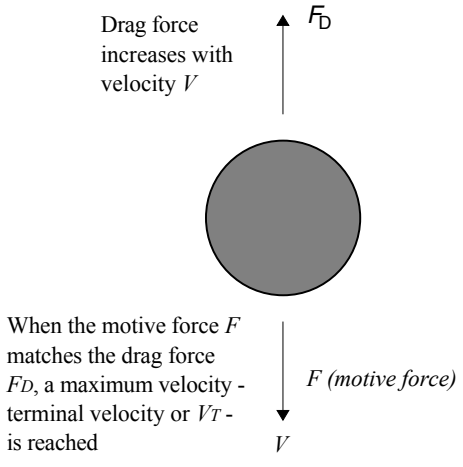

Fig. 2.3. Particle drag and terminal velocity

Particles traveling at their terminal velocity are said to be in *steady state motion*. A useful concept when considering the steady state motion of particles is their mobility**. Mobility (usually denoted by the symbol *B*) is a measure of the relative ease of producing steady state motion for an aerosol particle, and is defined as**:

$$B = \frac{V}{F_D} = \frac{1}{3\pi\eta d} \qquad 2.5$$

for spherical particles. Using particle mobility, terminal velocity, V_T, is expressed as by

$$V_T = FB \qquad 2.6$$

where F is the applied force.

An important application of Stokes law is the derivation of **the terminal velocity under gravity – in other words particle settling velocity V_{TS}**. The gravitational force on a particle is given by mg where particle mass $m=\pi d^3\rho/6$. Thus using equation 2.6,

$$V_{TS} = \frac{\pi d^3 \rho_p}{6} g \times \frac{1}{3\pi\eta d} = \frac{\rho_p d^2 g}{18\eta} \qquad 2.7$$

This expression is valid for spherical particles d > 1µm and Re < 1.0.

Slip Correction

The derivation of Stokes law assumes that particles are in the *continuum regime – i.e. that that the particle is much larger than the gas mean free path and that the gas velocity at the particle's surface is zero.* However, as particle diameter approaches and goes below the gas molecule mean free path, these assumptions begin to break down. The gas can no longer be treated as a continuous medium, and the assumption that gas velocity at the

particle surface is zero becomes meaningless. This is sometimes visualized as the gas flow 'slipping' across the particle surface. At the extreme, particles will behave like massive molecules, 'slipping' between the gas molecules until a random collision takes place. For Stokes law to be used in this region – typically at particle diameters < 1 μm, a correction needs to be applied. Not surprisingly, this is usually referred to as **Slip Correction**. The first derivation of the correction factor was proposed by Cunningham in 1910, leading to

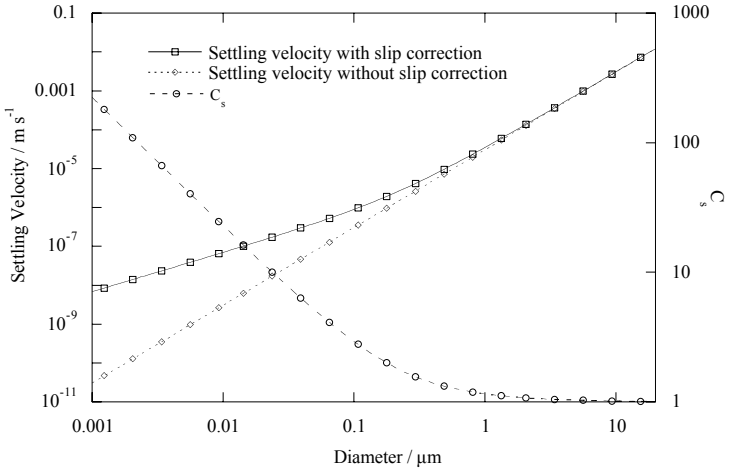

Fig. 2.4. Slip correction and settling velocity

$$F_D = \frac{3\pi\eta V d}{C_C} \qquad 2.8$$

where

$$C_C = 1 + \frac{2.52\lambda}{d} \qquad 2.9$$

***C_c* is the Cunningham Slip Correction Factor**. Use of the Cunningham slip correction factor extends the applicable range of Stokes law to particles of diameter 0.1 μm. A more generally applicable empirical form of the slip correction factor is given by

$$C_S = 1 + \frac{\lambda}{d}\left(2.34 + 1.05e^{-0.39\frac{d}{\lambda}}\right) \qquad 2.10$$

which is applicable for all particles smaller than 1 μm**.** **Particle settling velocity** for all particle sizes with *Re* < 1 therefore becomes

$$V_{TS} = \frac{\rho_p d^2 g C_S}{18\eta} \qquad 2.11$$

Particle Shape

The above expressions all assume that spherical particles are involved. If a particle is non-spherical, it will generally experience a different drag to a similarly sized sphere. Generally, it is unusual to find spherical solid aerosol particles (unless they are manufactured specifically to be spheres), and so is particularly useful to know how particle shape affects drag, and therefore mobility and terminal velocity.

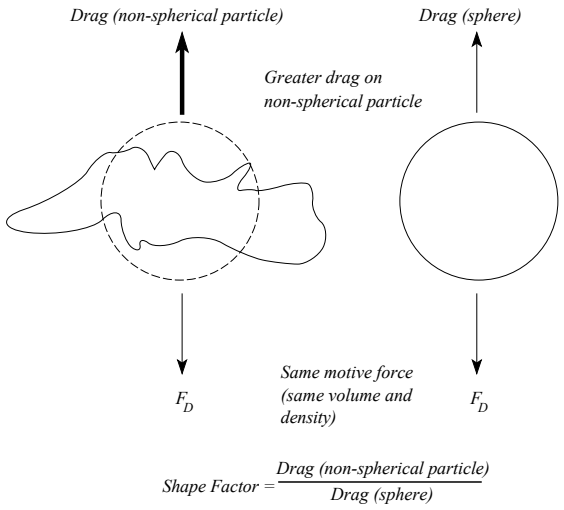

Fig. 2.5 Shape Factor

A correction factor – the **Dynamic Shape Factor** – is applied to Stokes law to account for the effect of shape on moving particles. The dynamic shape factor (χ) is essentially the ratio of the actual drag experienced by the particle, to that experienced by an equivalent spherical particle. *χ for a spherical particle is 1.* Mathematically the dynamic shape factor χ is given by

$$\chi = \frac{F_D}{3\pi\eta V d_e} \qquad 2.12$$

where d_e is **the equivalent volume diameter** – the diameter of a sphere having the same volume as the particle in question.

With the inclusion of particle shape, Stokes law becomes

$$F_D = \frac{3\pi\eta V d\chi}{C_s} \qquad 2.13$$

and particle terminal settling velocity becomes

$$V_{TS} = \frac{\rho_p d^2 g C_S}{18\eta\chi} \qquad 2.14$$

Calculation of χ is complex, and for all but the simplest geometries it must be measured experimentally. χ is always greater than 1.

Table 2.1. Dynamic Shape Factors. Taken from Hinds, p52

	Dynamic Shape Factor χ			
		Axial Ratio		
Shape		2	5	10
Sphere	1.00			
Cube	1.08			
Cylinder				
Vertical Axis		1.01	1.06	1.20
Horizontal Axis		1.14	1.34	1.58
Orientation-averaged		1.09	1.23	1.43
Straight Chain		1.10	1.35	1.68
Compact Cluster				
Three spheres	1.15			
Four spheres	1.17			
Bituminous coal	1.05-1.11			
Quartz	1.36			
Sand	1.57			
Talc	1.88			

Tranquil and stirred settling

Knowing V_{ts} allows an estimate to be made of how long it will take for an aerosol to settle out the air in a chamber or room. If there is no convective air motion within a room of height h, it will simply take a time of V_{ts} x h for all particles to settle out. If the aerosol concentration n at a given point was measured, it would remain constant to a point, them

abruptly fall to zero as the last particles settled past the point (fig 2.6). If the aerosol within the room was constantly stirred, particles would still be lost through gravitational settling. However, the constant re-dispersal of particles would lead to an exponentially decreasing concentration (fig. 2.6). In time *dt* the overall concentration would decrease by

$$dn = \frac{nV_{ts}}{h} dt \tag{2.15}$$

Integrating for the initial condition of $n = n_0$ at $t = 0$ gives

$$n(t) = n_0 e^{\left(\frac{-V_{ts}t}{h}\right)} \tag{2.16}$$

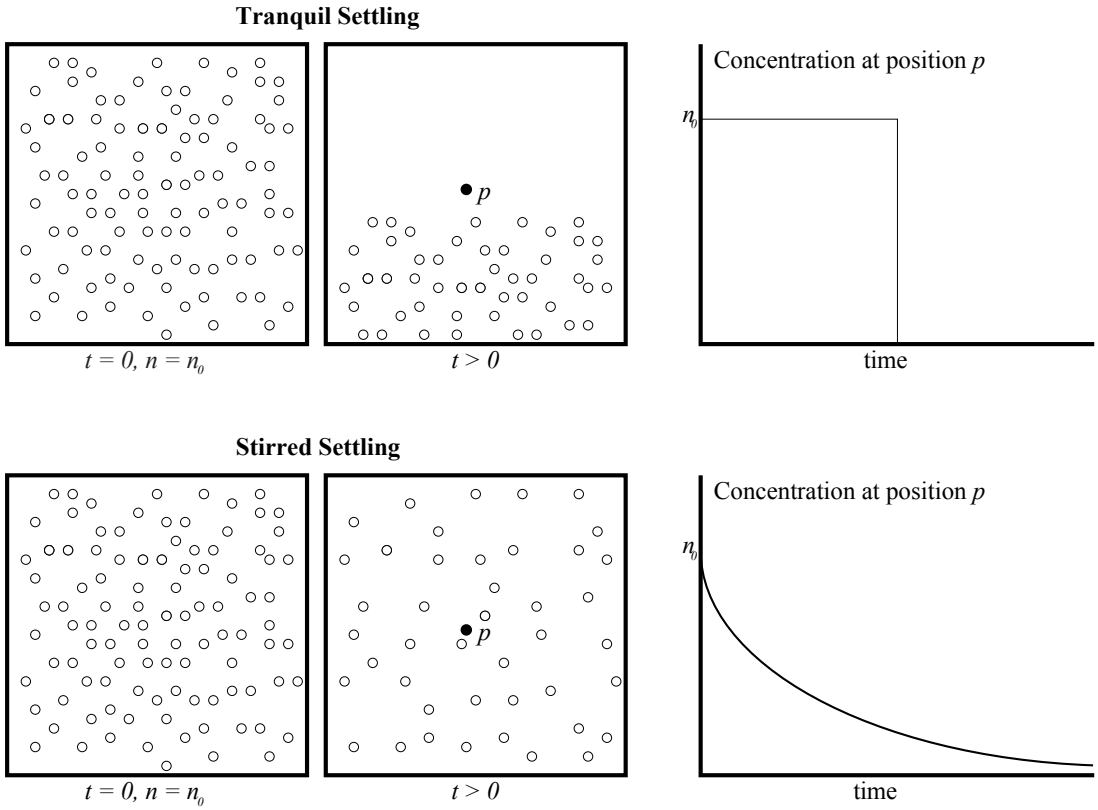

Fig. 2.6. Tranquil versus stirred settling

3. Definition of particle diameter – Aerodynamic diameter

We are now in a position to examine more closely the concept of particle diameter. So far we have assumed that diameter *d* refers to a particle's physical diameter – something like what you would see if you examined it under a microscope. However, the measured diameter of a particle depends strongly on the shape and composition of the particle, and on the measurement method (Measuring particle diameter using microscopy, settling velocity and light scattering will all give different answers in many cases). What is important is the measure of diameter that determines how a particle will behave in any given situation – and this may or may not be the same as its physical diameter. Differences in the measure of diameter are particularly pertinent for non-spherical particles, where expressing particle size by a single parameter alone is an approximation in the first place. ***The concept that the measured diameter of a particle is dependant on the way it is measured is particularly important when interpreting aerosol measurements***.

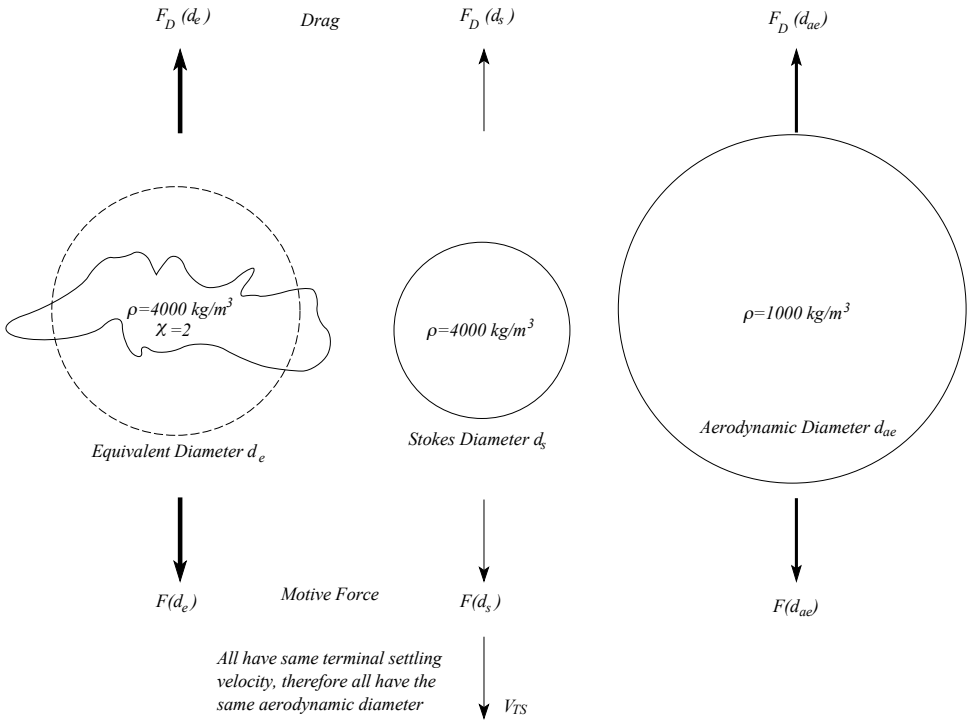

Fig. 2.7. Aerodynamic diameter

To a first approximation, particles being measured characterized or separated by inertial forces such as gravity or 'centrifugal' force are characterized by their settling velocity. In other words, *two particles with the same settling velocity will behave in the same manner, and be measured as being identical* – even though they may have very different physical characteristics. It is common to define particles under these conditions by their *aerodynamic diameter*. **Aerodynamic diameter is defined as the diameter of a sphere of density 1000 kg/m^3 with the same settling velocity as the particle of interest**. A similar definition, used occasionally, is the *Stokes diameter* (d_s), which is the diameter of a sphere *with the same density* as the particle in question, and the same settling velocity. Re-arranging equation 2.14 gives aerodynamic diameter (d_{ae}) as

$$d_{ae} = d_e\left(\frac{\rho_p}{\rho_0 \chi}\right)^{\frac{1}{2}} = d_s\left(\frac{\rho_p}{\rho_0}\right)^{\frac{1}{2}} \qquad 2.17$$

(ignoring slip correction. Refer to fig. 2.6 ρ_0 is 1000 kg/m^3 – sometimes referred to as 'unit' density. For spheres, d_{ae} is simply

$$d_{ae} = d_p\left(\frac{\rho_p}{\rho_0}\right)^{\frac{1}{2}} \qquad 2.18$$

For smaller particles where slip correction is important, equations 2.17 and 2.18 need to be modified to include C_s for each particle diameter (see Baron and Willeke chapter 4).

In general terms, it is common to speak of a particle's **mobility diameter**. Aerodynamic diameter is a special case, where mechanical mobility is being considered. However, a similar approach may be used for electrical mobility, diffusional mobility, thermophoretic mobility etc. ***The important point to realize is that there are no absolutes when it comes to particle diameter – diameter is defined by the method used to measure it***.

Settling at High Reynolds Number.

Before we move on from particle settling, it is important to realize that all of the above expressions are only valid for $Re < 1$ – the region where Stokes law is valid. A more general form of the settling velocity of a particle is obtained using equation 2.1;

$$V_{TS} = \left(\frac{4\rho_p d_p g}{3C_D \rho_g} \right)^{\frac{1}{2}} \qquad 2.19$$

This required knowledge of the drag coefficient C_D – which is fine in the Stokes regime, but not so easy to determine in the transition regime. V_{TS} for larger particles may be solved graphically, or iteratively. The 'Aerosol' spreadsheet by Paul Baron has a routine for doing this (available at www.tsi.com and www.bgiusa.com). The important thing to realize is that **for particle above 50 µm or so, particle Reynolds number at the settling velocity is high enough to lead to significant errors if V_{TS} is calculated using Stokes law** (equations 2.7, 2.11 and 2.14).

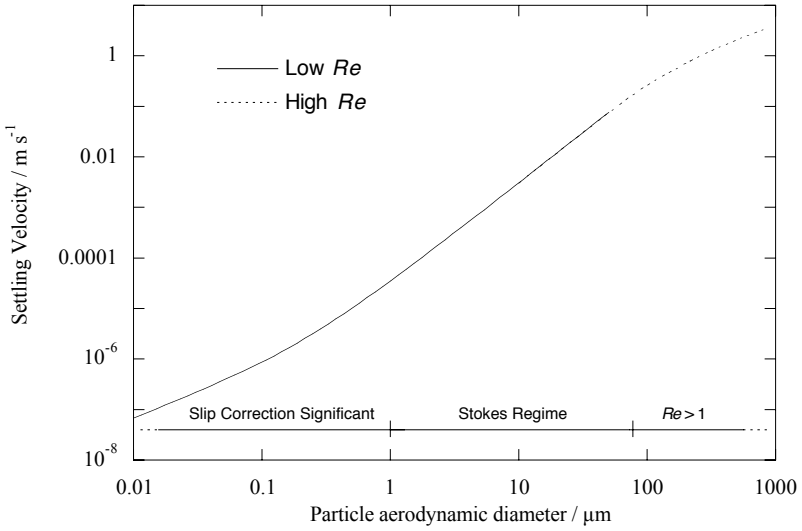

Fig 2.8. Settling velocity versus aerodynamic diameter

4. Particle motion under acceleration

A number of particle collection and measurement methods depend on the motion of particles under an accelerating force – either leading to straight line acceleration, or curvilinear motion (motion along a curved path**). Three quantities are of particular use in understanding particles undergoing acceleration –** ***particle relaxation time, stopping distance, and Stokes number***. The concepts behind each quantity will be developed, along with the necessary expressions to calculate them. However, a detailed derivation is beyond the scope of this course.

Relaxation Time

We have already established that if you apply a steady force to a particle, it will eventually reach a steady velocity as the drag force matches the applied force. The assumption was made earlier that this steady state is reached relatively rapidly. However knowing something about how long a particle takes to respond and 'adjust' to a change in applied force is a very useful tool for determining behavior under conditions of change.

Recall that under gravity, terminal settling velocity is given by *mobility* × *applied force*; in this case gravity (F_g=mg). V_{TS} can therefore be written as

$$V_{TS} = Bmg = \tau g \qquad 2.20$$

where τ has the units of time**. The quantity τ is referred to as Relaxation Time, and is essentially a measure of how rapidly a particle will respond or 'relax' to any changes in applied force**. τ occurs in many instances within aerosol science where a particle's

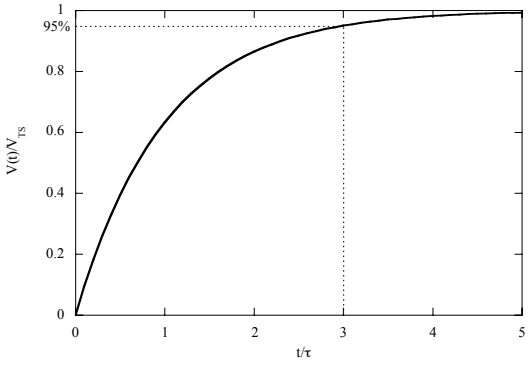

Fig 2.9. Velocity versus time for an accelerating particle

motion is governed by mechanical mobility. It is useful for looking at how rapidly different particles will respond to an applied force – for instance, if a group of particles with different diameters are moving under the influence of an electric field, it indicates which particles will continue to move for an appreciable amount of time when the field is switched off, and which will stop almost immediately. Re-arranging equation 2.20 and using the expression for mechanical mobility B (equation 2.5) gives

$$\tau = \frac{\rho_p d^2 C_s}{18\eta} = \frac{\rho_0 d_a{}^2 C_s}{18\eta} \qquad 2.21$$

It takes 3τ for a particle to reach 95% of its new terminal velocity following a change in the applied force.

Stopping Distance.

While relaxation time gives an indication of the time taken for a particle to adjust to a new set of forces, **Stopping Distance is a measure of how far a particle will travel until it reaches a new steady state velocity under these forces**. For instance, stopping distance S of a particle traveling at velocity V_0 will give the distance the particle will continue to travel after the applied force has been removed**. Stopping distance is particularly important when it comes to determining the likelihood of particle deposition due to inertia**. Stopping distance for the situation where the motive force in the direction of travel is removed is given by

$$S = V_0 \tau \qquad 2.22$$

or

$$S = BmV_0 \qquad 2.23$$

where V_0 is the initial velocity. While τ gives an indication of the time taken to travel

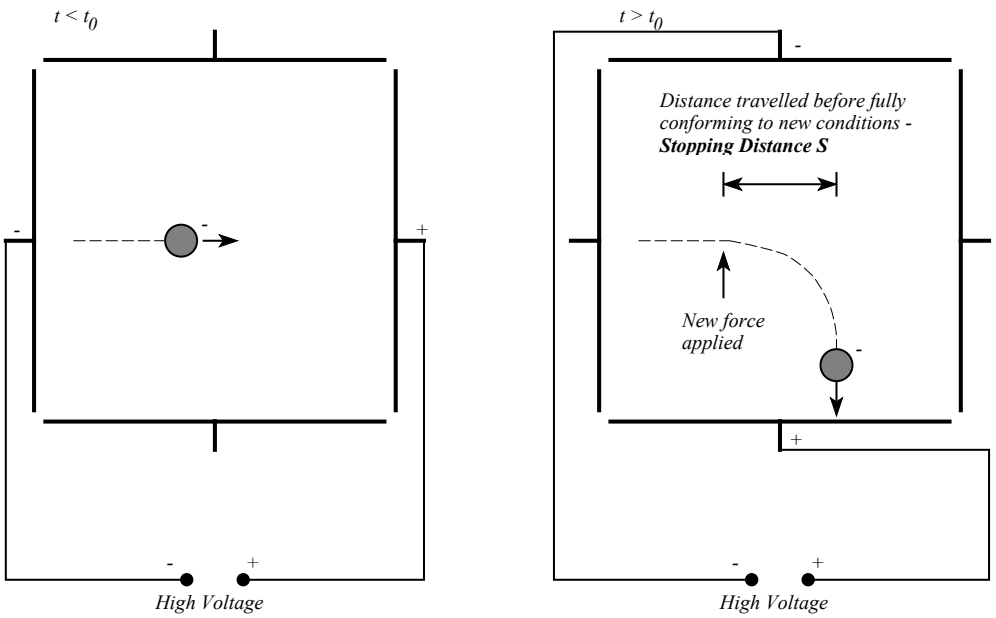

Fig. 2.10. Schematic representation of particle stopping distance

distance S, the actual time will be much longer – as the particle slows down, the drag force will reduce and the particle's rate of deceleration will decrease, leading to the distance traveled exponentially approaching the stopping distance S. *In the absence of other forces, a particle will travel 95% of the distance towards S in a time of* 3τ

Curvilinear motion

Curvilinear particle motion is an extension of straight-line motion, and occurs **when a particle experiences forces that are changing with respect to time and/or position**. A good example is of particles in an aerosol flowing around an obstruction, or through a series of constrictions. The gas streamlines depicting flow in these situations will curve in response to the flow conditions. Particles entrained in the flow will also attempt to follow the streamlines as the varying flow direction exerts a force upon them.

The degree to which particles will 'stick' to the streamlines, or diverge from them, is characterized by the Stokes number *Stk*. *Stk* is the ratio of particle stopping distance to some measure of the size of the object causing the flow to diverge:

$$Stk = \frac{S}{D} = \frac{\tau U_0}{D},\ \mathrm{Re}_0 < 1.0 \qquad 2.24$$

where D is a characteristic length of the obstruction, or flow system (for instance the diameter of a regular obstruction, or the radius of a pipe of nozzle) and Re_0 is the initial

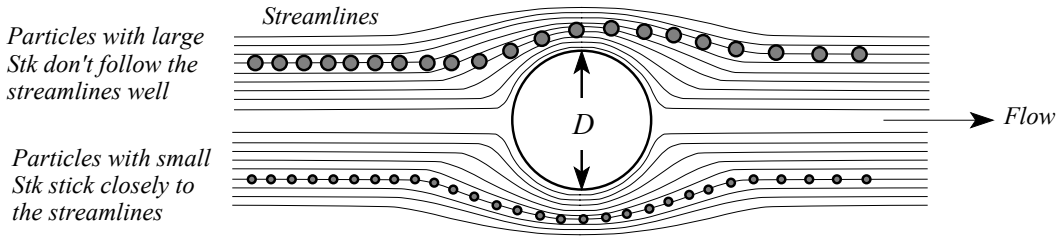

Fig 2.11. Aerosol flow around an obstruction with characteristic length D

particle Reynolds number. Like Reynolds number, Stokes number is dimensionless. Stokes number can be understood as the 'persistence' of a particle divided by the size of an obstruction. As *Stk* approaches zero, particles will follow the streamlines perfectly. As *Stk* increases, a particle's resistance to any changes in direction will increase, resulting in increasingly more streamlines being crossed by the particle in regions of rapid flow direction change.

If a particle has the same values of *Re* and *Stk* for similar geometric conditions, particle motion will be the same – **equality of *Re* ensures that the flow conditions are similar, while equality of *Stk* ensures that particle motion in the flow fields is similar**.

PARTICLE MOTION IN AIR II

Suggested reading: [1]Baron and Willeke chapter 4
[2]**Hinds chapters 7, 15**
[3]Vincent, chapter 4.

Material Covered:

- Brownian Motion
  - Diffusion
  - Mean particle velocity
  - Particle Mean Free Path
- Motion in an Electric Field
  - Charged particle motion - electrophoresis
  - Charging mechanisms
  - Boltzmann equilibrium charge
  - Motion in a non-uniform electric field – dielectrophoresis

[1] Aerosol Measurement. Principles, Techniques and Applications. 2nd Ed. Baron, P A and Willeke, K (Eds.). Wiley Interscience, New York. 2001
[2] Aerosol Technology. 2nd Edition. Hinds, W C. Wiley Interscience, New York. 1999.
[3] Aerosol science for Industrial Hygienists. Vincent, J H. Elsevier Science, Bath, UK. 1995.

BACKGROUND NOTES

Background notes include supplemental material that is useful, but not essential, to the course.

1. Brownian Motion

In 1827 the botanist Robert Brown first observed the random motion of pollen grains in water – what we now call Brownian Motion. Around 50 years later similar behavior was noticed with smoke particles, and the connection was made between gas molecule motion, and random particle motion.

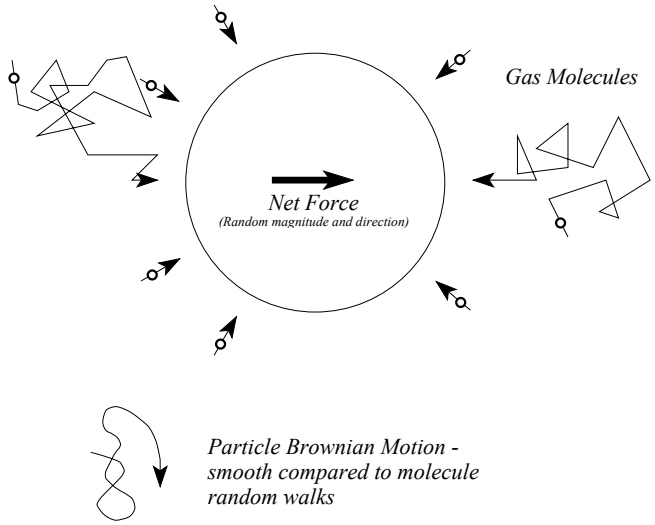

Fig. 3.1. Particle Brownian motion

We saw previously that the molecules in a gas are in a continuous state of motion. Clearly any aerosol particles present will be constantly bombarded by these molecules. If the particle are of similar mass to the gas molecules, they will move around in a similar way, and follow a similar random walk. For particles very much larger than the gas mean free path, the collision rate with air molecules on all sides will be approximately equal, and there will be no net force leading to motion. However, in the transition region between these extremes, there is a finite probability of more collisions from one direction than the opposite direction, leading to a net force in that direction. The net direction, magnitude and persistence of the force is itself random, leading to the random particle motions seen in Brownian Motion**. The motion is analogous to molecular motion although it is important to remember that the particle motion is a result of many collisions with molecules, and not single collisions**.

Particle Brownian motion leads to three characteristics of particle behavior that are analogous or similar to molecular behavior in an ideal gas – *diffusion, mean velocity and mean free path*.

Diffusion.

The Brownian motion of aerosol particles leads to the bulk movement of particles through diffusion. As in the case of molecules, the flux of aerosol particles moving from a high to low concentration region through diffusion is given by Fick's first law of diffusion:

$$J = -D\frac{dn}{dx} \qquad 3.1$$

where D is the particle diffusion coefficient and dn/dx the particle concentration gradient. D can be derived from equating the Stokes drag force experienced by particles to the net force arising from molecular collisions, and is given by

$$D = \frac{kTC_s}{3\pi\eta d} \qquad 3.2$$

k is the Boltzmann constant (1.38×10^{-23} J K^{-1}), and T the temperature of the gas. The diffusion constant can be expressed in terms of particle mobility B:

$$D = kTB \qquad 3.3$$

D is proportional to temperature, but inversely proportional to particle diameter. For small particles with high values of C_s, D is approximately proportional to $1/d^2$ – an intuitive result if you consider that d^2 represents the cross-sectional area of a particle as it collides with gas molecules.

Note that the diffusion coefficient of a 0.01 μm particle is still three orders of magnitude smaller than that of a typical gas molecule.

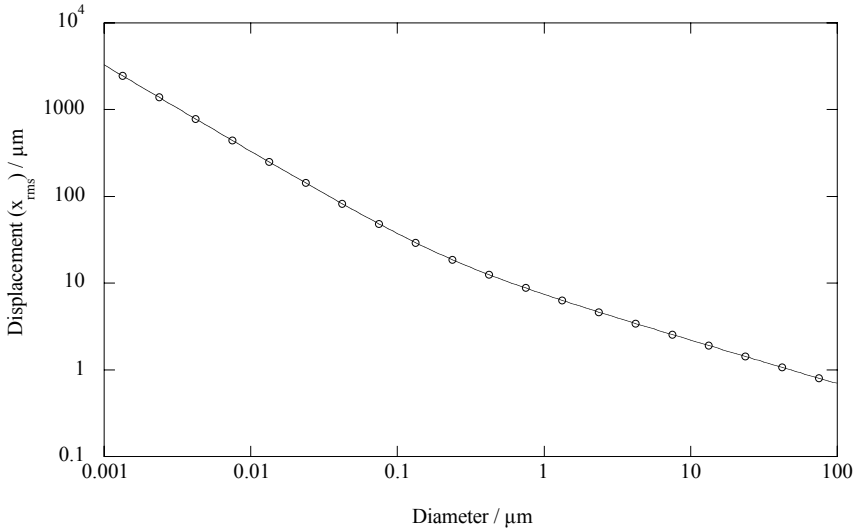

Fig. 3.2. Brownian displacement in 1 second.

The average distance a particle will travel from its starting position in a given time through diffusion is given by its **displacement** over time *t*. Brownian displacement is represented by the root mean square distance traveled, and is given by

$$x_{rms} = \sqrt{2Dt} \qquad 3.4$$

Mean particle velocity

As aerosol particles are constantly exchanging energy with the surrounding gas molecules, they have the same kinetic energy as the molecules. Therefore in the same way that the root mean square and arithmetic mean velocities for gas molecules were derived, the same quantities can be derived for aerosol particles:

$$c_{rms} = \left(\frac{3kT}{m}\right)^{\frac{1}{2}} = \left(\frac{18kT}{\pi\rho_p d^3}\right)^{\frac{1}{2}}$$

$$\bar{c} = \left(\frac{8kT}{\pi m}\right)^{\frac{1}{2}} = \left(\frac{48kT}{\pi^2\rho_p d^3}\right)^{\frac{1}{2}} \qquad 3.5, 3.6$$

Mean Free path

Particle mean free is not directly analogous to molecule mean free path. As most aerosol particles are much more massive than gas molecules, it takes many collisions to lead to a

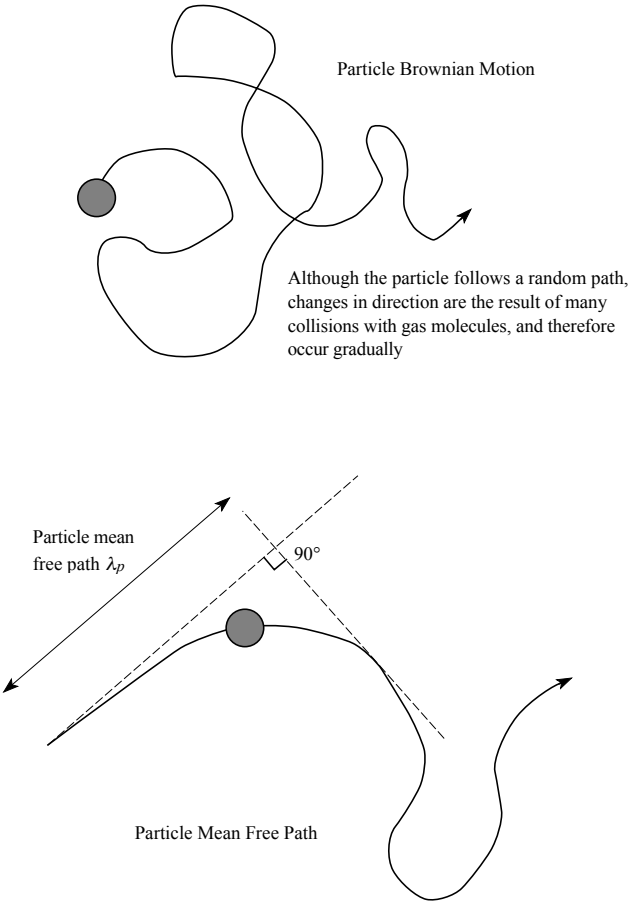

Fig. 3.3. Particle Brownian motion and mean free path

change in direction of particle motion. However, the concepts are similar**.** ***Particle mean free path is defined as the distance traveled before molecular collisions have led to a complete (i.e. 90°) change in direction***. This is essentially the stopping distance of the particles under the influence of Brownian motion, and is given by

$$\lambda_p = \tau \bar{c} \qquad 3.7$$

The diffusion coefficient of an aerosol particle can be expressed in terms of particle mean free path and mean velocity:

$$D = \frac{\pi}{8}\lambda_p \bar{c} \qquad 3.8$$

2. Motion in an electric field.

Charged aerosol particles in the presence of an electric field will experience a force leading to a terminal velocity V_{TE} (**electrophoresis – motion in an electric field**), where

$$V_{TE} = F_E B \qquad 3.9$$

F_E is the force resulting from the electric field, and B is the particle's mechanical mobility. In an electric field of strength E, $F_E = neE$ where n is the number of elementary charges on the particle, and e is the elementary charge – the charge of one electron (1.6×10^{-19} C) (Coulombs Law). It is more usual to use electrical mobility (Z) for charged particles, given by $Z = neB$, leading to

$$V_{TE} = ZE \qquad 3.10$$

$$Z = \frac{neC_s}{3\pi\eta d} \qquad 3.11$$

As the electrical forces on a charged particle can be very high, it is not uncommon for a particle traveling at its terminal velocity in an electric field to have $Re>1$. As in the case for gravitational settling with large particles, graphical or iterative methods need to be used to calculate V_{TE} in many cases. If a voltage V is placed between two parallel plates separated by distance h, $E = V/h$ and has the units of volts per meter.

Charging Mechanisms.

Particle motion in electric fields ca be useful, but also leads to aerosol sampling and handling problems. A number of instruments use electrophoresis to classify particles, or to sample them. However, electrophoresis is also a significant source of unwanted particle losses during sampling. The key to controlling aerosol behavior in electric fields is an understanding of how particles gain and loose electrical charge.

Aerosol particles principally obtain charge **through flame charging, static electrification, diffusion charging and field charging**. *However the most important of these from the aerosol sampling and measurement perspective are diffusion and field charging*.

Diffusion charging results from random collisions between particles and unipolar ions. It does not depend on the particle material, or the presence of an electric field. As charge accumulates on a particle, ions below a threshold energy (governed by their mean velocity) are repelled, and the charging rate decreases. ***Diffusion charging is dominant for particles smaller than 0.1 µm. Above 1 µm field charging dominates in the presence of an electric field.***

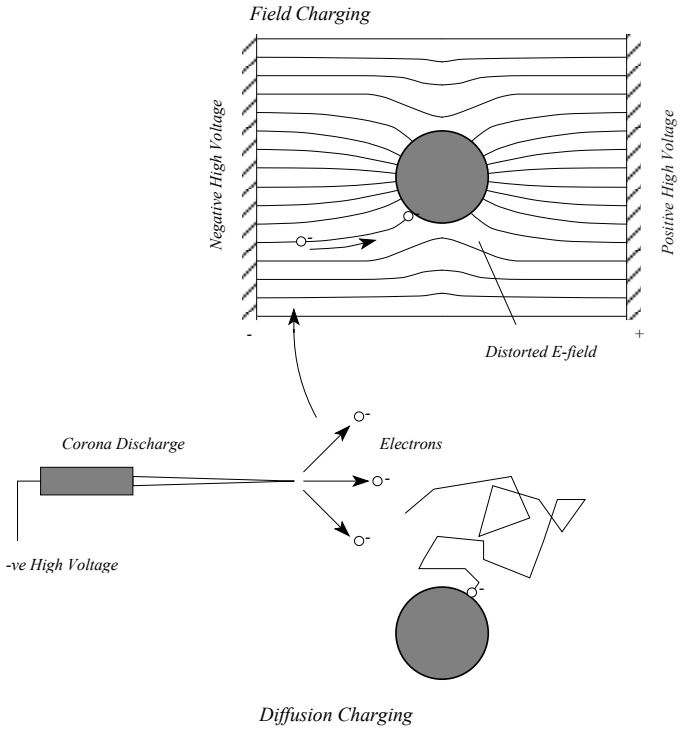

Fig. 3.4. Particle charging through field and diffusion charging mechanisms.

A common method of giving aerosol particles high charges is to pass them close to a **corona discharge**. If a very high electric field is sustained across a gas, sufficient energy

is given to existing ions to ionize neutral atoms. Sufficiently high fields may be formed around thin wires or sharp points, leading to **a self-sustaining avalanche of atom ionization that leads to a cloud of free electrons and positive ions – the corona discharge**. Ions of the same polarity as the electrode will be repelled, forming a *unipolar* ion cloud (all ions having the same polarity). Aerosol particles passing through the cloud will become charged through both diffusion and field charging mechanisms.

Charging of particles through diffusion charging is a function of the ion concentration N_i, and the residence time t spent in the ion cloud. As a rule of thumb, $N_i t$ should be greater than around 10^{12}-10^{13} ions s/m^3 for effective charging. For negatively charged solid particles, a maximum charge limit is reached when the self-generated field reaches that required for spontaneous electron emissions from the particle's surface. A similar mechanism limits the charge on positively charged solid particles, but as the energy required to remove a positive ion is greater than that to remove an electron, the charge limit is higher. As would be expected, ***the charge limit is proportional to the surface area of the particle.***

Flame Charging: Molecule ionization and thermionic electron emission from particles within the flame leads to a net charge on the emerging particles. **Static electrification** leads to particles becoming charged through mechanical action as they leave a bulk material or a surface, in the same manner that rubbing certain materials together leads to static electrification. **Field charging** occurs when a particle is placed in the presence of single-charge ions (unipolar ions) in a strong electric field. The particle distorts the field, causing ions to collide with it. As the charge on the particle increases, a maximum charge is reached where incoming ions are repelled by the particle's own electric field. At this point the particle is said to be at saturation charge. ***Field charging is proportional to the square of particle diameter.***

For liquid particles the charge limit is governed by the **Rayleigh limit** – the point at which the repulsive forces of the charges exceeds the surface tension at the droplet's surface, and it disintegrates into smaller droplets.

Equilibrium charge.

When sampling and transporting an aerosol, it would be useful if the charge on the particles could be reduced to zero, thus eliminating depositional losses due to particle charge. In practice, this is hard to achieve. The easiest way to reduce the charge on a charged particle is to expose it to ions of the opposite charge. However, once the particle has been neutralized, diffusion charging will occur, leading to the particle ending up carrying an opposite charge to the one it started with. It would seem reasonable therefore to expose the charged particle to both positive and negative ions simultaneously (**bipolar ions**). Ions of the opposite charge to the particle would always be preferentially attracted to it, thus leading to the particle having no net charge.

The principle behind this approach to **charge neutralization** is good, **and exposing a charged aerosol to a source of bipolar ions will lead to no net charge on the aerosol as a whole**. However recall that diffusional processes are dynamic – particles within the aerosol will continually be gaining and loosing charge as they collide with ions. Therefore although the overall net charge will be zero, *there will always be some particles that have a positive charge, and some that have a negative charge*.

The distribution of charges on aerosol particles at charge equilibrium follows a Boltzmann distribution, and is frequently referred to as **the Boltzmann equilibrium charge distribution** (the Boltzmann distribution is characteristic of distributions resulting from random gas molecule collisions). For particles larger than around 0.5 μm, this becomes equivalent to a normal distribution. The fraction of particles of diameter d_p having n positive or negative elementary charges is then given by

$$f_n = \left(\frac{K_E e^2}{\pi d_p kT} \right)^{\frac{1}{2}} \exp\left(-\frac{K_E n^2 e^2}{d_p kT} \right) \qquad 3.12$$

where K_E is the electrostatic constant of proportionality (9×10^9 N m^2/C^2), e is the charge on an electron, k is the Boltzmann constant and T the gas temperature [in Kelvin]. At Boltzmann charge equilibrium there is equal probability of a particle having n positive or n negative elementary charges. In practice the distribution is slightly skewed, but the Boltzmann charge equilibrium is a good approximation.

From the Boltzmann charge equilibrium, the average number of charges (positive or negative) on a particle of diameter d_p can be estimated using

$$\overline{n} = 2.37\sqrt{d_p} \qquad 3.13$$

for particles larger than 0.2 μm. The number of charges on a particle at a given time, *n(t)*, that starts off with n_0 charges is given by

$$n(t) = n_0 e^{-4\pi K_E e Z_i N_i t} \qquad 3.14$$

where Z_i is the ion electrical mobility, and N_i the number concentration of the ions. As can be seen, **the rate of 'neutralization' is governed by the product of the ion concentration and the time that the aerosol is exposed to the ions – $N_i t$**. A value of $N_i t$ of 6×10^{12} ions s/m^3 is required for complete 'neutralization' of highly charged particles. This is usually achieved using a radioactive α or β source such as Polonium-210 (α) or Krypton-85 (β). The β radiation from these sources ionizes air molecules in their vicinity, thus providing a bipolar ion cloud. However

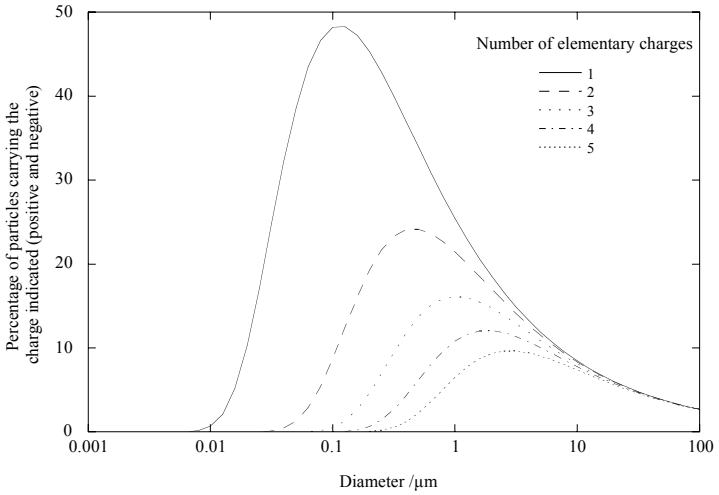

Fig. 3.5. Boltzmann charge equilibrium – charge held as a function of particle size

sufficient ion concentrations typically only exist a few mm from most commercial neutralization sources, and so the aerosol needs to be brought close to the source. ^{85}Kr is a gas, and so to be effective it is generally contained in a thin-walled stainless steel tube, or behind a thin metal window, and the aerosol allowed to flow past or across the tube/window.

An alternative approach to reducing the charge on an aerosol is to introduce bipolar ions from a corona discharge. To achieve an ion cloud with equal numbers of positive and negative ions, two opposite-polarity corona electrodes are needed, and the current to each carefully monitored to ensure equal ion generation rates. The advantage of such systems is that the ions can be introduced directly to the aerosol by introducing air flow passing the corona electrodes, although care must be taken to ensure good mixing of the aerosol and introduced flow.

Atmospheric and aged aerosols tend to have a Boltzmann charge distribution as a result of the omnipresent bipolar ions in the air (resulting from various generation mechanisms, including cosmic rays). **The normal atmospheric bipolar ion concentration is around 10^9 ions/m^3, and thus residence times of the order of 100 minutes will lead to 'neutralization'.**

A practical note: where the predicted number of charges on a particle is less than 1 (or not an integer), this is the *average* charge, resulting from some particles having an integer number of elementary charges, and others having none.

Relative deposition velocities

In general, different deposition forces become dominant at different particle sizes. For large particles gravitational deposition (or inertial deposition) is important. Electrostatic deposition becomes more important at smaller particle diameters, but for most aerosols the Boltzmann charge equilibrium inhibits very small particles having sufficient charge

for electrostatic deposition to be significant. In this region diffusion rapidly becomes the dominant deposition mechanism (fig. 3.6).

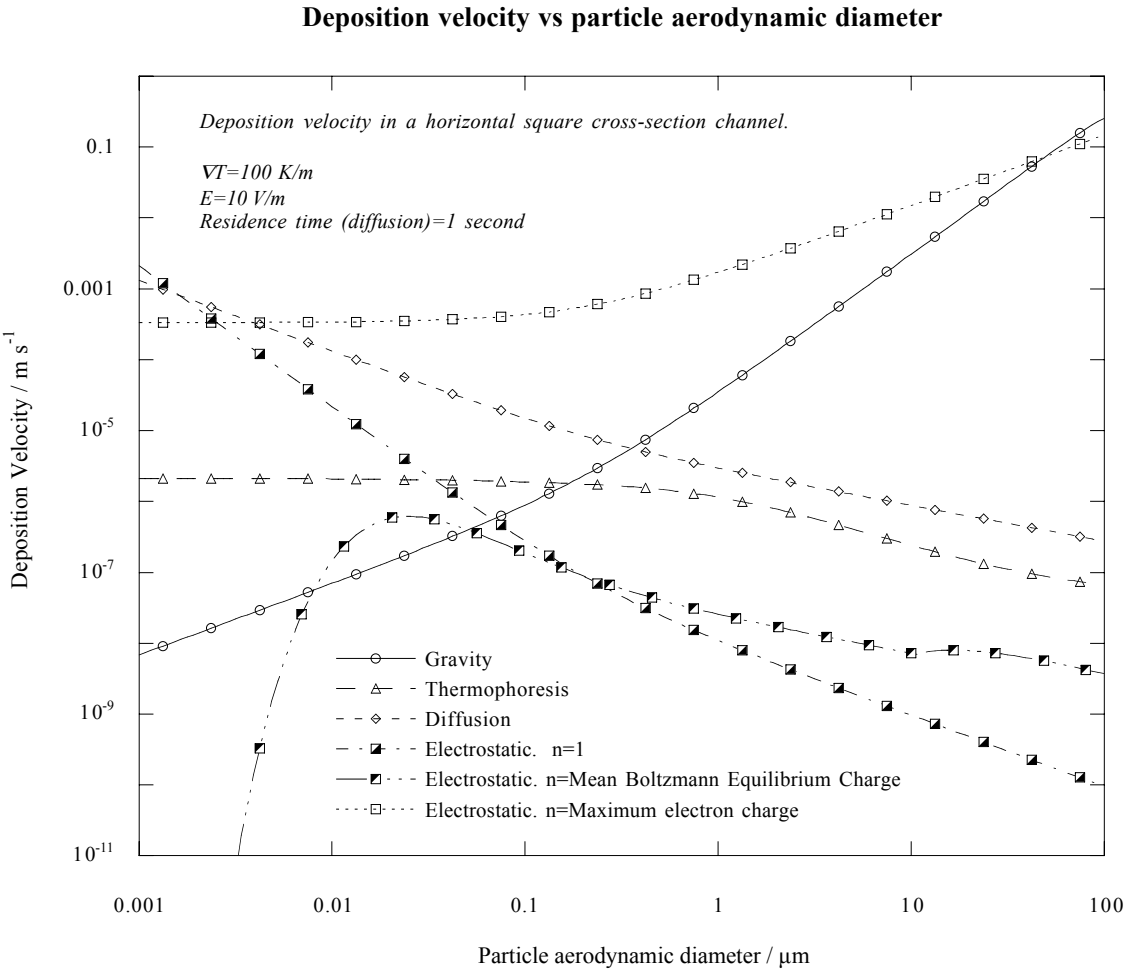

Fig. 3.6. Summary of deposition velocities arising from various mechanisms. Note that exact velocities will depend on the magnitude of the motive force, although the plot gives a fair representation of relative orders of magnitude between different mechanisms.

AEROSOL SIZE DISTRIBUTIONS

Suggested reading: [1]Baron and Willeke chapter 6
[2]**Hinds chapters 4**
[3]Vincent, chapter 3

Material Covered:

- Size distribution characteristics
  - Discrete distributions
  - Continuous distributions
  - Geometric bin sequences
  - Lognormal size distributions
  - Cumulative size distributions
  - Number, surface area and mass weighting

[1] Aerosol Measurement. Principles, Techniques and Applications. 2nd Ed. Baron, P A and Willeke, K (Eds.). Wiley Interscience, New York. 2001
[2] Aerosol Technology. 2nd Edition. Hinds, W C. Wiley Interscience, New York. 1999.
[3] Aerosol science for Industrial Hygienists. Vincent, J H. Elsevier Science, Bath, UK. 1995.

BACKGROUND NOTES

Background notes include supplemental material that is useful, but not essential, to the course.

1. Background

So far, we have focused on the behavior of individual suspended particles. However if we are to draw any meaningful conclusions about the behavior of an aerosol as a single entity, we need to consider the properties of large groups of particles. At its simplest, aerosol characterization consists of measuring bulk physical and chemical quantities such as particle mass or number concentration within a given volume of air. While such measurements are useful, they greatly simplify the aerosol. The next level of complexity involves considering physical and chemical quantities as a function of particle size. This approach still represents a great simplification of the complexity represented by a collection of (sometimes) millions of particles. However it does enable a sophisticated understanding of aerosol behavior to be developed in many cases, allowing particle behavior as a function of size and composition to be addressed. Inclusion of particle size provides most of the information on an aerosol needed for basic characterization in many cases, and it is common to see aerosol size distributions as a function of mass, number or surface area versus particle diameter. This lecture covers the basics of describing and understanding aerosol size distributions.

2. Aerosol Size Distribution Characterization

Most instruments capable of measuring a particle size distribution will initially measure the number (mass, or surface area) of an aerosol between a series of set particle diameters. The diameters define 'bins', and during the measurement process, each particle detected and characterized is added to the appropriate bin. These data are not directly useful in themselves, as the aerosol quantity (particle number concentration will

be used in this example) in any bin is dependent on how wide the bin is, as well as the actual aerosol size distribution. The first step to transforming binned particle numbers to a useable distribution is to create a histogram of the data, by dividing the particle number in each bin by the bin width. The area of each bin on the histogram now represents the

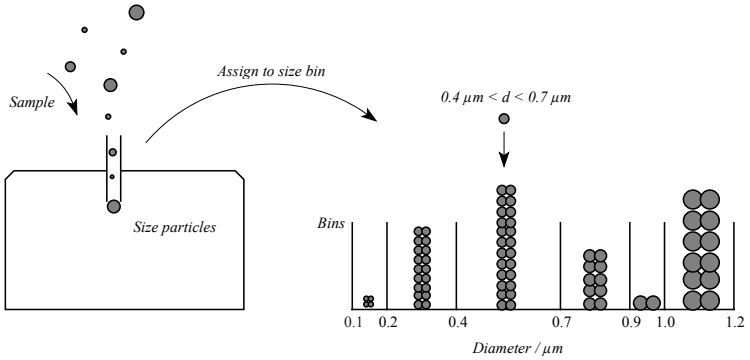

Fig. 4.1. Aerosol particle sizing. Particles are assigned to bins according to their diameter.

integral number concentration between the bin limits, and the total area represented by all of the bins represents the total aerosol number concentration. The beauty of this approach is that the center points of each bin may be plotted, and the points joined to give a representation of the continuous aerosol size distribution. The center diameter is the arithmetic mean of the bin diameter limits.

As each bin on the histogram represents the particle number concentration δn over a particle diameter range δd, the vertical scale is referred to as the differential particle concentration, and written $\mathrm{d}n/\mathrm{d}d$. This makes sense if you consider that the integrated area under the curve equals the total number concentration n: in mathematical terms:

$$\int \frac{\mathrm{d}n}{\mathrm{d}d}\mathrm{d}d = n \qquad 4.1$$

Geometric Bin Sequences. Most aerosol size distributions cover several orders of magnitude of particle diameter, and the use of measurement bins with similar diameter widths would lead to excessive bins. For instance, if a distribution extends from 0.01 µm

to 10 μm, a choice of 0.01 μm width bins would give reasonable resolution, but would require 999 bins! Using a bin width of 1 μm would reduce this to 10 bins, but no detailed information would exist for particles smaller than 1 μm. To cover such large diameter ranges, it is more usual to use a geometric progression of bins. In this case each subsequent bin edge is a constant multiplied by the previous bin edge

$$edge_i = edge_{i-1} \times c$$
$$\text{or} \qquad 4.2$$
$$edge_i = edge_0 \times c^i$$

If there are to be 10 bins per decade, c=1.2589. An alternative definition of bin edge diameters in a geometric progression that is often useful is

$$d_i = d_0 \times 10^{\frac{i}{x}} \qquad 4.3$$

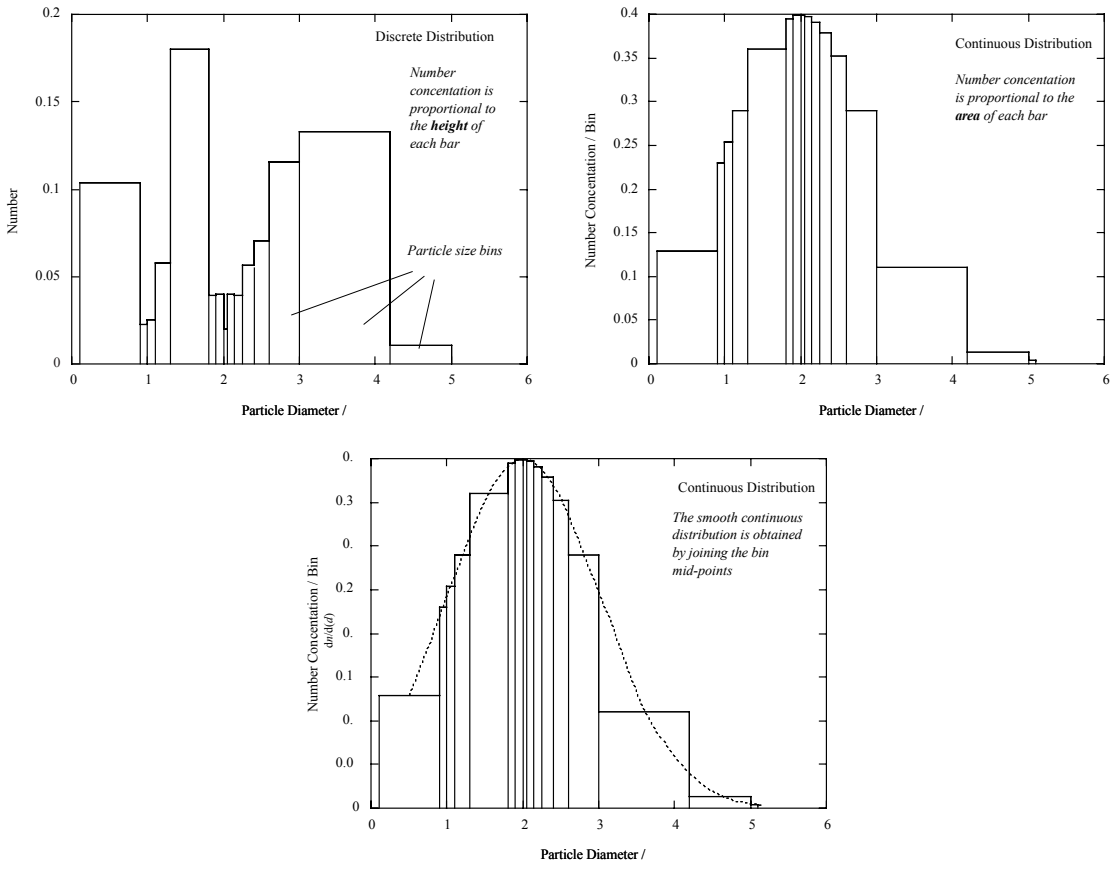

Fig. 4.2. Conversion of a discrete particle size distribution to a continuous distribution

where d_0 is the first diameter in the sequence, d_i the ith diameter, and x the number of bins per decade. Using the above example, a particle size distribution between 0.01 µm and 10 µm could be characterized using 30 bins, and still have good resolution at small particle diameters.

Using a geometric sequence of bin edges still allows the data to be converted into a continuous distribution by dividing through by the bin width for each bin. However, plotting the resulting distribution on a linear diameter scale will hide any data at smaller diameters – the additional resolution gained by using geometric bins will effectively be lost on plotting the data. *This is particularly important, as aerosol size distributions tend to contain features on logarithmic scales rather than linear scales*. ***It is therefore usual***

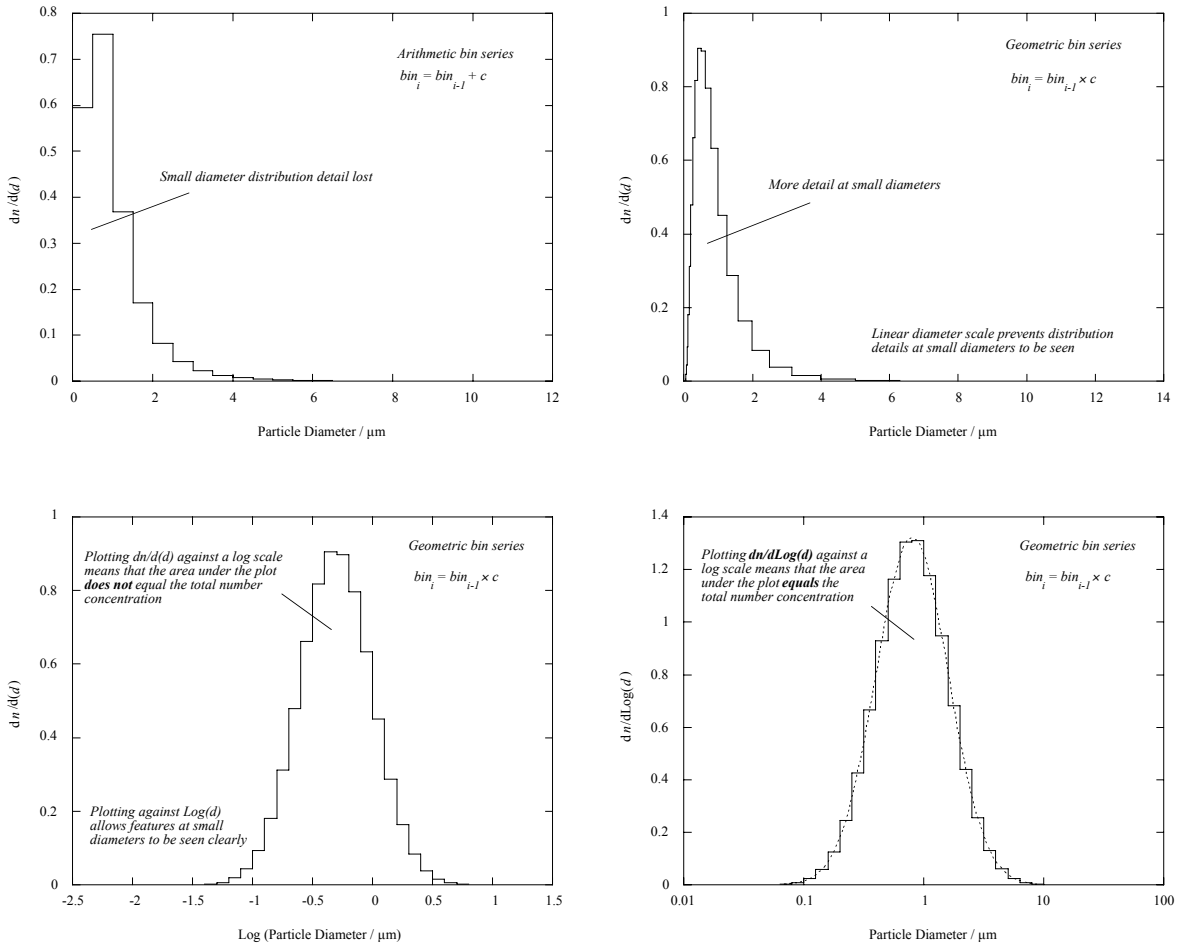

Fig. 4.3. Plotting skewed size distributions with a geometric bin series against Log(d)

to plot size distributions against the log of particle diameter (or on a logarithmic axis). An added advantage of this approach is that many aerosol distributions approximate a lognormal distribution (normal with respect to the log of particle diameter), and thus plotting the distribution on a log axis simplifies characterization considerably.

The one drawback of plotting distributions on a logarithmic axis is that while the area under the normalized or continuous distribution represents total particle number concentration when plotted on a linear scale, this relationship is lost when the same data are plotted on a log scale. The solution is to divide the particles in each bin by the difference in log(d) across the bin, rather than the difference in d. The resulting distribution represents differential concentration in terms of dn/dLog(d) versus diameter, and ***on a log axis, the area under the curve represents particle concentration between selected diameters***. This is the usual way of representing aerosol size distributions. When deriving the continuous particle distribution from the histogram of dn/dLog(d) versus diameter, dn/dLog(d) is plotted against the geometric mean diameter for each bin (and not the arithmetic mean diameter). Geometric mean diameter is given by

$$\text{Geometric Mean Diameter} = \sqrt{d_{lower} \times d_{upper}} \qquad 4.4$$

where d_{lower} and d_{upper} are the lower and upper diameter bounds of the bin. It is important to remember that to calculate the actual particle number concentration between two diameters from a plot of dn/dLog(d), you MUST integrate with respect to Log(d) and not d.

Even though we have already simplified the characterization of an aerosol considerably by focussing on a single parameter – particle size – the resulting size distribution can still represent a lot of data if many particle size intervals are used. An elegant solution to simplifying the data further is to represent the distribution by a mathematical function where possible, which allows the size distribution to be described by relatively few parameters. Fortunately this is possible in many cases using a *lognormal distribution*.

Lognormal Distribution

The normal function is a common symmetrical mathematical function used to describe the frequency of occurrence of a given measurement – for instance, the number of times particles of a given diameter occurs in a given aerosol volume. In terms of a particle size distribution, the number dn of particles of diameter d_p over a diameter interval dd_p is given by

$$dn = \frac{n}{\sigma\sqrt{2\pi}} e^{-\frac{\left(d_p - \bar{d}_p\right)^2}{2\sigma^2}} dd_p \qquad 4.5$$

where d_p is the arithmetic mean particle diameter, σ the standard deviation and n is the total particle number concentration. dn at any d_p is defined now by just three parameters – d_p, n and σ. Unfortunately, the normal distribution is applicable to relatively few aerosol size distributions. Most are skewed (not symmetrical about d_p), and have long tails at large particle sizes. Furthermore, the normal distribution extends to negative values of d, which isn't helpful in the real world.

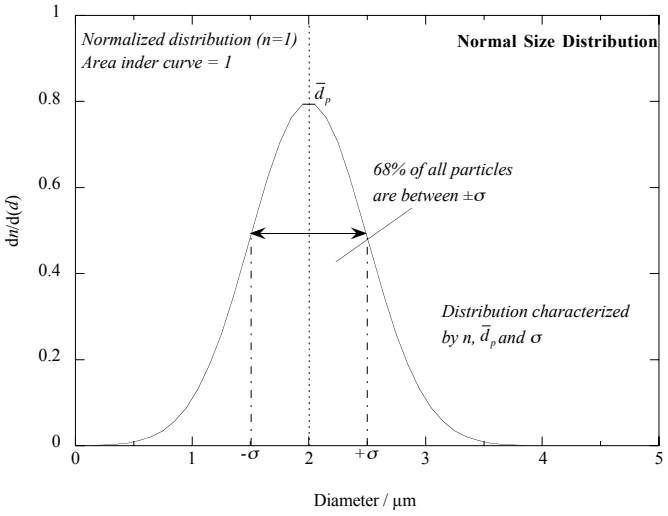

Fig. 4.4. Normal Distribution

The lognormal function gives the *distribution of the logarithm of particle diameter about the log of a mean diameter*, and has two advantages over the normal distribution: it 'compresses' the distribution, thus allowing distributions extending over several orders of magnitude of diameter to be dealt with, and it never extends to negative particle diameters. It also often provides a good approximation to single-mode aerosol size

distributions. The lognormal distribution represents the normal distribution of Log(d) about the arithmetic mean of Log(d), and the distribution is characterized by particle number concentration n, Count Median Diameter (CMD) (which is the same as the

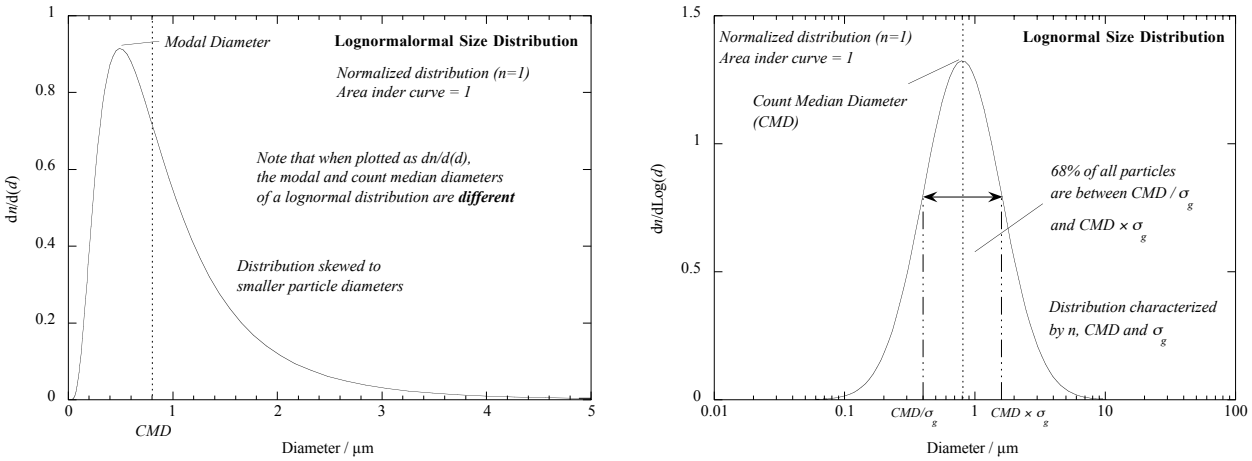

Fig. 4.5. Lognormal Distribution

geometric mean of diameter d and the diameter corresponding to the arithmetic mean of Log(d)), and Geometric Standard Deviation (GSD, σ_g). Log(σ_g) is the standard deviation of Log(d). Note that CMD represents the particle diameter for which 50% of the particles are smaller, and 50% larger. In mathematical terms, the fraction of particles having diameter d over the log diameter interval dLog(d) is given by

$$dn = \frac{n}{\sqrt{2\pi}Log(\sigma_g)} e^{-\frac{\left(Log\left(d_p\right)-Log(CMD)\right)^2}{2Log\left(\sigma_g\right)^2}} dLog\left(d_p\right) \qquad 4.6$$

Note that for simplicity logs to the base 10 have been used here – however it is more usual for natural logs to be used.

For the normal distribution, 95% of the distribution lies within the limits $d_p \pm 2\sigma$. ***For the lognomal distribution this range is assymetrical, and goes from*** $\frac{CMD}{\sigma_g^2}$ ***to CMD× σ_g^2.***

Thus if σ_g =2, 95% of the distribution will lie between a quarter of CMD and four times CMD.

Similarly, ***68% of the distribution lies between*** $\frac{CMD}{\sigma_g}$ ***and CMD×*** σ_g. If the lower and upper limits of this region are represented by d_{16} (16% of the distribution lies below this diameter) and d_{84} (84% of the distribution lies below this diameter), then

$$\sigma_g = \frac{d_{84}}{CMD} = \frac{CMD}{d_{16}} = \sqrt{\frac{d_{84}}{d_{16}}} \qquad 4.7$$

Cumulative size distribution

The lognormal distribution can be plotted as a cumulative distribution – giving the number concentration of particles below a given diameter. *CMD* (given by d_{50}), d_{16} and

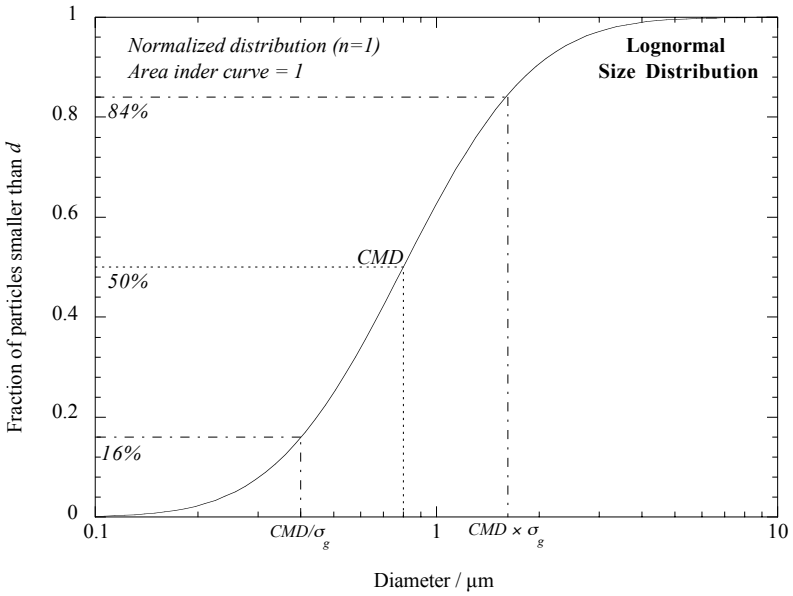

Fig. 4.6. Cumulative size distribution – lognormal distribution

d_{84} can be directly read off a cumulative distribution plot, allowing simple calculation of σ_g, and the overall lognormal distribution. This is particularly useful for deriving the

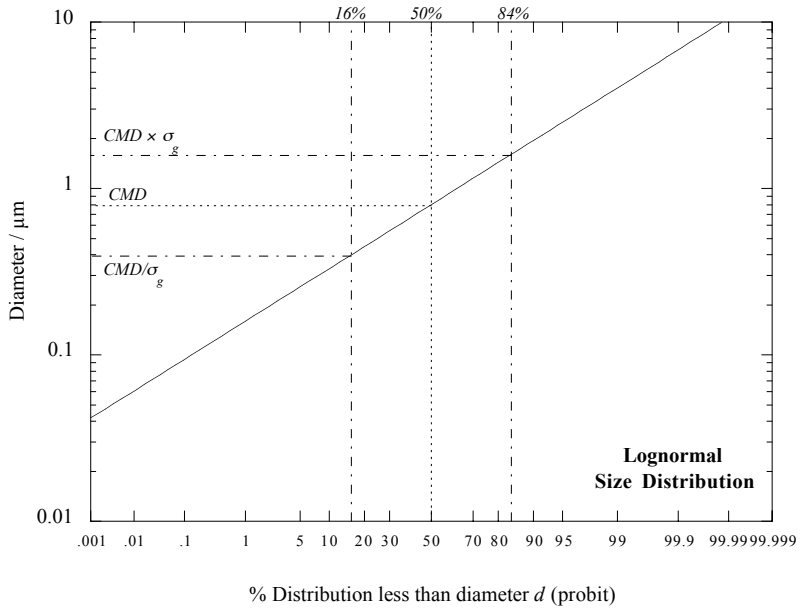

Fig. 4.7. Log-probability plot – lognormal distribution

lognormal parameters describing an experimental distribution. Instead of using complex fitting routines on the continuous distribution derived from experimental data, the cumulative distribution of particle below a given size can be plotted, and the relevant parameters simply read off the plot.

Although the cumulative lognormal plot with a linear vertical axis has a distinctive shape, it is not sufficiently distinctive to indicate how close an experimental distribution is to a lognormal distribution. An alternative is to use a log-probability plot. Particle diameter is plotted on a vertical log axis and the percentage of the distribution less than the indicated diameter is plotted on a probability scale – giving the *probit* of the cumulative number concentration. The probit scale is designed to result in a straight line when a lognormal distribution is plotted, and so plotting experimental data on a log-probability plot gives an immediate indication of how close the lognormal approximation is. As for the cumulative lognormal distribution, σ_g and CMD for an experimentally measured distribution can be measured by simply reading the 16^{th}, 50^{th} and 84^{th} percentiles from the plot.

Dangers of assuming a lognormal size distribution. If the size distribution is not lognormal, the log-probability plot will not give a straight line. However many real distributions only approximate to a lognormal distribution, and it is usual to approximate this by a lognormal distribution by reading the 16^{th}, 50^{th} and 84^{th} percentiles from the cumulative plot. However, if the distribution is bimodal, this approach will lead to a serious mis-representation of the distribution (see next page).

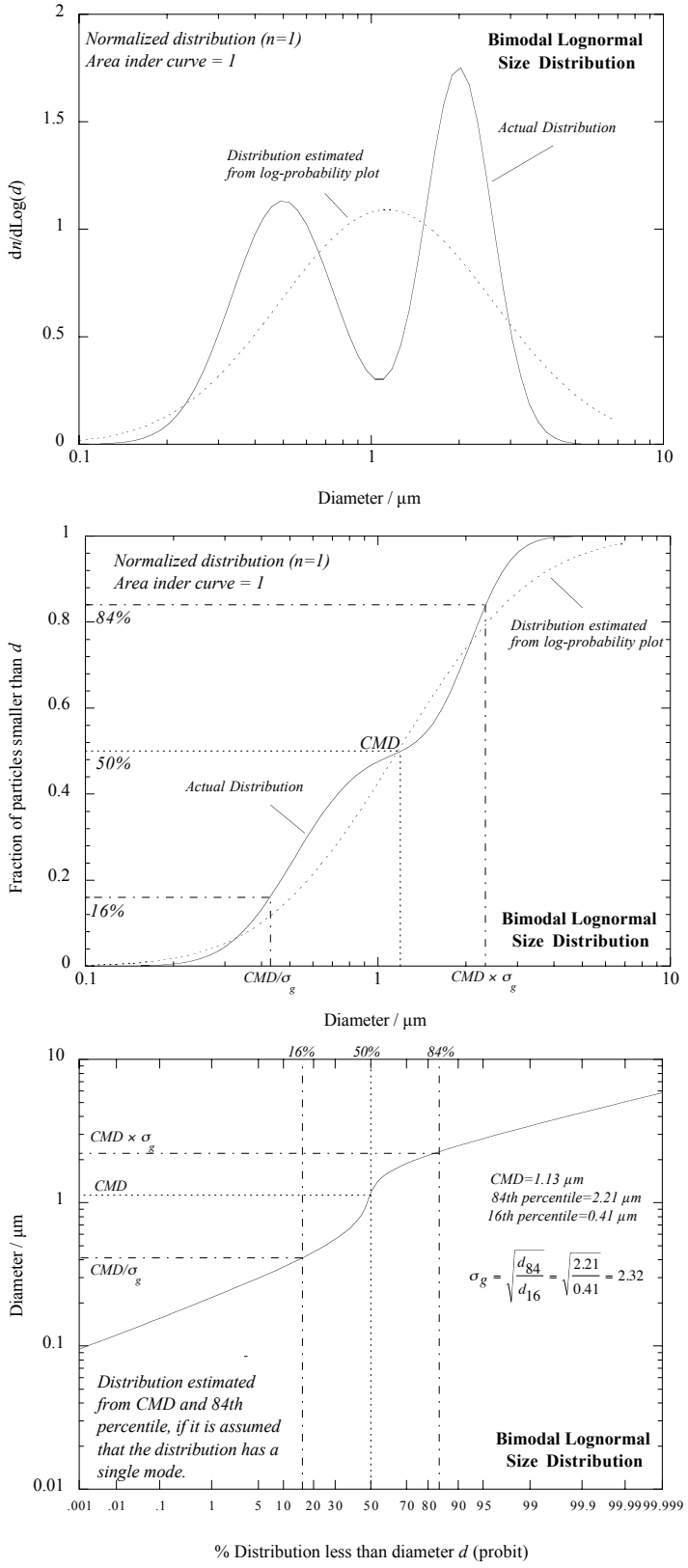

Fig. 4.8. False interpretation of a bimodal distribution as a single mode distribution

Number, surface area and mass weighting

A particle of a given diameter has three primary physical characteristics – its size, mass, and surface area. Likewise, aerosol size distributions can represent three primary physical characteristics of the aerosol – particle number concentration as a function of diameter, particle mass concentration as a function of diameter, and particle surface area concentration as a function of diameter. Each weighting, or moment – number, mass or surface area –leads to different distribution functions and different mean, median and geometric mean diameters. For instance, while *CMD* represents the diameter that 50% of the particle **number** is smaller than, Mass Median Diameter (*MMD*) represents the diameter that 50% of the particle **mass** is below. As the mass at a given diameter is the particle number weighted by diameter cubed (mass is proportional to diameter cubed for compact particles), ***MMD will be different to CMD***.

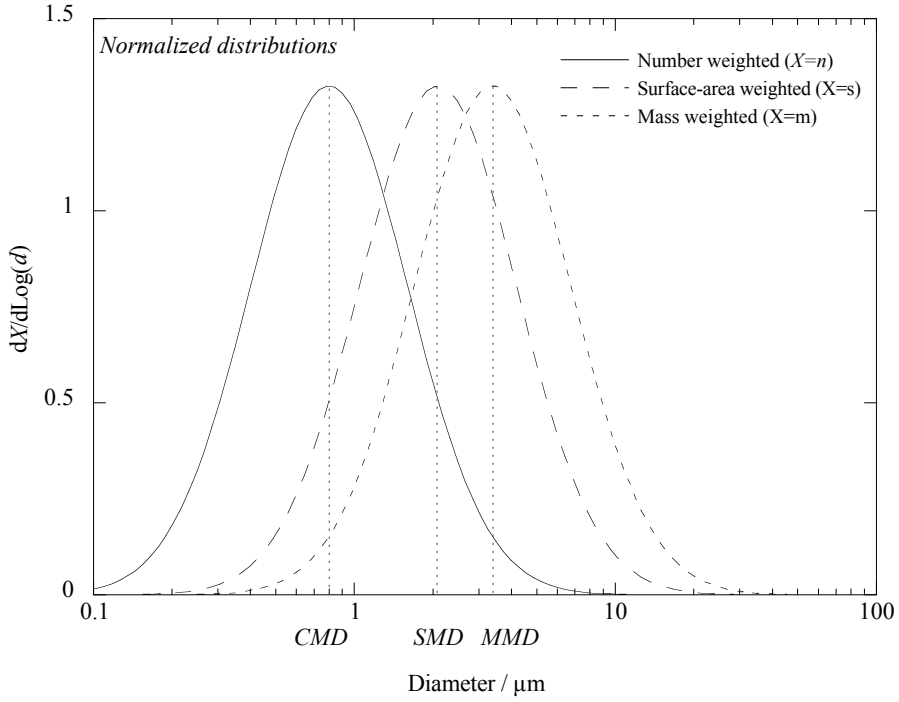

Fig. 4.9. Number, surface-area and mass weighted lognormal size distributions

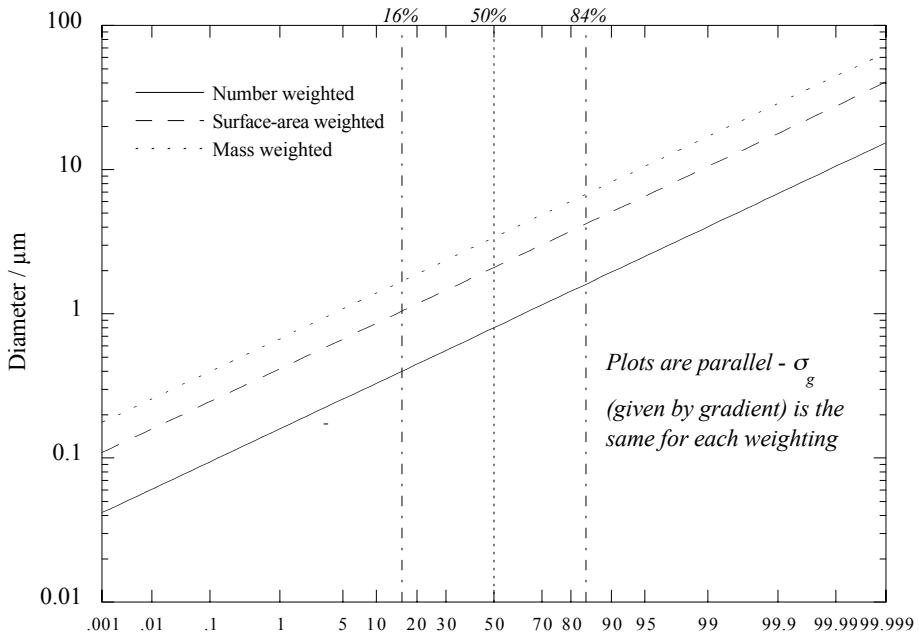

Fig. 4.10. Log-probability plot of number, surface-area and mass weighted lognormal distribution

A lognormal distribution remains lognormal whichever moment is used to describe the distribution. Furthermore, the geometric standard deviation of a lognormal distribution is independent of distribution weighting (or moment). In other words, a lognormal distribution of particle number concentration as a function of diameter (dn/dLog(d)) with σ_g =2 will remain lognormal with σ_g =2 when converted to a mass-weighted distribution – dm/dLog(d). There are also simple relationships between the characteristic average diameters for lognormal distributions with different weightings. These are the **Hatch-Choate** equations. They allow conversion between mean particle diameters for different distribution moments. Note that for particle number, the moment is 0, 2 for surface area, and 3 for mass. In its most basic form, the Hatch-Choate equation is used to convert between median diameters:

$$MMD = CMDe^{3Ln^2\sigma_g}$$
$$SMD = CMDe^{2Ln^2\sigma_g} \qquad 4.8$$

where *MMD* is the Mass Median Diameter and *SMD* is the Surface Median Diameter.

Weighting a distribution by number, surface-area or mass can lead to visually very different distributions. Thus a number distribution that is dominated by very small particles may be dominated by large diameter particles when weighted by particle mass (recall that surface area is proportional to diameter squared, and mass is proportional to diameter cubed).

Weighting by particle volume is also commonly used – the result is the same as mass weighting for spherical particles, but without the inclusion of particle density.

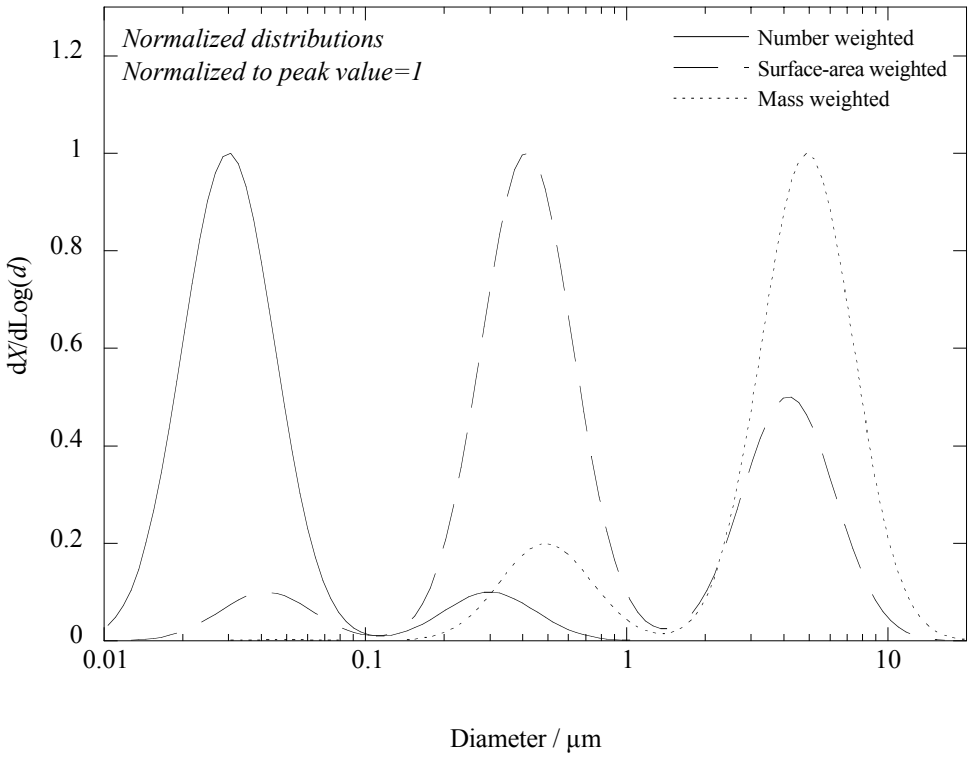

Fig. 4.11. Weighting a trimodal distribution by particle number, surface-area and mass (or volume)

AEROSOL GENERATION AND DISPERSION

Suggested reading: [1]Baron and Willeke chapter 5, 21
[2]Hinds chapters 12, 14, 21
[3]Vincent, chapter 3

Material Covered:

- Aerosol generation and formation mechanisms
  - Ambient aerosol size distribution
  - Mechanical generation
  - Nucleation
  - Coagulation
- Laboratory aerosol generation
  - Monodisperse aerosols
  - Polydisperse aerosols

[1] Aerosol Measurement. Principles, Techniques and Applications. 2nd Ed. Baron, P A and Willeke, K (Eds.). Wiley Interscience, New York. 2001
[2] Aerosol Technology. 2nd Edition. Hinds, W C. Wiley Interscience, New York. 1999.
[3] Aerosol science for Industrial Hygienists. Vincent, J H. Elsevier Science, Bath, UK. 1995.

BACKGROUND NOTES

Background notes include supplemental material that is useful, but not essential, to the course.

1. Background

The nature of an aerosol is often governed by its beginnings – its generation, and the underlying mechanisms leading to generation. In this lecture, the formation of aerosols through natural and human processes will be looked at. We will also briefly consider the generation of well-defined aerosols in the laboratory

2. Primary aerosol generation mechanisms

If the relative abundance of aerosol particles in the *environment* is measured as a function of particle size, a similar size distribution emerges wherever the measurements are taken (within reason). Between diameters of approximately 1 nm and 100 µm, three modes dominate the size distribution, each representing a different set of generation and formation mechanisms.

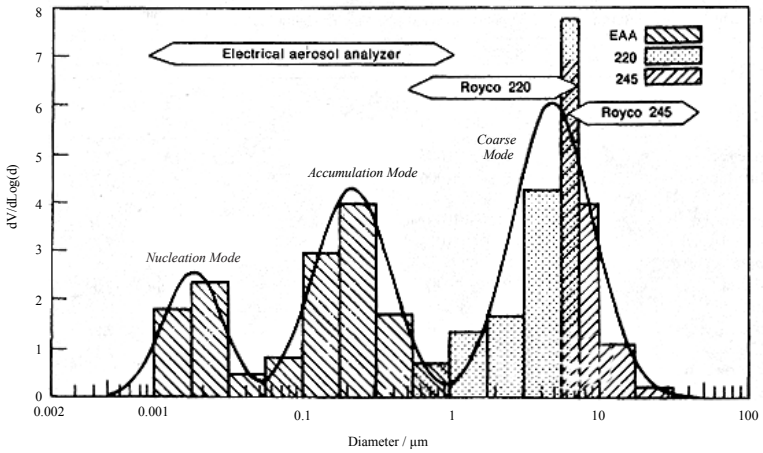

Fig. 5.1. Ambient aerosol size distribution measured by Whitby in 1978 [B&W p104]

Coarse Mode

The particles of the greatest diameters in the distribution make up the upper most mode – the *coarse mode*. For the most part these particles are generated through mechanical processes such as re-entrainment of dust from surfaces, the attrition of bulk material (for instance, rocks), the grinding together of materials, and the spraying of liquids. It takes increasingly higher energies to mechanically form increasingly smaller particles (the energy required is depends on the surface area of the generated aerosol, among other factors, and is approximately inversely proportional to the diameter of the generated particles for a given mass of material). The naturally occurring forces typically found in the environment tend not to lead to particles much smaller than 1 μm being generated through this route – hence the lower limit of the coarse mode. Much larger particles may be generated, but will rapidly settle out of suspension, thus limiting the upper end of the coarse mode to around 100 μm or so.

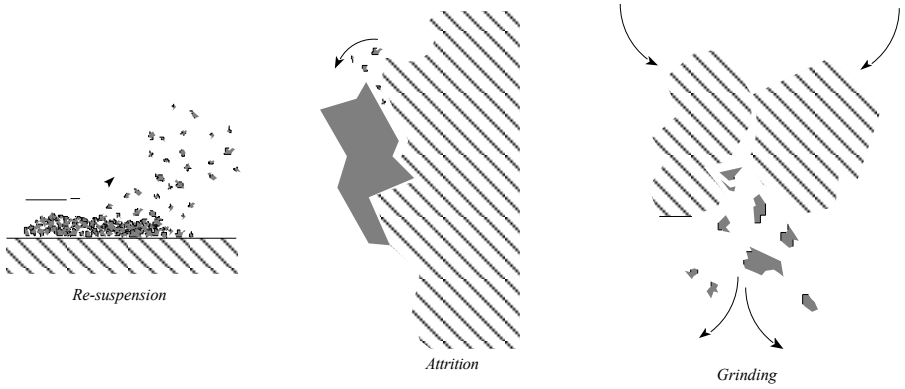

Fig. 5.2. Coarse mode generation mechanisms

In the workplace, much higher mechanical forces are encountered – grinding and drilling for instance, and the potential for producing very much smaller particles through mechanical means exists. However even with high-energy mills, used to produce fine powders, it is difficult to generate significant numbers of particle smaller than around 0.1 μm in diameter.

As mechanically generated particles are produced as a result of particles shearing off the parent material, they typically have a very uneven, jagged shape. Aerosols generated from crystalline material will typically shear along crystalline planes, leading to very

sharp edged particles. Crystalline silica is a prime example. Asbestos is a unique example in that the cleavage planes within the bulk material lead to the generation of increasingly fine fibers – in this case, it is possible to form very high aspect ratio particles with very small physical diameters through mechanical generation

Nucleation Mode

The first mode, usually referred to as the nucleation mode, consists of the smallest particles in the distribution. As it requires extremely high amounts of energy to break large particles into small particles, very few if any of the particles in this region are generated through mechanical means. Two processes dominate in the atmosphere – particle nucleation from supersaturated vapors, and gas-to-particle conversion.

Gas-to-particle conversion in the atmosphere is dominated by the oxidation of sulfur dioxide (SO_2) to sulfuric acid (H_2SO_4), which then forms an aerosol. Reversible reactions between ammonia (NH_3 – the most common alkaline gas in the atmosphere) and Nitric acid (HNO_3) and hydrochloric acid (HCl) lead to solid ammonium chloride and ammonium nitrate aerosol particles:

$$\begin{aligned} NH_4OH(s) &\leftrightarrow NH_3(g) + HNO_3(g) \\ NH_4Cl(s) &\leftrightarrow NH_3(g) + HCl(g) \end{aligned} \qquad 5.1$$

HNO_3 in the atmosphere results from the oxidation of NO_x – mainly from vehicle emissions and other combustion sources. The main source of HCl is from refuse incineration and coal combustion. The initial particles generated through gas-to-particle conversion are of the order of nanometers in diameter.

Aerosol particle nucleation occurs when the molecules in a supersaturated vapor begin to coalesce together to form particles. *Note: saturation is the point at which a liquid and a vapor are at equilibrium.* At higher vapor pressures or vapor concentrations *(supersaturation)* there will a net movement from the vapor to the liquid, and at lower vapor pressures, there will be a net movement of molecules from the liquid to the vapor. In a pure vapor, it is difficult to persuade molecules to remain together after random

collisions, even at high supersaturation ratios. It can be shown that a vapor at a given **saturation ratio (vapor pressure/saturation vapor pressure)** particles must initially reach a diameter d^* before they are able to grow into stable droplets. A theoretical saturation ratio of 220 would be required for particle growth to commence on a single water molecule. However because of the random formation of molecular clusters in the vapor, nucleation begins in practice at much lower saturation values (3.5 for water at 293K). The process of nucleation within a pure vapor is referred to as ***homogeneous nucleation***.

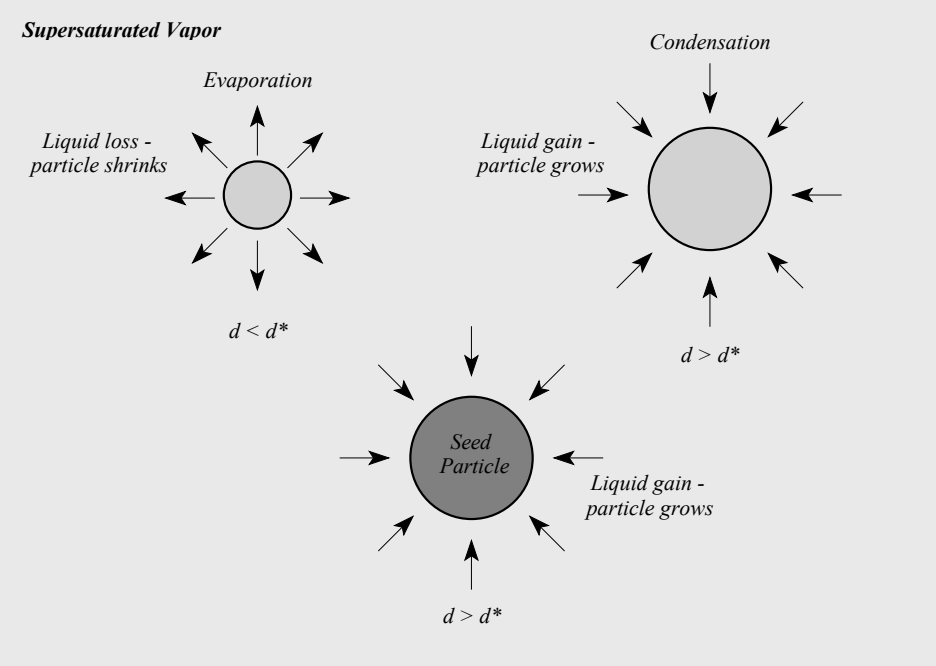

Fig. 5.3. Particle nucleation

Clearly, as particles above a critical diameter d^* form stable nuclei for the nucleation process, if a supersaturated vapor is 'seeded' with such nuclei, particle growth will occur much more rapidly. The process is referred to as ***nucleated condensation, or heterogeneous condensation***. If the seed particles are soluble, a resulting droplet will have a lower vapor pressure than a droplet of the pure liquid, and thus the critical particle diameter for a stable droplet d^* will be reduced. Similarly, the presence of ions (charged clusters of molecules) in a vapor slightly reduce the critical droplet diameter, thus leading

to nucleation at reduced saturation ratios – this is the basis of cloud chambers used to track radioactive particles. Seed particles – usually referred to as nucleation particles – are formed through homogeneous nucleation or gas-to-particle conversion. Ions that act as nucleation centers are omnipresent in the atmosphere.

Homogeneous nucleation is not common in the atmosphere, where saturation ratios rarely approach the necessary levels. Instead, heterogeneous nucleation dominates aerosol production and growth. However in many workplaces processes lead to relatively high levels of vapor, making homogeneous nucleation much more commonplace. *The generation process typifies the aerosols found from hot processes, including combustion processes, metal refining, welding and grinding*. The initial particles formed tend to be spherical, although crystalline forms may be generated under the right conditions. The initial particles also tend to be of the order of a few nanometers in diameter.

Once particles have formed through nucleation or gas-to-particle conversion, *they will continue to grow in the presence of a supersaturated vapor through condensation*. Competition between nucleation and condensation leads to the particle sizes that make up the nucleation mode. Typically these are between 5 and 50 nm in diameter.

Accumulation Mode

Particles forming in the nucleation mode will have very high diffusion coefficients due to their small size, and will rapidly collide with one another. Unlike gas molecules, that tend not to stick together after collisions (apart from at high saturation ratios),

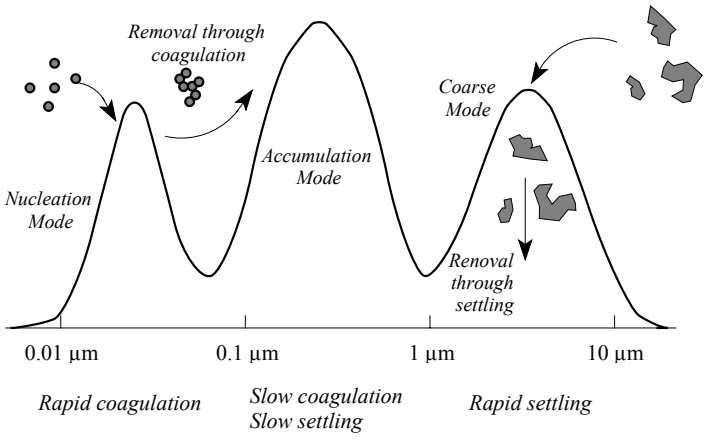

Fig. 5.4. Low particle removal rate from the accumulation mode.

aerosol particles are attracted by adhesive *van der Waals forces* at short range that tend to be greater than the particles' kinetic energy – they therefore tend to stick together and form agglomerates. The process is referred to as ***Brownian coagulation***, and is the primary mechanism leading to particle removal from the nucleation mode. (liquid particles coalesce to form larger droplets). Particles in this region rapidly coagulate with each other, and with larger particles, until they are several hundred nanometers in diameter. They eventually reach a point where their diffusion coefficient is sufficiently small to prevent coagulation with larger particles, while the mass of small particles coagulating with them is too small to lead to a significant increase in diameter. Furthermore particle losses through gravitational settling are small, as the particles have insufficient mass to settle out rapidly.

Thus the accumulation mode represents a region where smaller particle migrate to, but find it difficult to leave. It typically occurs between 0.1 and 1 μm, with a mode around 0.3 μm. *Remember these values, as a very similar behavior will be seen when we look at filtration and particle deposition.*

Coagulation

A full blown treatment of coagulation is beyond this course. However it is an important mechanism where large numbers of small particles are being generated, and it is useful to get a feel for what conditions lead to it being significant.

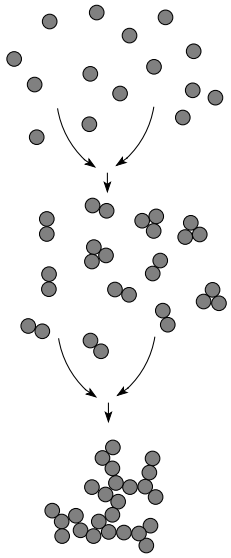

Fig. 5.5. Coagulation

The simplest case to consider is an aerosol consisting of particles with the same diameter – a monodisperse aerosol. Collisions between particles are due to particles diffusing towards each other, and therefore the rate of collisions between particles can be calculated by considering the rate of diffusion of one particle onto the surface of another. Following the calculation through gives the number of collisions per unit volume of an aerosol, dn_c/dt as

$$\frac{dn_c}{dt} = 4\pi d_p D n^2 \qquad 5.2$$

where D is the diffusion coefficient of the particles, and n is the number of particles per unit volume (number concentration). If it is assumed that the particles always stick together following a collision, then the collision rate is equal to the rate of change of the number concentration, dn/dt:

$$\frac{dn}{dt} = -4\pi d_p D n^2 \qquad 5.3$$

Note the change of sign, as we are now looking at a decrease in particles.

This is more usually expressed as

$$\frac{dn}{dt} = -K_0 n^2 \qquad 5.4$$

where K_0 is the coagulation coefficient.

$$K_0 = 4\pi d_p D \qquad 5.5$$

For particles larger than 0.1 μm, K_0 simplifies to

$$K_0 = \frac{4kTC_s}{3\eta} \qquad 5.6$$

and thus for particles greater than 1 μm, K_0 is approximately constant. Under standard conditions, equation 5.6 simplifies to $K_0=3.0\times10^{-16}\ C_s$ m^3/s (C_s is the Slip correction factor).

As dn/dt is dependent on n^2, the coagulation rate increases rapidly as particle number concentration increases.

If K_0 is considered to be constant, the particle number concentration at time t can be estimated from

$$\frac{n(t)}{n_0} = \frac{1}{1 + n_0 K_0 t} \qquad 5.7$$

and the mean particle diameter at t can be estimated from

$$\frac{d(t)}{d_0} = \left(1 + n_0 K_0 t\right)^{1/3} \qquad 5.8$$

These equations are clearly approximations, as even if you start with a monodisperse aerosol, coagulation will rapidly lead to a polydisperse aerosol (containing a range of particle diameters). However they are suitable for estimating aerosol behavior where K is constant, and are often applied to polydisperse aerosols (using the aerosol particle count median diameter).

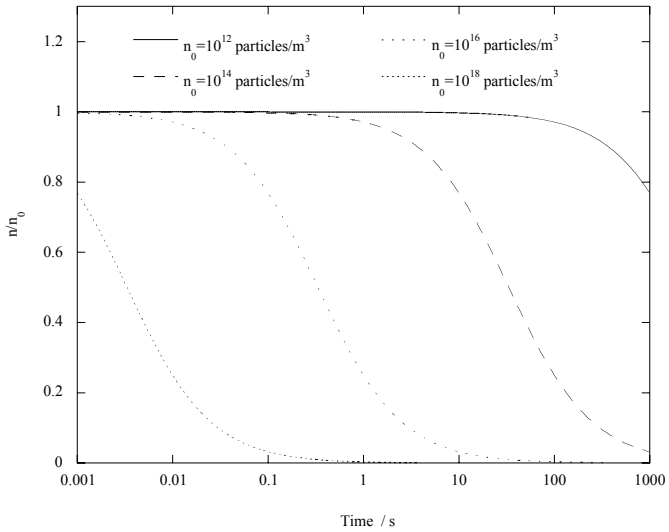

Fig. 5.6. Effect of coagulation on particle number

A more accurate consideration of coagulation becomes significantly more complex. Below 0.1 μm a correction factor has to be applied to K, which is analogous to the slip correction factor in calculating Stokes drag force. In a polydisperse aerosol, this leads to analytical solutions for particle coagulation only in specialized cases (e.g. when the aerosol size distribution is log-normal – see next section). In all other cases, numerical modeling is required to predict changes in the aerosol with time. The above expressions also assume a liquid aerosol. As solid particles coagulate, they are more likely to form

open complex shapes, with fractal-like properties, adding a further layer of complexity to determining aerosol behavior.

Kinematic Coagulation

Large particles moving under a motive force have a finite probability of colliding with other more slowly-moving particles in their path. This leads to kinematic coagulation, which is typified by the removal of very small particles by very large particles in an aerosol (scavenging). (Note that kinematic coagulation can occur whenever particles moving with different velocities are able to collide). Scavenging through Brownian coagulation is also seen in aerosols dominated by large particles. The coagulation coefficient between particles of very different sizes is dominated by the diffusion coefficient of the smaller particles, and the diameter of the larger particles. Thus if a number of small particles are introduced to an aerosol primarily consisting of large particles, they will preferentially and rapidly coagulate with the large particles, thus being removed or scavenged form the aerosol.

4. Aerosol Generation in the Laboratory

There are many instances where aerosols with specific characteristics are required – for instance in testing instrument response, preparing standard samples or using aerosol particles as the starting point in a manufacturing process. Although there are many ways of producing aerosols, there are a number of standard methods and instruments that are widely used. Most methods allow some control over the size and number concentration of the particles produced. Many methods lead to the generation of spherical particles, thus removing ambiguities of diameter definition and instrument response associated with non-spherical particles. However some methods are specifically designed to produce non-spherical particles with well defined shapes.

Laboratory generated aerosols are generally categorized into those predominantly consisting of ***particles of a single diameter – monodisperse aerosols***, and those with a ***wide range of particle sizes – polydisperse aerosols***. Aerosols with a geometric standard deviation below 1.1 are generally considered to be monodisperse.

Monodisperse aerosols

There is a clear advantage to using aerosols with a narrow range of particle diameters when evaluating instrument response.

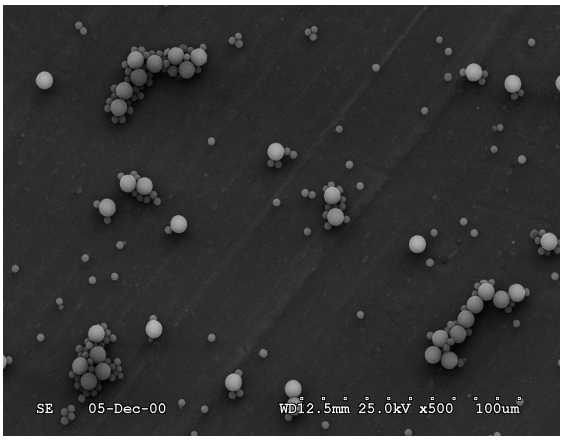

Fig. 5.7. SEM Image of two sizes of polystyrene latex spheres

Polystyrene Latex Spheres (PSL). Spherical polystyrene spheres are commercially available in closely graded sizes, allowing the formation of an aerosol of spherical particles with a *GSD* of less than 1.1. The density of PSL particles is around 1050 kg/m^3, resulting in their physical diameter being virtually equivalent to their aerodynamic diameter. They are available either in suspension, or in dry powder form, and may even be tagged with a fluorescent dye. They are widely used in many aspects of aerosol science, from measuring sampler performance, to measuring particle penetration through sampling systems, to observing and researching fundamental aerosol particle dynamics.

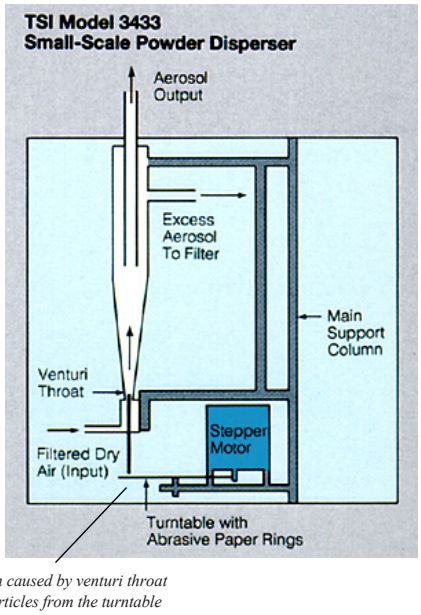

Fig. 5.8. Small scale powder disperser. Image from TSI Inc.

Generation of aerosols from dry powders is possible using a number of techniques, many of which will be covered under polydisperse aerosols below. However two methods are

often associated with PSL. The first is about the simplest method possible for generating a monodisperse aerosols – a small sample of the powder is spread out on a smooth surface such as a microscope slide, and brushed off into the air using a fine artists brush. Care has to be taken to apply enough force to break agglomerates into individual particles, but on the whole the method is surprisingly successful. A more sophisticated method is employed by a device called the Small Scale Powder Disperser (TSI). Dry PSL are applied to an abrasive pad, which is rotated under a Venturi nozzle. The high shear forces at the nozzle's entrance lift the particles from the surface (as well as aiding in their de-agglomeration), and result in the controlled generation of a monodisperse aerosol.

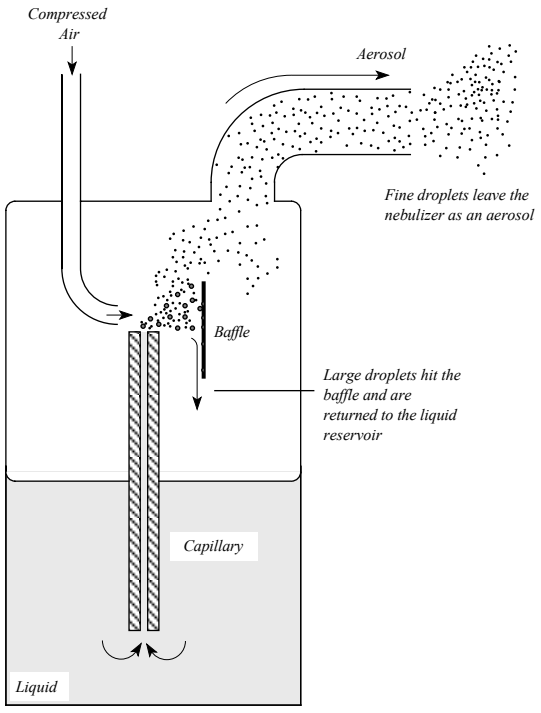

Fig. 5.9. Schematic of a nebulizer.

Generation from a liquid suspension is usually achieved using liquid nebulization or atomization. A capillary is placed in the particle suspension, and high velocity air blown over the top of it. The reduced pressure at the top of the capillary leads to liquid being drawn up it (venturi effect), where it is atomized by the shear forces in the air flow. Nebulizers tend to have a plate in front of the atomizer nozzle to catch the larger droplets, and return them to the liquid reservoir. The remaining aerosol particles are a few μm in diameter, and form a fine mist. PSL particles smaller than around 5 μm can be entrained in these droplets – evaporating the droplets then leads to am aerosol of dry PSL. To aid removal of the liquid vapor, the aerosol is usually passed through an air dryer – often an annular flow path surrounded with a drying agent such as silica gel. As a note of caution, PSL are usually suspended in a liquid containing surfactant and biocides

to ensure the particles remain separate and clean. If the concentration is too high, he residual surfactant and biocide in the nebulized droplets will lead to an outer coating on the PSL, and a high number of very fine particles resulting from droplets not containing PSL particles.

A number of other rather more exotic monodisperse particle preparations are available allowing the generation of aerosols of particles with distinct shapes. Particles of near-identical shape may be micromachined from silicon wafers in the same manner as electronic chips are manufactured. The method is ideally suited to the generation of disk and rod like particles with very well defined and controlled shapes and dimensions, although the production costs are high. Controlled crystal growth can also be used to produce near-monodisperse particles with somewhat unusual shapes. Such particles are useful for testing instrument response to particle shape.

Liquid monodisperse aerosol particles.

Although nebulizers can be used to generate aerosols with relatively low GSD's, with the exception perhaps of some ultrasonic nebulizers they are generally too high to be considered monodisperse (compressed air nebulizers generate aerosols with a GSD of typically between 1.5 – 2.5. Ultrasonic nebulizers may give an aerosol distribution with a GSD as low as 1.4-1.6). Two methods that do find widespread use for generating highly monodisperse droplet aerosols are the Vibrating Orifice Aerosol Generator (VOAG) and the Spinning Top Generator

Vibrating Orifice Aerosol Generator. If a jet of liquid is forced through a small nozzle, it is inherently unstable and will tend to break into small particles. These particles usually lead to a wide aerosol size distribution. However, if a regular mechanical disturbance is applied to the liquid jet the break-points, and thus the droplet sizes, can be closely controlled. In the Vibrating Orifice Aerosol generator (VOAG) a liquid is forced through an orifice with a diameter between 5 μm – 30 μm (20 μm is typical) using a syringe pump (capable of very low flow rates). The orifice is vibrated at a constant frequency using a piezoelectric crystal. As the oscillations are superimposed on the liquid flow, it breaks up at regular points, leading to uniformly sized droplets. Droplet diameter is given by

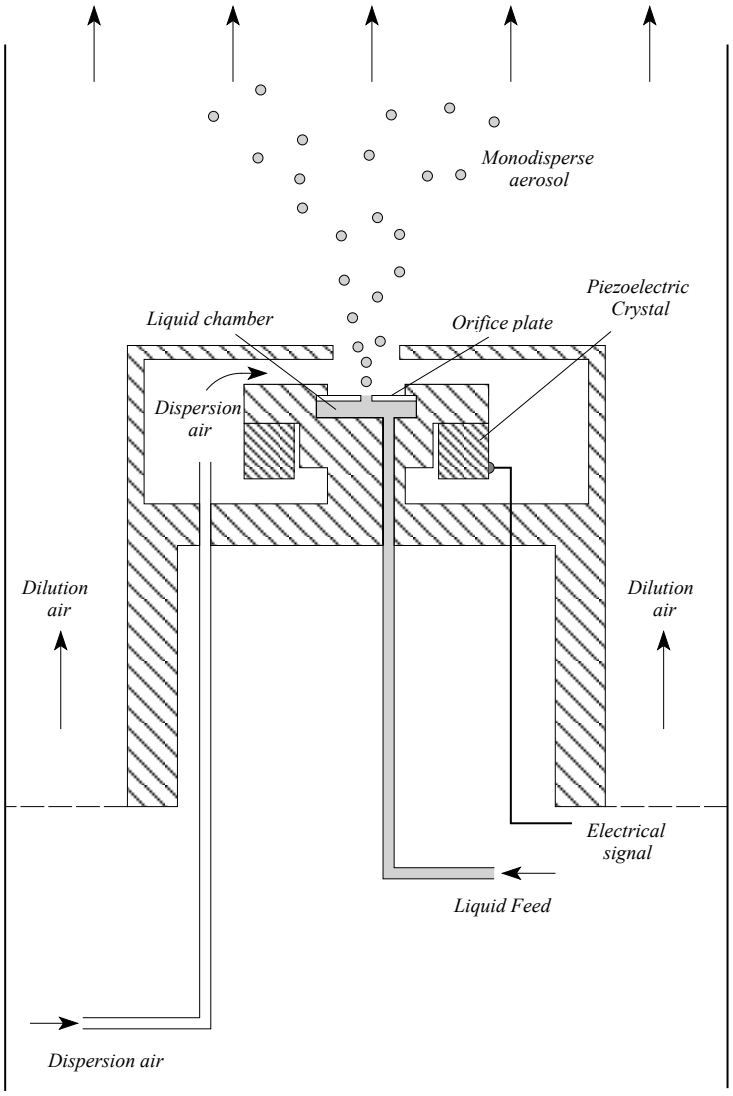

Fig. 5.10. Schematic of a Vibrating Orifice Aerosol Generator

$$d = \left(\frac{6Q}{\pi f}\right)^{\frac{1}{3}} \qquad 5.9$$

The generation rate is the same as the applied oscillation frequency. For a given jet diameter there is an optimum frequency for generating uniform droplets – hence the

availability of a range of orifice diameters. The ideal wavelength λ of the applied frequency is given by

$$\lambda = 4.508 d_j \qquad 5.10$$

where d_j is the jet diameter, although droplets will be formed within a factor of two of the ideal frequency.

The droplets formed by the VOAG are rapidly entrained in a turbulent airflow through an exit hole directly above the orifice (dispersion air), thus dispersing the particles and minimizing coagulation. In most applications the resulting aerosol is then entrained in a further airflow (dilution air) to transport it to its final destination, and brought to charge-equilibrium (particles may carry several thousand elementary charges). The uniformity of the aerosol particles generated make the VOAG a primary choice for laboratory-based test aerosol particles. Care has to be taken to avoid satellite particles (smaller than the primary particles, generated at the point where the liquid jet parts to form droplets – usually around a quarter of the diameter of the primary particles) and multiplets (coagulation of two or three droplets). Satellites and multiplets may be reduced by optimizing operating conditions and constantly monitoring output (using something like an optical particle counter/sizer). Satellites may also be removed from the aerosol by using a winnowing flow – an airflow that will remove the satellites with low Stokes numbers, but not the primary particles with relatively high Stokes numbers. Generation rates are also relatively low, and not suited to situations where large volumes need to be filled with an aerosol, such as in large scale wind-tunnel testing.

Note that as the primary particle size from the VOAG can be accurately predicted from theory, it is often considered a primary particle size standard.

Spinning-disk aerosol generator.

The spinning disk (or spinning top) generator leads to particle generation from liquid streams in a similar manner to the VOAG. In this case, a steady flow of liquid is introduced to the center of a disk rotating at up to 70,000 rpm. The liquid flows to the edge of the disk through centrifugal force, where it accumulates until inertial forces overcome surface tension. Liquid filaments then separate from the disk, and break up into droplets. Droplet diameter is given by

$$d = K\sqrt{\frac{\gamma}{\rho_f \omega^2 d_{disk}}} \qquad 5.11$$

γ is surface tension, ρ_f the fluid density, ω the angular velocity of the disk and d_{disk} the disk's diameter. K is a constant and varies in the range 2 – 7. The disk may be rotated mechanically, or in the case of more modern models, using compressed air. Primary particles may be formed with diameters between 20 μm – 100 μm, with a GSD of about 1.1 – not as good as the VOAG, but narrow enough to be considered monodisperse. As with the VOAG, satellite particles with diameters around a quarter of the primary particles are also formed. These may be removed by a peripheral winnowing flow that sweeps them away while allowing the more massive primary particles to reach the mainstream flow.

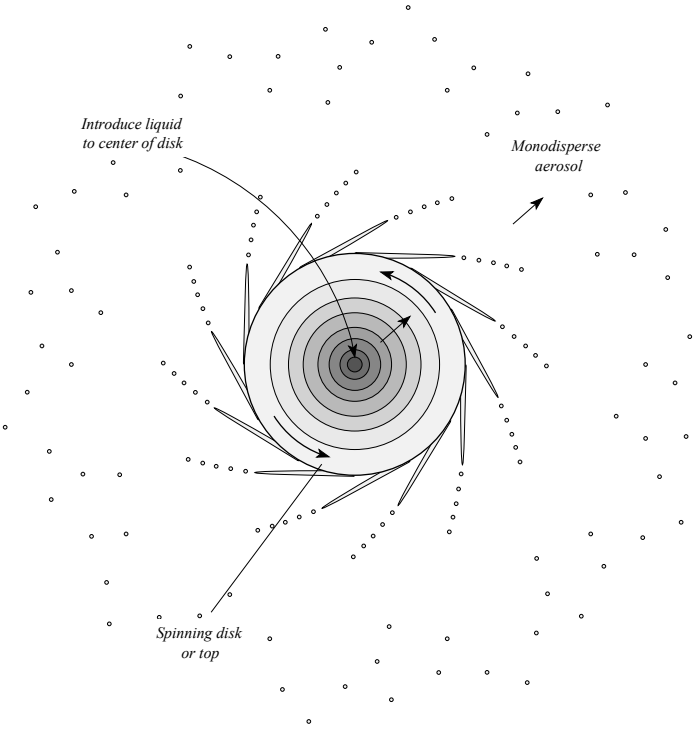

Fig. 5.11. Principle of the spinning disk aerosol generator

A significant advantage of the spinning-disk generator is the ability to generate large numbers of particles into a test volume, making it particularly suitable for testing samplers in large scale wind tunnels at high aerosol mass concentrations

Sub-micrometer monodisperse aerosols

If either the VOAG or spinning disk generator are used with a solution of a low volatility solute in a volatile liquid, solid monodisperse particles may be generated by evaporating the droplets to leave the low volatility 'residue'. This is a common methods of obtaining monodisperse particles smaller than 1 μm. Common solutes include oleic acid, sodium chloride and fluorescin. The diameter of the resulting particles is given by

$$d = C^{\frac{1}{3}} d_d \qquad 5.12$$

where C is the concentration of the solute in the solvent, and d_d is the initial droplet diameter. The minimum particle diameter attainable is determined by the level of impurities in the solvent. Note that a solution of flourescin in ammonium hydroxide is often used to generate ammonium fluorescin particles. These have the advantage of

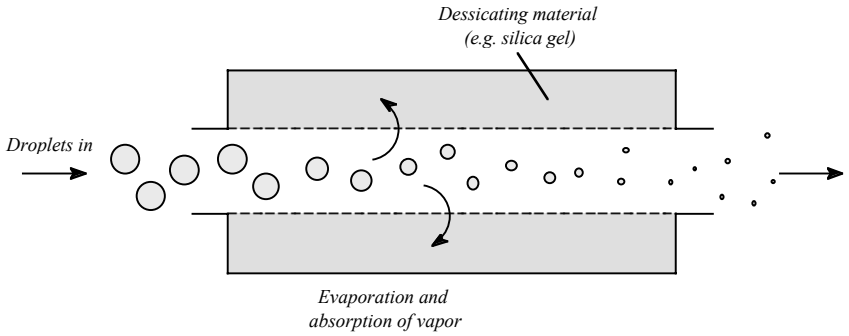

Fig. 5.12. Drying droplets of solute in solvent to obtain small diameter monodisperse particles

being spherical and smooth with the same density as the bulk material, while allowing quantitative detection using fluorescence spectroscopy (which is much more sensitive than mass analysis using weighing).

Electrospray generators rely on a similar approach to generating very fine aerosol particles. If a conducting liquid is passed through a capillary and subjected to a high electric field at the capillary exit, a fine stream of particles is generated. The use of an appropriate solute concentration can lead to monodisperse particles as small as 2 nm in diameter.

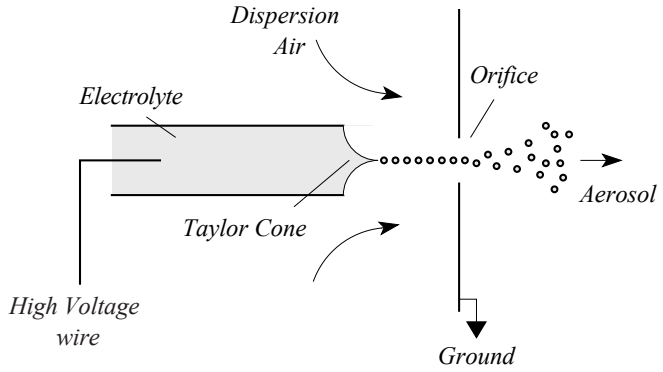

Fig. 5.13. Principle of electrospray generation

Polydisperse aerosols

There are many occasions where polydisperse test aerosols are more useful than monodisperse test aerosols. Perhaps the best case is where the behavior of aerosol particles is being measured using an instrument capable of discriminating between particles of different sizes. If the sampling efficiency of a device is being measured as a function of particle diameter, the traditional approach has been to carry out a series of measurements using monodisperse particles. However if measurements are made using an instrument that can also measure particle diameter, the use of a polydisperse aerosol is the equivalent of carrying out many tests with monodisperse aerosols in parallel – the time savings and increase in precision can be very large indeed (it may take a week to make measurements with monodisperse particles that take just 5 minutes with a polydisperse aerosol). Polydisperse aerosols are also more convenient to use when particle diameter is of secondary importance. For instance, if the performance of a

sampler is being tested, and it is known that sampling efficiency varies slowly with particle diameter above 30 μm, it is more convenient to use a polydisperse aerosol with a narrow GSD than a monodisperse aerosol, and the resulting errors will not be significant. In the case where the performance of an instrument is being tested with a realistic workplace or ambient aerosol, the use of polydisperse aerosols is a necessity.

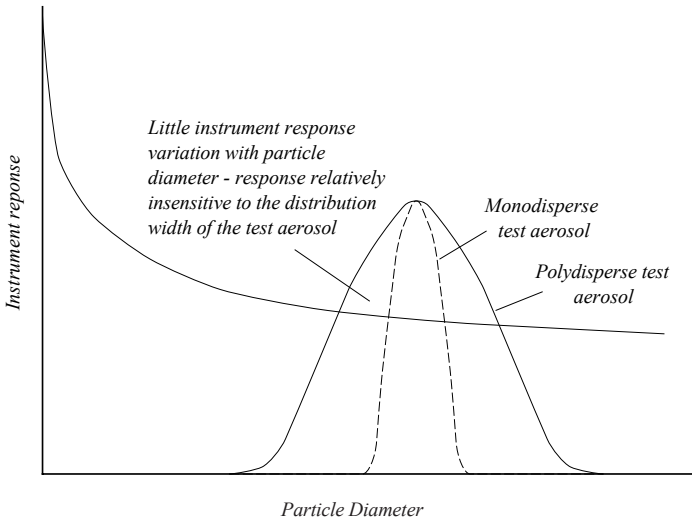

Fig. 5.14. Use of narrow polydisperse aerosols when testing instrument response

Most aerosol generation processes result in polydisperse aerosols, and so at a first glance their generation shouldn't be too difficult. However within a laboratory environment *it is important to ensure that both the size distribution and the aerosol concentration remain constant with time*, and this is often not trivial. Two approaches are commonly employed when generating aerosols to test instrumentation and samplers: direct generation from a bulk source, and re-suspension of powders.

Direct generation.

With the exception of nebulization, direct polydisperse generation methods tend to give aerosols dominated by sub-μm particles. Compressed air (pneumatic) nebulizers and ultrasonic nebulizers are capable of generating polydisperse aerosols with mass median aerodynamic diameters below around 5 μm. They may also be used with solutions of low volatility solutes in high volatility solvents to generate sub-μm polydisperse aerosols. Pneumatic nebulizers will generate an aerosol with a large GSD. However output tends not to be constant with time as conditions within the nebulizer change. Ultrasonic nebulizers tend to have a more stable output, but lower GSD's. However one solution to

their use for producing a wide range of particle diameters in the same aerosol is to use a number in parallel, each producing a different range of droplet diameters.

Nucleation and combustion both lead to the direct generation of polydisperse aerosols. Combustion is rarely used as a controlled aerosol source, although it is sometimes employed in smoke generators for air movement visualization. However homogeneous nucleation may be used to generate stable aerosols from a number of materials. Heating metals to above their melting point in a flow of inert gas (e.g. N_2 or Ar) leads to the generation of particles from around 5 nm in diameter upwards. Particle size and generation rate are dependant on the vapor pressure of the material, its temperature, and the gas flow rate. Silver is commonly used as it gives high nanometer-sized particle concentrations at relatively low temperatures (less than 1200 °C). The carbon vapor produced within an electric discharge between carbon electrodes is also a good source of nucleation particles, and is used to generate stable polydisperse aerosols.

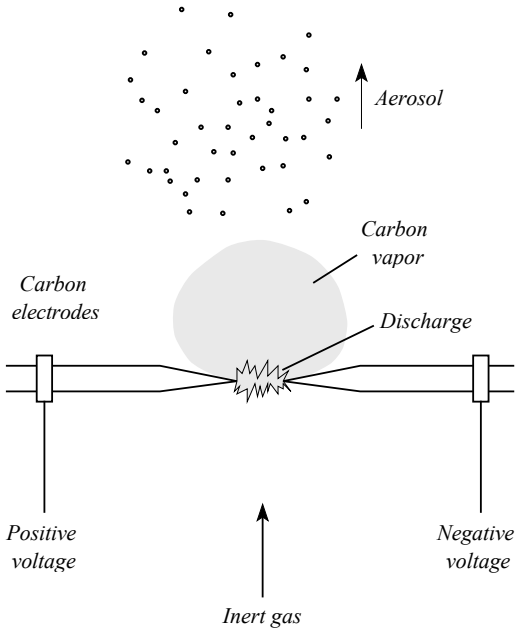

Fig. 5.15. Aerosol generation from a carbon arc

Powder dispersion

Many laboratory-based aerosol instrument evaluations rely on the use of powder dispersion to form a polydisperse aerosol. For aerosolizing small amounts of fine powders the Small Scale Powder disperser is a useful tool (described earlier). This instrument is primarily aimed at generating an aerosol from a powder in order to characterize it, and gives a very low aerosol generation rate. To generate aerosols in

sufficient quantities to allow instrument evaluation a number of dispersion methods are used, but four methods find particularly widespread use. Note that most powder dispersers result in a high level of charge on the particles generated, thus requiring some form of charge neutralization before the aerosol is used.

Fluidized bed generation.

If air is passed up through a bed of particles, the particles may be buoyed up by the air, and begin to act like a fluid. The resulting close and constantly changing contact between particles within the powder, as well as the air, forms an ideal environment for aerosolizing small particles. The simplest form of a fluidized bed is a single-component bed, consisting of just the powder to be aerosolized. Passing air up through the powder separates individual particles through shear forces within the flow, and also through mechanical collisions between particles within the powder, leading fine particles becoming detached and entrained in the flow. A more efficient approach is often to form a fluidized bed from a separate material consisting of particles too massive to be entrained in the flow, and then to introduce the powder to be aerosolized (a two-component bed). The introduced powder is fully exposed to the flow, thus allowing the finest particles to become airborne. Energetic collisions with the massive particles forming the bed detaches further particles from the powder. Glass or metal beads several hundred μm in diameter are often used to form the bed.

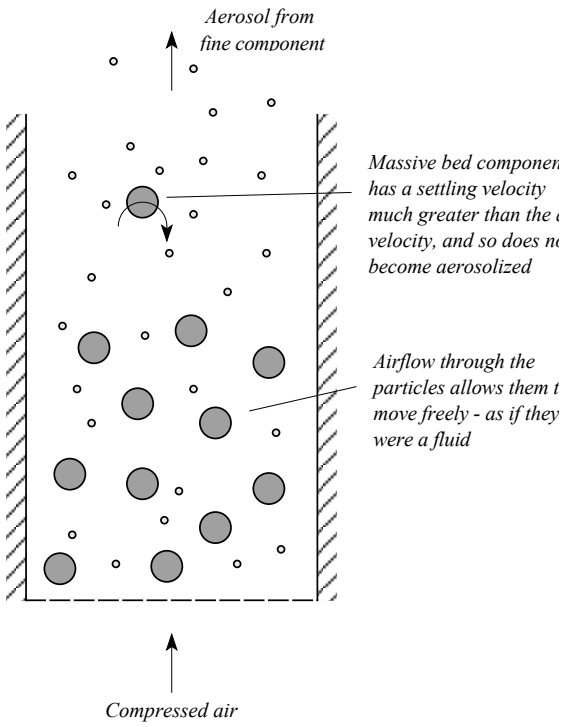

Fig. 5.16. Schematic of a simple two-component fluidized bed

Fluidized beds are generally capable of producing aerosols of particles from around 100 nm in diameter up to 3 – 5 μm in diameter. Smaller particles need increasingly more energy to detach them from agglomerates in the powder, and are correspondingly more difficult to generate. Particles much larger than 5 μm have settling velocities greater than the air velocity through most beds, and thus settle back down into the bed. Note that this separation by aerodynamic diameter also prevents the massive bed component particles from being entrained in the air flow.

Fluidized beds may also be fluidized using mechanical means rather than air flow through the bed itself. This may be achieved by mechanically oscillating the bed (using a speaker placed under a flexible membrane for instance), or by shaking the bed. In either case, passing air through the upper regions of the bed allows generated aerosol particles to be entrained in the flow.

The TSI 3400A is a commercially available two-component fluidized bed frequently used for powder aerosolization. The generator achieves relatively stable generation rates by introducing powder to the fluidized bed at a constant rate.

Wright Dust Feed.

An alternative approach to forming an aerosol from a powder is to 'scrape' particles off the surface of a compacted powder. The scraping process provides the mechanical force to separate individual particles and agglomerates of particles from the powder. Entraining these particles in a narrow jet of air provides shear forces that further break up the agglomerates.

This form of aerosol generator is embodied in the Wright Dust Feed. Powder is compacted in a cylinder that is rotated and slowly advanced onto stationary scraper blade. At the same time air flows at high speed over the compacted cylinder's surface to break up agglomerates, and entrain aerosol particles. Generation rate is a function of the compacted column feed rate. The generation methods isn't particularly suitable for generating particles much smaller than 1 μm as the adhesive forces between individual particles become too great for the mechanical and shear forces to overcome. However it is an effective method of generating aerosols of particles between 1 – 20 μm in diameter. In principle it is possible to aerosolize much larger particles, but in practice few powders consisting of large particles will remain sufficiently compacted to prevent the powder column from collapsing when scarping starts. At the other end of the spectrum, powders which compact particularly well are not broken up fast enough, leading to the generator jamming.

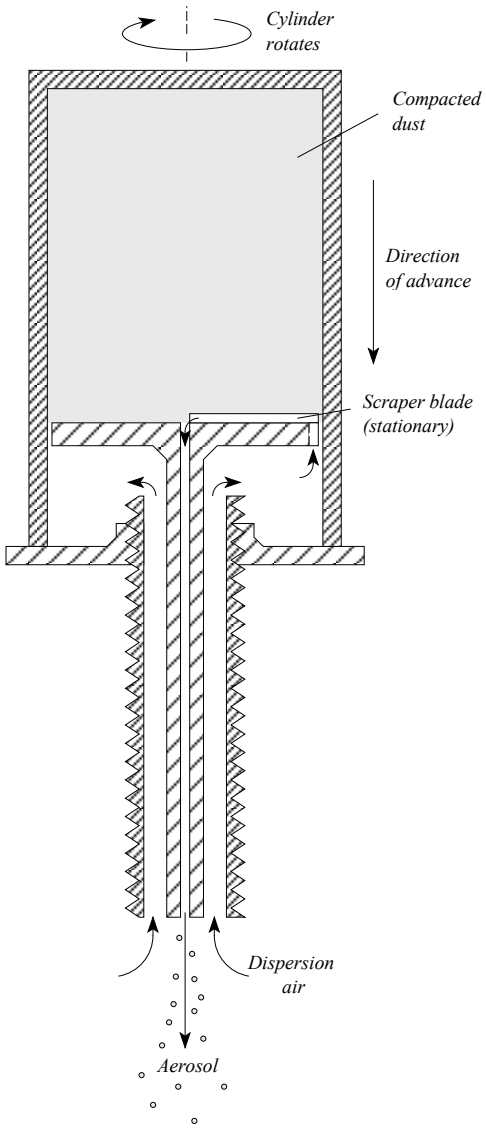

Fig. 5.17. Operating principle of the Wright Dust Feed

With a suitable powder the dust feed can give a stable aerosol with a wide range of concentrations.

Rotating Brush Generator.

The rotating brush generator uses the same principle as the dust feed, but modifies it in two respects to allow a greater range of powders to be aerosolized. Powder is still compacted into a cylinder. However this is not rotated, but is advanced vertically upwards onto the wire bristles of a brush rotating at up to 1100 rpm. Particles are removed from the dust column onto the bristles, and partially broken up. As the bristles reach the top of the brush, they enter a narrow region of high velocity air flow – particles are removed from the bristles in the flow, and broken up in the shear forces as the flow enters a narrow restriction.

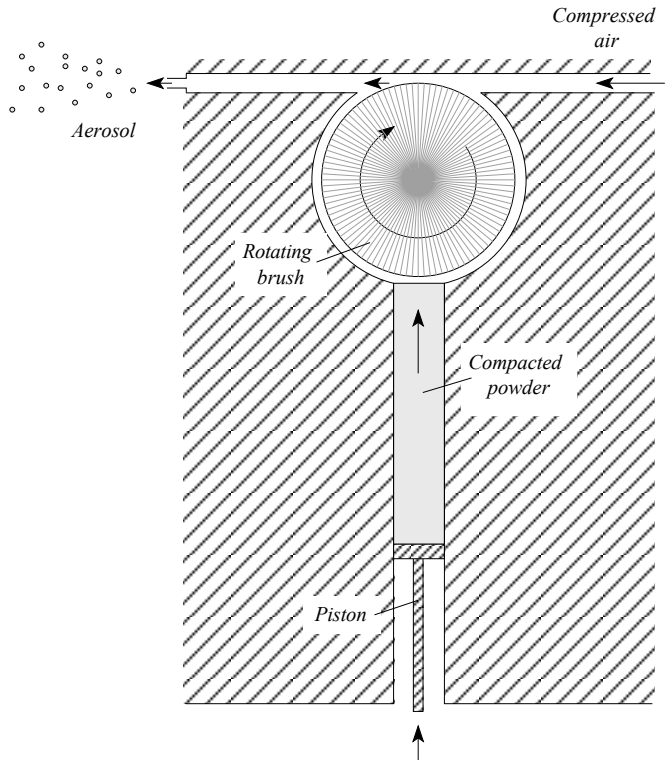

Fig. 5.18. Operation of the rotating brush generator

The method has similar limitations to the dust feed, although it is easier to generate an aerosol from material that is harder to compact down successfully. By using narrow bore cylinders it is possible to achieve very low constant aerosol generation rates. However the method is superceded by the dust feed in maximum generation rates.

Rotating Table

A particularly effective approach to aerosolizing large quantities of powder that has been used for many years is the rotating table generator. Powder is fed from a hopper into a groove on a rotating table (the hopper is usually vibrated to aid powder flow). The powder-filled groove then passes under an aspirator or air-mover (a device using the

Venturi effect to give an air-flow using compressed air). Powder is picked up from the groove, broken up and diluted in the aspirator, and generated as a high concentration aerosol. The generation rate is controlled by the groove length and depth, and the speed of rotation. This method has been used widely to fill large chambers and wind tunnels with aerosol for instrument performance testing.

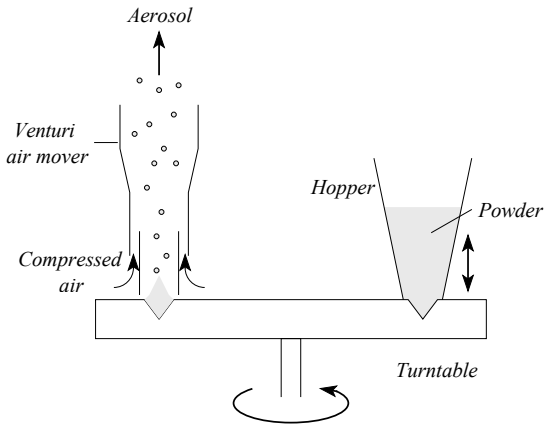

Fig. 5.19. Rotating table dust disperser

5. Test systems.

Aerosol instrumentation is generally tested in two types of environment: horizontal laminar flows and calm air. In each environment, the test aerosol needs to remain constant with respect to size distribution, concentration, space and time – a reference measurement at position and time 1 needs to give the same results as another reference measurement at position and time 2. The first requirement is therefore for the aerosol generator to produce an output which doesn't vary in size distribution or generation rate with time. The second requirement is for that aerosol to be homogeneously distributed across the cross-section of the test system. Although there are many ways of achieving this, most methods rely on introducing turbulence to

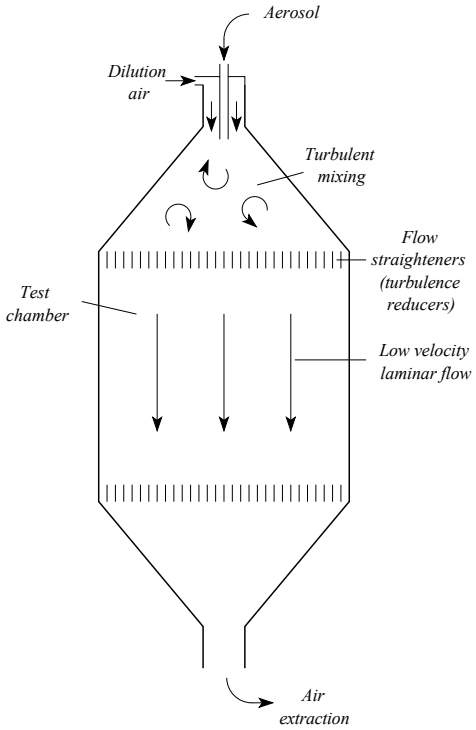

Fig. 5.20. Schematic of a 'calm air' aerosol instrument test chamber

the aerosol to give good mixing, then reducing turbulence as the aerosol enters the test region. Recall that conditions of high *Re* will lead to turbulent flow. A complete reduction of turbulence is often impractical, as the length of flow-line or wind tunnel that would allow the establishment of laminar flow would also lead to the loss of many aerosol particles through deposition. Flow-straighteners or turbulence-reducing grids are therefore employed to minimize turbulence where aerosol measurements are made. The flow is passed through an array of narrow flow channels. As the flow passes through the channels lateral flow patterns longer than the width of the channel are damped out, leaving most of the localized flow traveling parallel to the channels – conditions approaching laminar flow. Hexagonal-celled aluminum honeycomb material is frequently used.

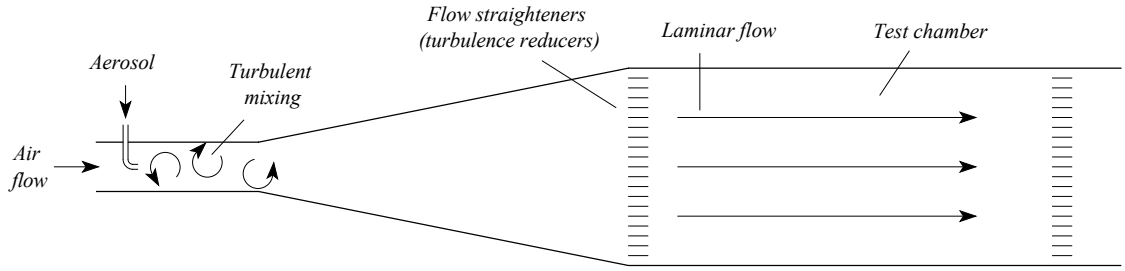

Fig. 5.21. Schematic of a laminar horizontal flow aerosol instrument test chamber (aerosol wind tunnel)

AEROSOL SAMPLING AND COLLECTION I: BASIC PRINCIPLES

Suggested reading: [1]Baron and Willeke chapter 8, 9
[2]Hinds chapters 10, 9
[3]Vincent, chapter 9, 11

Material Covered:

- Aerosol sampling – concepts involved
- Aspiration
- Aerosol transport
  - Electrostatic losses
  - Diffusional losses
  - Settling losses
  - Inertial losses
- Aerosol Pre-classification
  - Principles of Inertial Pre-classification
- Sample collection
  - Principles of Filtration

[1] Aerosol Measurement. Principles, Techniques and Applications. 2nd Ed. Baron, P A and Willeke, K (Eds.). Wiley Interscience, New York. 2001
[2] Aerosol Technology. 2nd Edition. Hinds, W C. Wiley Interscience, New York. 1999.
[3] Aerosol science for Industrial Hygienists. Vincent, J H. Elsevier Science, Bath, UK. 1995.

BACKGROUND NOTES

Background notes include supplemental material that is useful, but not essential, to the course.

1. Introduction

As we've discussed, aerosols are complex, and can only be completely characterized by looking at many, many parameters. For most practical situations, it is not feasible to even begin to attempt this, and so a number of simplifications need to be made. For instance, we have seen that approximating an aerosol size distribution with a lognormal distribution leads to a much simpler analysis of the size distribution. Likewise, the use of aerodynamic diameter allows the dynamics of particles with potentially complex shapes and structures to be characterized by a single parameter.

Understanding that any aerosol measurement is just an estimate or an indicator of the aerosol's characteristics is a key step to understanding the measurement process and the ensuing results. Another key step is understanding the relationship between the measurement and the aerosol characteristic being measured. For instance, if a device measuring aerosol mass concentration is insensitive to particles larger than 10 μm, measurements made on an aerosol with most of its mass in particles greater than 10 μm will not be particularly representative. ***Knowing the limitations of a measurement method is probably the single most important aspect of choosing the most appropriate approach to aerosol characterization, and interpreting the results.***

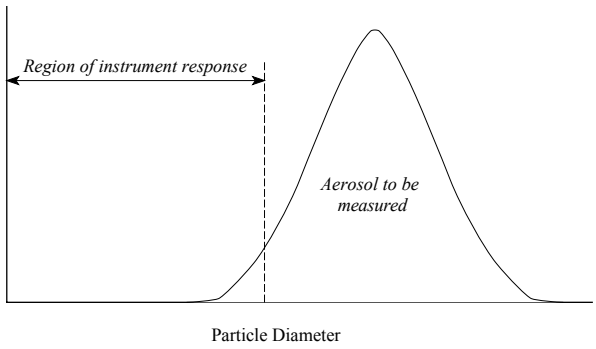

Fig. 6.1. Instrument response needs to be matched to the nature of the aerosol being sampled

2. Aerosol sampling - concepts

The process of aerosol measurement can be divided into a number of sequential sub-processes. The first part of the process is the removal of a small sample from the bulk aerosol for analysis -usually achieved by drawing it through a tube connected to the measurement system. The process is referred to as aspiration. The sampled particles are then transported from sampling inlet to the measurement instrument. The particles may be collected for future analysis, or may be analyzed in real-time (dynamic measurement). Each part of the process - aspiration, transportation and analysis - has the potential to introduce error into the measurement. An additional step – pre-classification - is sometimes added prior to collection or analysis to introduce an intentional bias. An example would be the removal of all particles larger than 10 μm in cases where only the mass of particles smaller than 10 μm is considered of relevance. The final quantity measured therefore has to be interpreted in the context of the influence of aspiration, transportation, pre-classification and analysis.

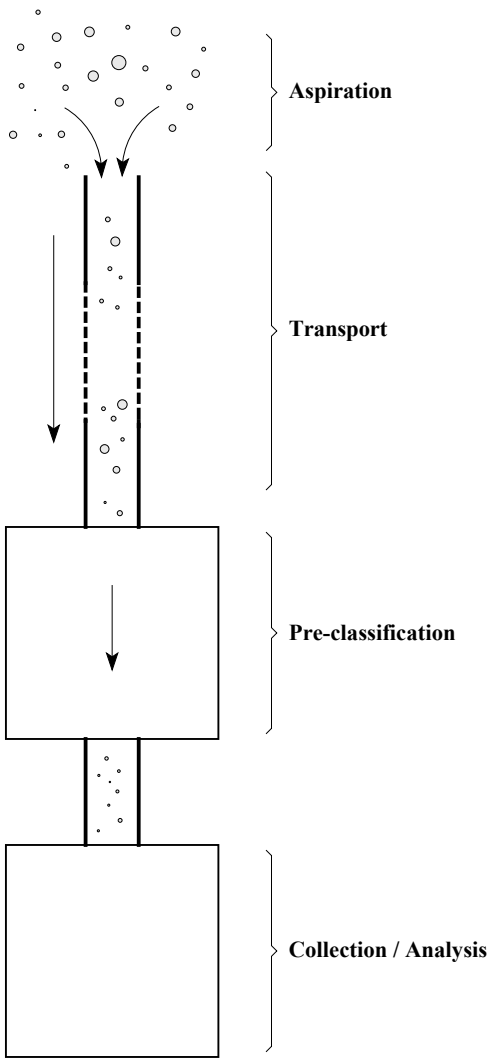

Fig. 6.2. Stages in the aerosol sampling process.

The aspiration, transport and pre-classification of aerosol particles are dominated by the probability of particles of a given diameter passing through each stage of the sampling process. If the aerosol remains well-mixed as it passes through the sampling system, *the probability of a particle of diameter d penetrating through the system is the product of the penetration probability through each leg of the system*. Thus if the penetration

probability (or penetration efficiency) of a particle being aspirated is $P_A(d)$, the probability of it being transported to the pre-classifier is $P_T(d)$, the probability of it passing the pre-classifier is $P_C(d)$, the overall penetration efficiency P is

$$P(d) = P_A(d) \times P_T(d) \times P_C(d) \qquad 6.1$$

Note that if there are several legs to the aerosol transport system, $P_T(d)$ will be the product of the penetration efficiency of each leg. To calculate how the measured quantity compares to the actual quantity in the aerosol, P needs to be multiplied by instrument response $T(d)$. Thus if the actual quantity to be measured is $\Gamma(d)$, what an instrument will measure is $\Gamma_M(d)$

$$\Gamma_M(d) = \Gamma(d) \times P(d) \times T(d) = \Gamma(d) \times P_A(d) \times P_T(d) \times P_C(d) \times T(d) \qquad 6.2$$

Γ may be any aerosol parameter, including mass and number concentration. Note that when a sample is collected for future analysis, $T(d)$ may be replaced by the sample collection efficiency – $E(d)$.

3. Aspiration

In most cases, the process of sampling an aerosol through a small inlet results in particles having to change direction to enter the opening. This can be seen most effectively by looking at the streamlines of a gas being sampled through an opening. If the gas velocity at the opening is greater or less than the gas velocity far away (the free stream velocity), the streamlines will have to diverge ($U > V$) or converge ($U < V$). Aerosol particles that follow the streamlines into the sampling precisely into the inlet will be aspirated with 100% efficiency (as the gas itself is). However, we know from looking at particle motion that not all particles will be able to follow the change in direction. Particles with high inertia (large Stokes number) will diverge substantially from the streamlines. Where the streamlines diverge ($U > V$), this will result in more particles entering then inlet than the

streamlines would dictate - aspiration efficiency will be greater than 100%. Where the streamlines converge ($U < V$), not all particles will be able to make it into the inlet, and aspiration efficiency will be less than 100%. It should be clear that for the special case where $U = V$, all particles will follow the streamlines into the inlet, and aspiration efficiency will be 100%. *This is referred to as isokinetic sampling, and is the most desirable way of sampling an aerosol*. Any other condition is referred to as *anisokinetic*, and will result in aspiration efficiency differing from 100% at high Stokes numbers.

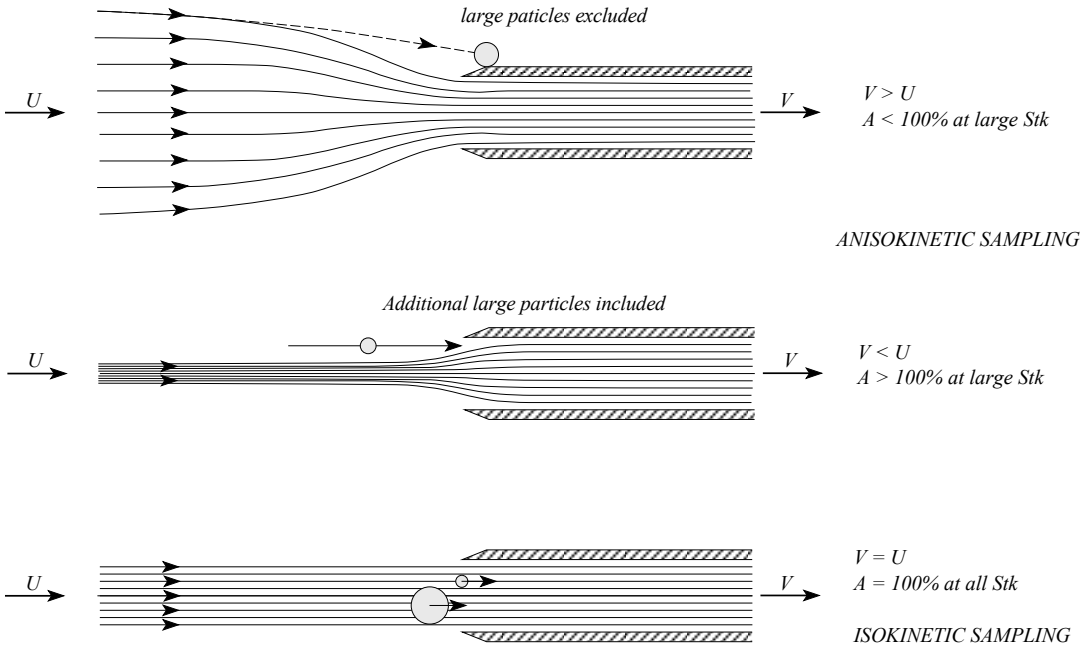

Fig. 6.3. Aspiration from an aerosol flow with velocity U.

A special case is when an aerosol is being sampled from calm air. Virtually all streamlines will curve as they enter the sampler, ensuring that it is impossible to sample 100% of all particles of all diameters from calm air. However it is possible to estimate at which diameters aspiration efficiency decreases significantly. C. N. Davies was the first to point out that two conditions must be met if all particles of a given diameter are to be sampled through a small inlet from calm air. The first condition states that the particles must have insufficient inertia to deviate significantly from the gas streamlines when

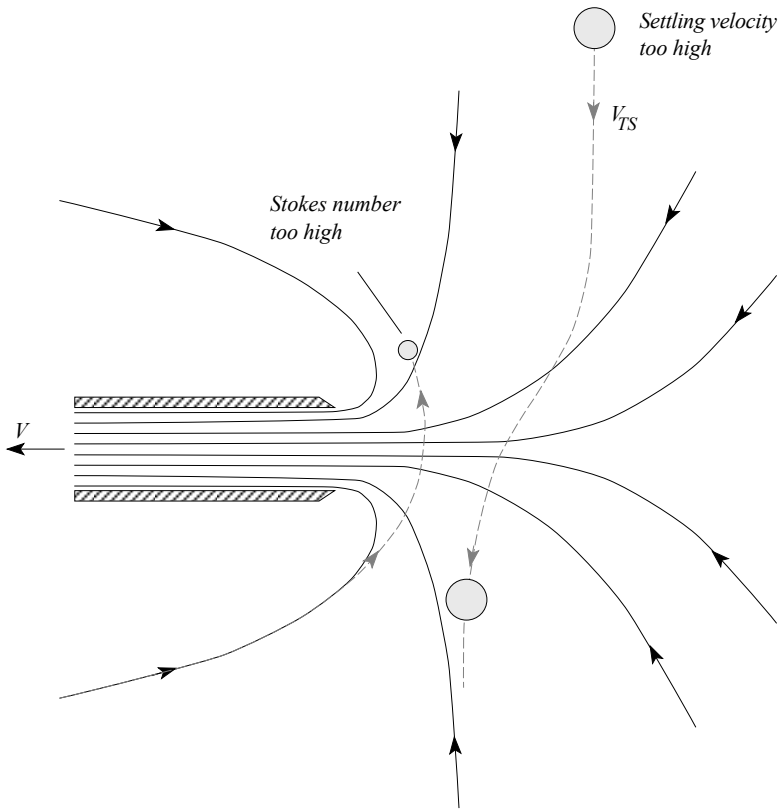

Fig. 6.4. Aerosol aspiration in calm air

being sampled. This is expressed by the particle Stokes number, using the average sampling velocity V and the inlet diameter D

$$Stk = \frac{\tau V}{D} \leq 0.016 \qquad 6.3$$

The second condition states that particle settling velocity must be sufficiently small that any effect of inlet orientation with respect to the direction of settling is insignificant. Davies calculated this to be the case when the ratio of settling velocity V_{TS} to sampling velocity is less than or equal to 0.04:

$$\frac{V_{TS}}{V} \leq 0.04 \qquad 6.4$$

Equations 6.3 and 6.4 together make up the Davies criteria for taking representative samples from calm air.

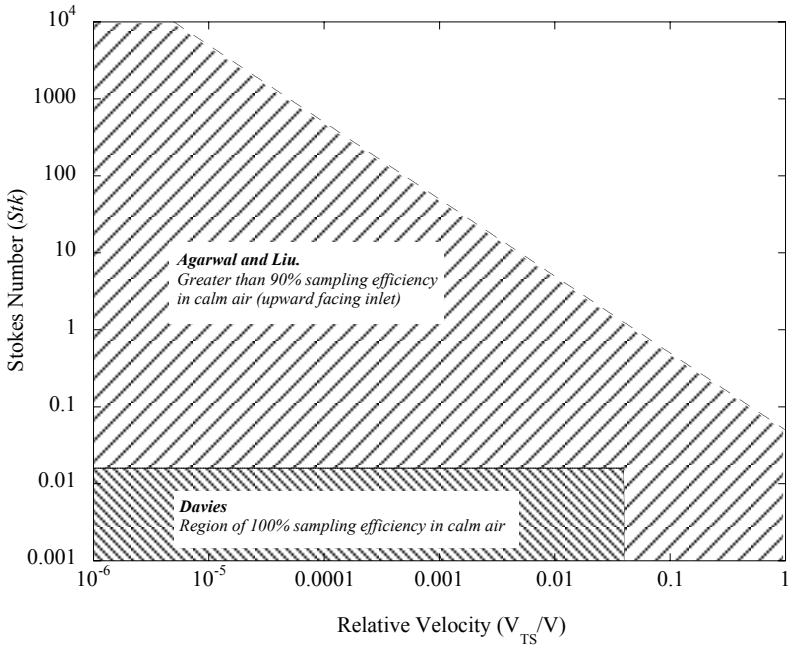

The Davies criteria is pretty restrictive when it comes to practical sampling. A more relaxed criteria that is widely used was formulated by Agarwal and Liu from theoretical predictions. The Agarwal-Liu criteria (based on an upward-facing inlet), follows similar arguments to the Davies criteria, and gives the conditions that should lead to an aspiration efficiency of 95% or higher:

$$Stk\frac{V_{TS}}{V} \le 0.05 \qquad 6.5$$

or

$$V_{TS}\frac{\tau}{d} \le 0.05 \qquad 6.6$$

4. Transport.

All mechanisms leading to particle movement discussed in previous lectures may lead to particles being deposited in an aerosol transport system, and thus not penetrating with 100% efficiency. The main mechanisms are shown in fig. 6.6.

Electrostatic deposition occurs predominantly when particles are charged, and the system they are being transported through is electrostatically charged. Losses may be significant when sampling using non-conductive tubing or samplers, and the use of materials that tend to accumulate a high electrostatic charge (e.g. Teflon) should be avoided. Electrostatic losses may often be minimized by 'neutralizing' the aerosol prior to sampling, using a bipolar ion source such as a corona neutralizer or a radioactive source (e.g. polonium 210). Charged particles may also deposit electrostatically within conducting tubing (the image charge effect). Although the use of a conductor eliminates electric fields arising from a buildup of electrostatic charge, a charged particle will induce a charge of opposite polarity in the wall of the conductor (an image charge), and be attracted to it.

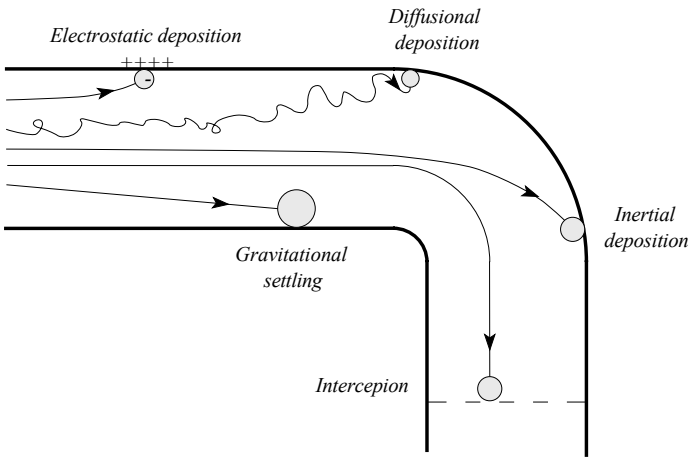

Fig. 6.6. The five main deposition mechanisms encountered when transporting aerosols

Diffusion losses dominate at very small particle diameters, as Brownian motion leads to diffusive deposition velocity exceeding gravitational settling

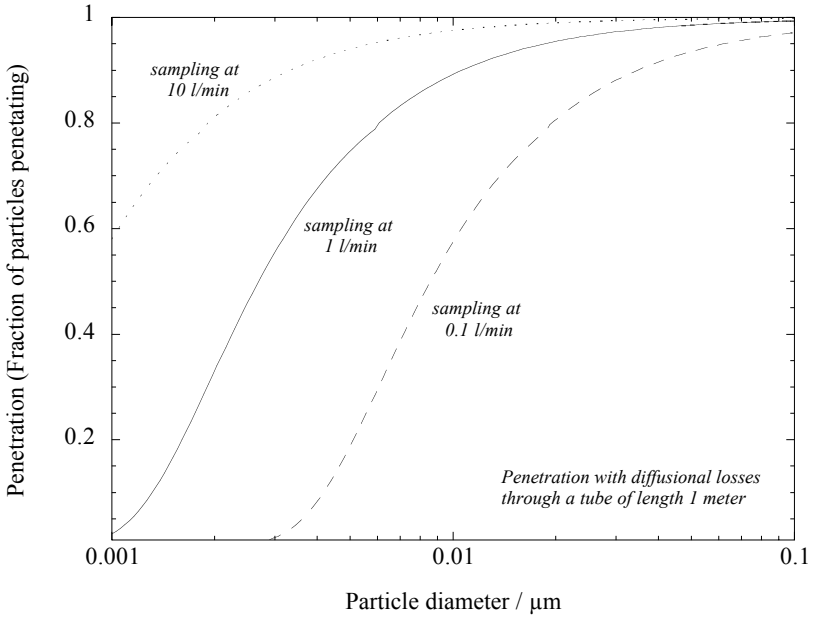

Fig. 6.7. Aerosol penetration through a tube with diffusional deposition losses.

velocity, and in many cases electrostatic deposition velocity. For particles smaller than 20 nm, diffusive deposition is the most significant source of particle losses in most cases. For the relatively simple case of laminar flow through a circular cross-section tube, penetration P as a function of particle diameter is approximated by an expression developed by Gormley and Kennedy in 1949

$$P = \frac{n_{in}}{n_{out}} = 1 - 5.5\mu^{\frac{2}{3}} + 3.77\mu \text{ for } \mu < 0.009 \quad 6.7$$

$$P = 0.819e^{-11.5\mu} + 0.0975e^{-70.1\mu} \text{ for } \mu \geq 0.009 \quad 6.8$$

where μ is the dimensionless deposition parameter

$$\mu = \frac{DL}{Q} \quad 6.9$$

D is the diffusion coefficient, L the length of tube and Q the flow rate (in m/s). Note that for a given particle diameter (and thus diffusion coefficient), penetration can only be increased by decreasing L, or increasing Q . ***Tube diameter does not influence deposition***.

Gravitational settling becomes significant at large particle diameters when long lengths of horizontal tubing are used to transport the aerosol. Losses can be estimated using particle settling velocity and the tube diameter, assuming laminar flow (no aerosol mixing) and plug flow (flow through all parts of the tube is moving at the average flow velocity U). If a particle is settling with a velocity V_{TS}, it will settle a distance $V_{TS} \times t$ in time t. It will also travel a horizontal distance $U \times t$ in the same time. All particles closer to the bottom of the tube than distance $V_{TS} \times t$ will

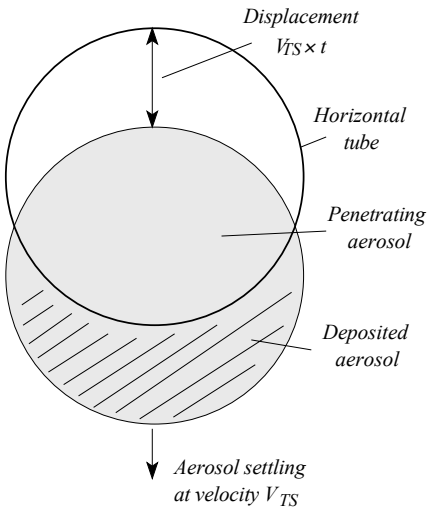

Fig. 6.8. Simplified aerosol settling in a horizontal tube with laminar flow.

deposit out over tube distance $U \times t$. Total deposition will occur when $V_{TS} \times t$ is equal to the tube diameter D_T. For a given length of tube L, the time taken for the flow to pass along it is

$$t = \frac{L}{U} \qquad 6.10$$

The time required for total deposition (t_{td}) is given by

$$V_{TS} \times t_{td} = D_T \text{ therefore } t_{td} = \frac{D_T}{V_{TS}} \qquad 6.11, 6.12$$

and thus from 6.10 and 6.12, the tube length leading to total deposition (L_{td}) is

$$L_{td} = \frac{U}{V_{TS}} D_T \qquad 6.13$$

Re-arranging equation 6.13 allows the particle diameter (d_{crit})to be estimated that will have zero penetration through a tube of length L_{td}.

$$L_{td} = \frac{U}{V_{TS}} D_T = \frac{18\eta}{\rho_p d_{crit}^2 g} U D_T \text{ therefore } d_{crit} = \sqrt{\frac{18\eta 4Q}{L_{td}\rho_p g \pi D_T}} \qquad 6.14$$

(replacing the average flow velocity with $\frac{4Q}{\pi D_T^2}$). The particle diameter at which penetration reduces to zero is therefore a function if $Q/D_T L$ – as a first approximation reducing both L and D_T and increasing Q will lead to an increase in penetration.

Gravity-dominated penetration in a horizontal circular cross-section tube before total deposition occurs can be understood by visualizing the aerosol settling within the tube as a circle of aerosol particles overlaying the tube's cross-section, but moving with respect to it with a velocity of V_{TS}. At time t, the centers of the two circles would be a distance $V_{TS} \times t$ apart, with some of the aerosol remaining within the tube's cross-section, and

some lying outside it. If it is assumed that the region where the two circles intersect represents aerosol particles that haven't deposited out of the flow, (relatively) simple geometry may be used to calculate the fraction of particles remaining after a time *t*, and

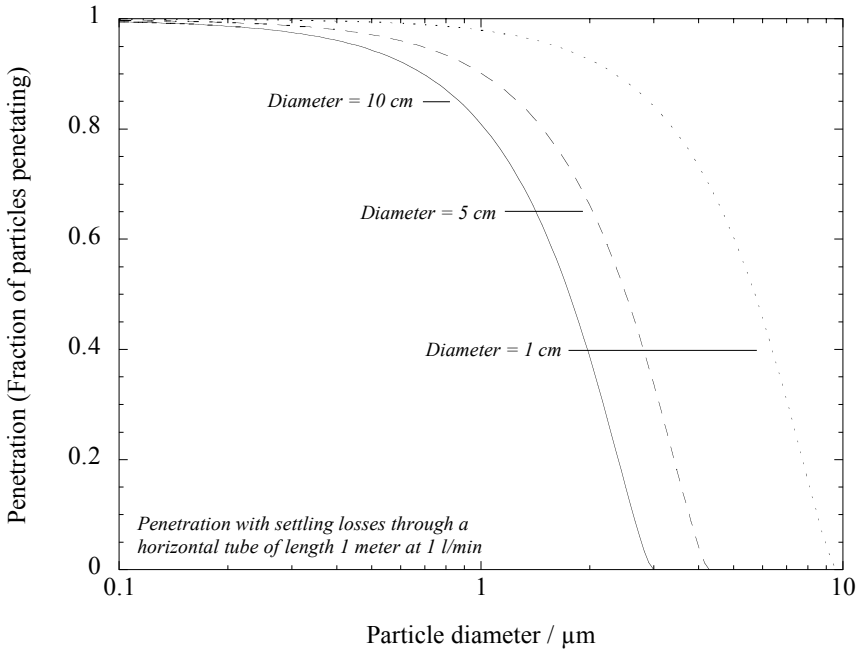

Fig. 6.9. Penetration through a horizontal tube with gravitational settling

thus the penetration efficiency of particles as a function of diameter. If these calculations are carried through, and expression approximating the penetration through the tube is arrived at. A more accurate analysis taking into account the parabolic flow velocity profile within the tube gives

$$P = 1 - \frac{2}{\pi}\left(2k_1k_2 - k_1^{\frac{1}{3}}k_2 + \arcsin\left(k_1^{\frac{1}{3}}\right)\right) \qquad 6.15$$

where

$$k_1 = \frac{3LV_{TS}}{4D_TU}Cos\theta \text{ and } k_2 = \left(1 - k_1^{\frac{2}{3}}\right)^{\frac{1}{2}} \qquad 6.16$$

θ is the inclination of the tube from the horizontal, and arcsin(θ) is in radians.

Inertial losses occur when particles with high inertia are required to follow rapidly changing flow conditions – such as flow around a bend, or flow through a narrowing tube. Recall that a particles Stokes number provides an indication of whether a particle's inertia is sufficiently small for it to follow the streamlines, or large enough to lead to little or no conformity to the changing flow pattern. Thus particles with very small *Stk* would be expected to have a high penetration efficiency through a convoluted flow system, and particles with a high *Stk* would be expected to deposit out of the aerosol rapidly. Flow around bends is particularly important for industrial hygiene sampling, where it is often difficult to avoid them in sampling tubing. For laminar flow, the penetration efficiency around a bend of ϕ radians may be estimated using the empirical expression

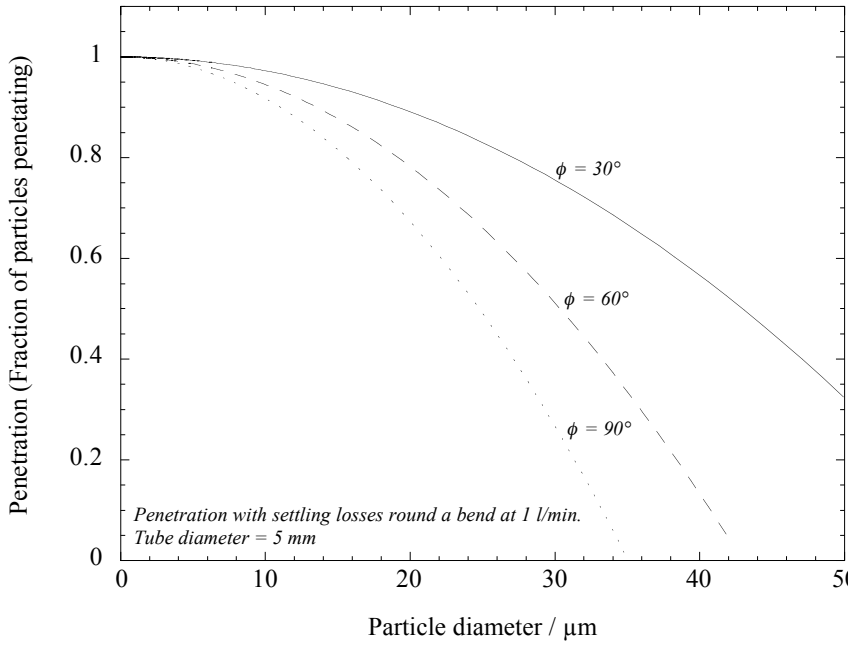

Fig. 6.10. Aerosol penetration round a bend (circular tubing)

$$P = 1 - \phi Stk \qquad 6.17$$

where

$$Stk = \frac{\tau U}{D_T} \qquad 6.18$$

U is the average flow velocity of the aerosol.

5. Pre-classification

There are a number of reasons why particles above (or below) a certain size may need to be excluded from a aerosol sampler. In some cases pre-classification is used to remove particles that may interfere with the response of an instrument. In some particle sizing instruments, narrow ranges of particle diameters are selectively sampled (either in parallel or in series) to allow measurements of particle size distributions to be made. However the overriding reason for using pre-classifiers within occupational and environmental hygiene is to restrict aerosol measurements to particles that are likely to be harmful to health. As we shall see later, the toxicity of many aerosol particles is associated with where they deposit in the respiratory system. As this is highly dependant on particle size, exposure measurements need to be targeted to similar size ranges to avoid unrepresentative samples arising from the presence of unwanted particles. As an example, inhaled particles that reach the deep lung (alveolar region) are typically smaller than 5 μm in diameter. If a mass-based sample of particles that would reach this region contained 1% by ***number*** of 50 μm particles, they would represent over 90% of the ***mass*** (particles smaller than 5 μm would represent less than 10% of the sample mass), and the sample would not reflect the harmfulness of the exposure to the recipient. Thus sampling bias without the use of pre-classification can be highly significant.

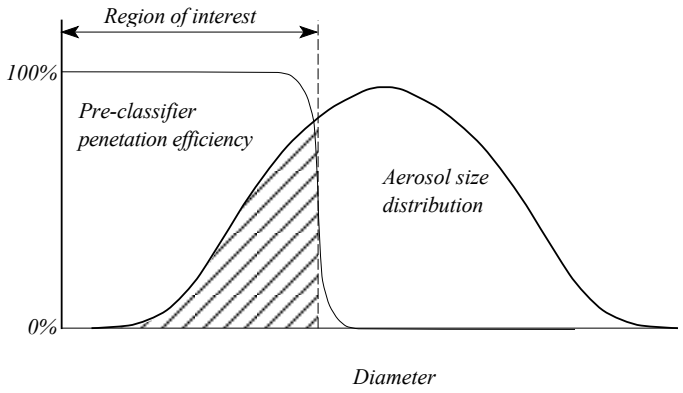

Fig. 6.11. Pre-classification – selecting the aerosol particles of interest

Most pre-classifiers are designed to remove particles a few tenths of a μm and greater in diameter from an aerosol, and tend to rely on inertial separation of the particles. Five families of pre-classifier are of particular interest from an industrial and environmental hygiene sampling perspective: impactors, cyclones, elutriators, aerosol centrifuges and porous foams.

Impactors

Inertial impactors are perhaps the most versatile, and most widely used aerosol pre-classifiers. The basic concept of operation is simple – aerosol flowing through a narrow nozzle is forced through a sharp 90° change in flow direction. Particles with high Stokes

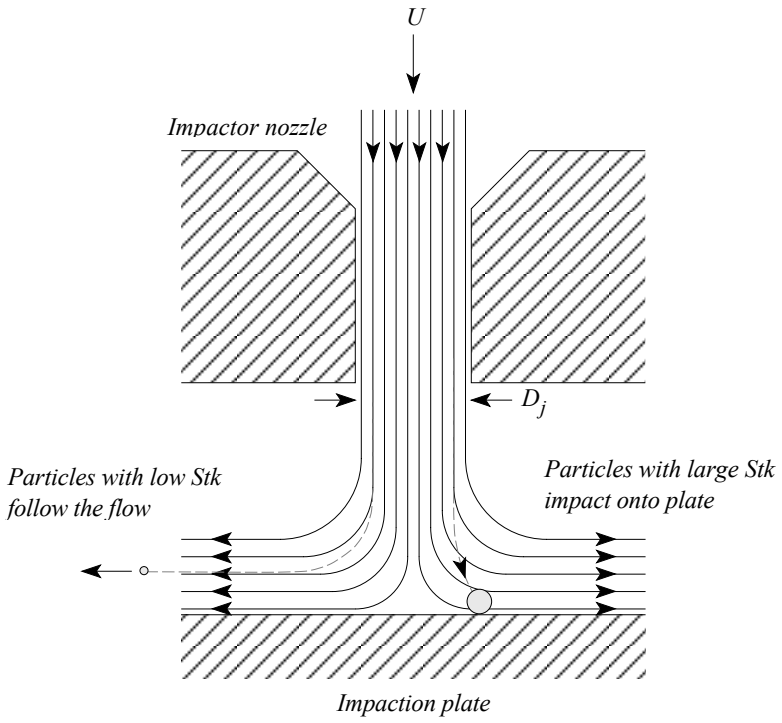

Fig. 6.12. Schematic of an inertial impactor

numbers have too great an inertia to follow the flow, and deposit or 'impact' on the impaction plate directly below the nozzle. Particle penetration may be defined in terms of *Stk*, given by

$$Stk = \frac{\tau U}{D_j/2} \qquad 6.19$$

U is the mean aerosol velocity in the nozzle, and D_j is the nozzle diameter. At a first glance it may seem sensible to use the nozzle to plate distance as the characteristic length when determining *Stk*. However in practice this distance has relatively little influence on the flow pattern within the impactor.

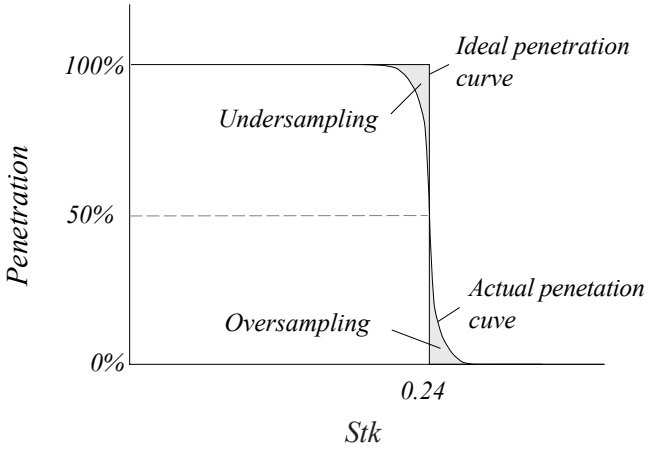

Fig. 6.13. Penetration through a circular jet impactor.

Particles with a Stokes number of Stk_{50} have a 50% probability of passing through the impactor (50% penetration efficiency). In a well designed impactor the penetration curve about Stk_{50} is relatively sharp, and as a first approximation it may be assumed that $Stk < Stk_{50}$ have 100% penetration efficiency, and those with $Stk > Stk_{50}$ have 0% penetration. In practice there is a finite transition region. The recommended design criteria for an impactor that gives a sharp cut are as follows: The Reynolds number of the gas flow within the nozzle should be between 500 and 3000. The ratio of the distance between the nozzle and the impaction plate to the jet diameter (or width) should be between 1 and 5 for circular nozzles, and between 1.5 and 5 for rectangular nozzles (lower values are better). Impactors following these criteria will have a Stk_{50} of 0.24 for circular jets, or 0.59 for rectangular jets. The diameter corresponding to 50% penetration efficiency (the cut-point, or d_{50}) is given by evaluating Stk_{50} for a given geometry and flow velocity. Note that d_{50} is dependent on U, and thus flow rate Q.

Note that as inertial impaction is an aerodynamic process, it is governed by particle ***aerodynamic diameter***.

The relatively sharp penetration curve of inertial impactors is useful where a sharp distinction needs to be made between particle sizes entering an aerosol sampler, and those excluded. For instance, the current PM2.5 sampler used for environmental aerosol sampling was designed to exclude all particles larger than 2.5 μm, but to allow all particles smaller than this to be sampled. The sharpness of the penetration curve also lends itself to cascading impactors with different cut points to measure aerosol mass concentration within discrete size ranges. The result is a Cascade Impactor. Each impaction stage collects deposits of particles that are larger than that stage's 50% penetration diameter (cut-point), but smaller than the cut-points of all the preceding stages. Thus each stage acts as a sampling bin, retaining the aerosol mass of particles between the diameters of the collection stage, and the preceding stage. The aerosol deposit on each stage is analyzed by weighing the deposit, or by applying a specific chemical analysis. Note that in this case the impactors are used as pre-classifiers AND collection devices.

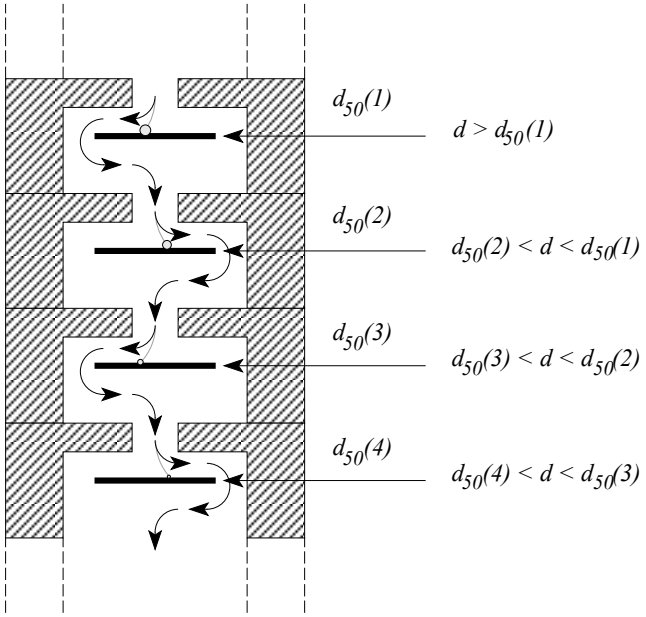

Fig. 6.14. Schematic of a cascade impactor

Although they are widely used, impactors suffer from a number of limitations.

- The high deposition forces involved may lead to solid particles bouncing rather than depositing.
- As deposition occurs below a narrow nozzle, overloading can occur rapidly.

- Under normal atmospheric conditions it is difficult to impart sufficient inertia to particles to enable particles much smaller than 0.2 – 0.5 μm in diameter to be collected.

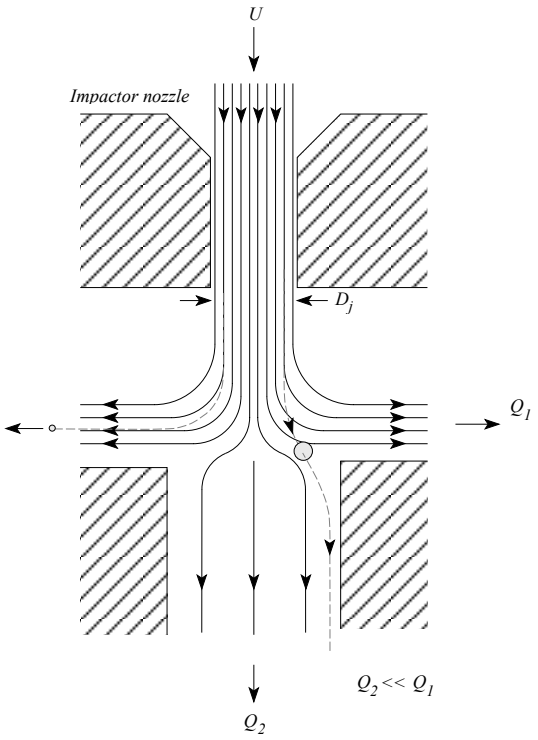

Fig. 6.15. Virtual impactor

In most impactors the impaction substrate is greased to inhibit particle bounce. Overloading is reduced by using impactors with a number of parallel nozzles leading to a single impaction surface (multi-orifice impactors). Particles smaller than 0.2 μm may be collected by impaction by using very narrow orifices that are chemically etched into an orifice plate. These micro-orifices may be as narrow as 50 μm, and are capable of reducing the achievable cut-point to around 0.06 μm. An alternative approach is to increase the apparent aerodynamic diameter of the particles. Recalling the equation defining aerodynamic diameter, this may be achieved by increasing the slip coefficient, which in turn depends on the mean free path of the suspension gas. Reducing gas pressure increases C_s, and thus apparent aerodynamic diameter, thus allowing impaction to operate successfully down to less than 50 nm. Impactors using this approach are termed Low Pressure impactors.

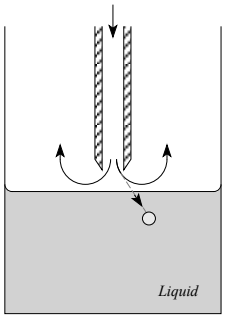

Fig. 6.16. Schematic representation of an impinger. Note that the nozzle is usually under the liquid surface

Other configurations of the impaction principle are found in regular use. Virtual impactors replace the impaction surface with a void , and a small secondary flow leading off it. Particles that would have impacted are entrained in the secondary flow, thus effectively splitting the aerosol into two

size-fractions. Complete separation is seldom possible however as a small portion of the smaller particles will be entrained in the secondary flow in most configurations.

Liquid impingers replace the solid impaction surface with a liquid. Using this approach particle bounce is eliminated, and particles may be delivered directly to an analysis reagent. However the liquid substrate also makes handling impingers more difficult than conventional impactors.

Cyclones

If a rotation is induced in an aerosol flow, the forces keeping the gas rotating will be insufficient to contain massive aerosol particles, and the particles will literally be flung from the flow by centrifugal force. The mechanisms are essentially the same as for impaction – particles with high *Stk* can not conform to the changing flow direction, and preferentially deposit out of the flow. Cyclones use this property by inducing rotational or cyclonic flow into the aerosol. Large particles deposit out on the side of the cyclone. Small particles remain entrained in the flow, and pass through the pre-classifier. The concept is simple, and with the right configuration allows the removal of large quantities of particles without significant overloading. For instance cyclones are often used to remove particles from gas flows in industrial processes. However the process isn't as simple to quantify as inertial impaction due to the complexity of flows within practical cyclones, and doesn't tend to lead to the same

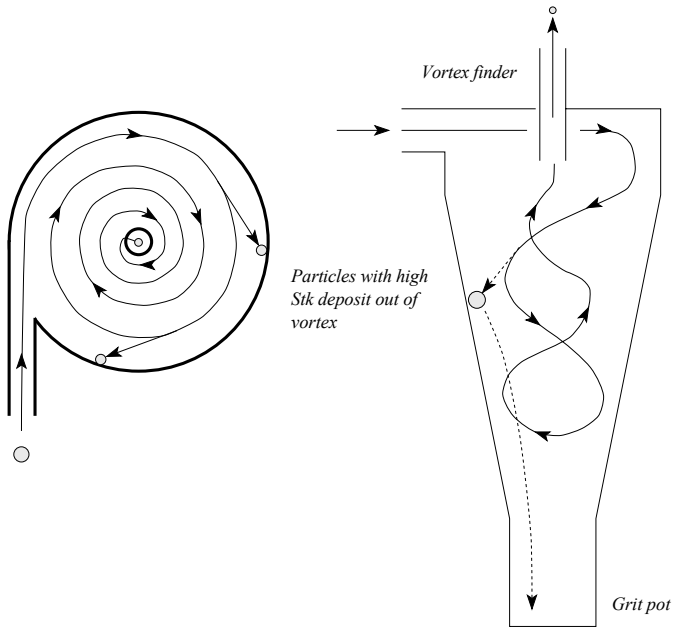

Fig. 6.17. Tangential flow cyclone

degree of sharpness in the penetration curve (although sharp-cut cyclones are now available). As a result, most cyclones are designed semi-empirically, and are used where a sharp penetration curve isn't essential. As for impactors, d_{50} is dependent on particle Stokes number and thus sampling flow rate. Interestingly, the curve defining particle penetration into the respiratory system is not sharp either, and is better represented by a cyclone than an impactor.

Most cyclone aerosol pre-separators are designed with a tangential flow geometry, although a number of flow geometries are possible. Aerosol enters a tangential cyclone at a tangent to a conical chamber, where the flow is forced to revolve in increasingly smaller circles until it leaves via the vortex finder at the center of the chamber. Particles larger than the 50% cut-point deposit on the cyclone walls, and migrate to the grit pot at the base of the cyclone. Tangential flow cyclones are used widely due to their simple geometry. The most widely used device for pre-classifying respirable dust (that capable of reaching the alveolar region of the lungs) in the US is the Dorr-Oliver or Nylon cyclone. In Europe the Higgins and Dewell tangential cyclone is used extensively as a respirable dust pre-classifier. Note that although attempts have been made to cascade tangential cyclones, they are not ideally suited to the purpose. 90° bends are necessary between the subsequent stages, leading to potentially large particle losses, and the penetration curves tend to be insufficiently sharp to prevent interference between adjacent cyclones. It is also not particularly easy to remove the deposit from within a cyclone for analysis.

Elutriators

Elutriators distinguish between particles with different settling velocities (hence differentiate with respect to particle aerodynamic diameter), and are perhaps the simplest form of pre-classifier. If an aerosol is flowing vertically upwards with an average velocity U, particles with a settling velocity V_{TS}

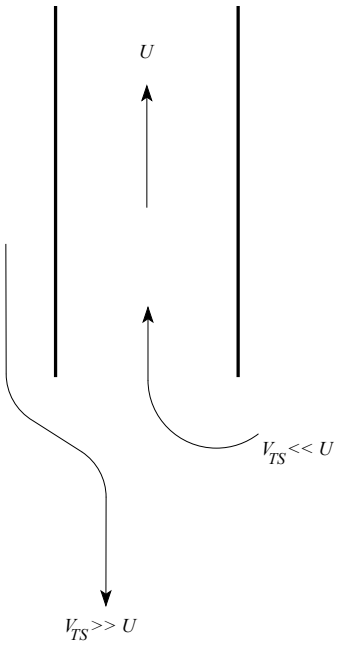

Fig. 6.18. Schematic of a vertical elutriator

greater than U will be unable to follow the flow, and will settle out. The use of a vertical aerosol flow – vertical elutriation – is therefore an effective way of removing particles greater than a given aerodynamic diameter from an aerosol. V_{TS} is given by

$$V_{TS} = \frac{\rho_0 d_{ae}^2 g}{18\eta} \qquad 6.20$$

(Notes 2), and so the aerodynamic diameter leading to 0% penetration efficiency may be found by equating equation 6.20 to the average flow velocity U, giving

$$d_{ae}(0\%) = \sqrt{\frac{18\eta U}{\rho_0 g}} \qquad 6.21$$

Note that this expression only gives an approximation of the cut-point in a vertical tube (for instance), as the actual flow velocity will be parabolic. There will be regions where the air velocity is lower than U, thus allowing particles of diameter $d_{ae}(0\%)$ to pass through the pre-classifier. Vertical elutriation is employed in a static sampler used for sampling cotton dust. The sampler is designed to collect particles able to penetrate to the thoracic region of the respiratory system (below the larynx), and uses a vertical elutriator to exclude particles larger than 10 μm from the sample.

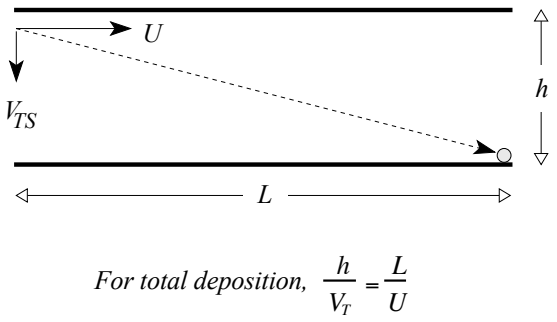

Fig. 6.19. Horizontal elutriation

A form of elutriator in more widespread use is the horizontal elutriator. Aerosol is passed through a horizontal channel (usually rectangular in cross-section), and unwanted particles are removed through gravitational settling. The conditions for total deposition are the same as for a horizontal tube, with tube diameter D_T replaced by the channel height h (see equation 6.14). Note that an effective method is decreasing the critical particle size for which total deposition occurs is to introduce a

series of evenly spaced plates into the elutriator. The effective distance particles need to settle for total deposition is now reduced to the channel height divided by the number of plates:

$$h_{effective} = \frac{h}{N} \qquad 6.22$$

where N is the number of parallel plates.

Horizontal elutriation does not give a sharp decrease in penetration with respect to particle size due to the finite distance particles at the top of the channel need to travel before depositing. An approximation of particle penetration as a function of aerodynamic diameter through a rectangular cross-section horizontal elutriator can be made by assuming plug flow (all air moving at the same average velocity U), and assuming all particles of diameter d are displaced vertically by the same distance $V_{TS} \times t$ in time t. The approach is the same as was used for the circular tube, although in this case the geometry is much easier to deal with.

In a rectangular channel of width w and height h, we can assume (as a rough approximation) that the aerosol retains the overall shape of the cross-sectional area, but is displaced a distance $V_{TS} \times t$ in time t. It is assumed that all aerosol particles in the aerosol rectangle lying outside the channel cross-section are deposited on the channel walls. The fraction of particles penetrating is then given by the intersecting area of the two rectangles divided by the channel area

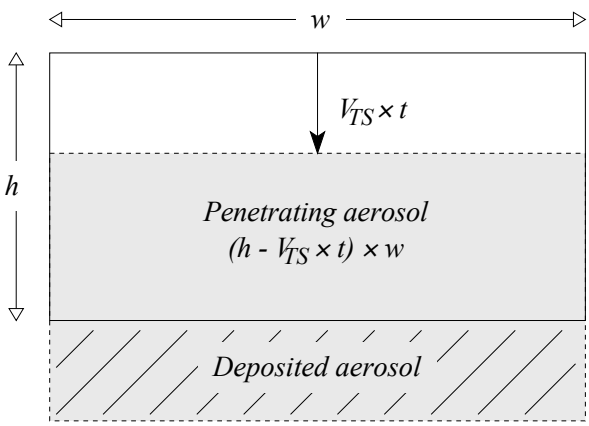

Fig. 6.20. estimating horizontal elutriator penetration efficiency

$$P = \frac{(h - V_{TS}t)w}{wh} = 1 - \frac{V_{TS}t}{h} \qquad 6.23$$

Time t is simply given by the length of the elutriator L divided by the mean flow velocity U. Re-writing equation 6.23 substituting for t and expanding the term for V_{TS} in terms of aerodynamic diameter gives

$$P = 1 - \frac{\rho_0 g L C_s}{18\eta U h} d_{ae}^2 \qquad 6.24$$

With the right parameters, this expression can approximate the function giving the probability of particles reaching the alveolar region of the lung reasonably, and for many years horizontal elutriation has formed the basis of respirable pre-classification when taking industrial hygiene dust samples underground.

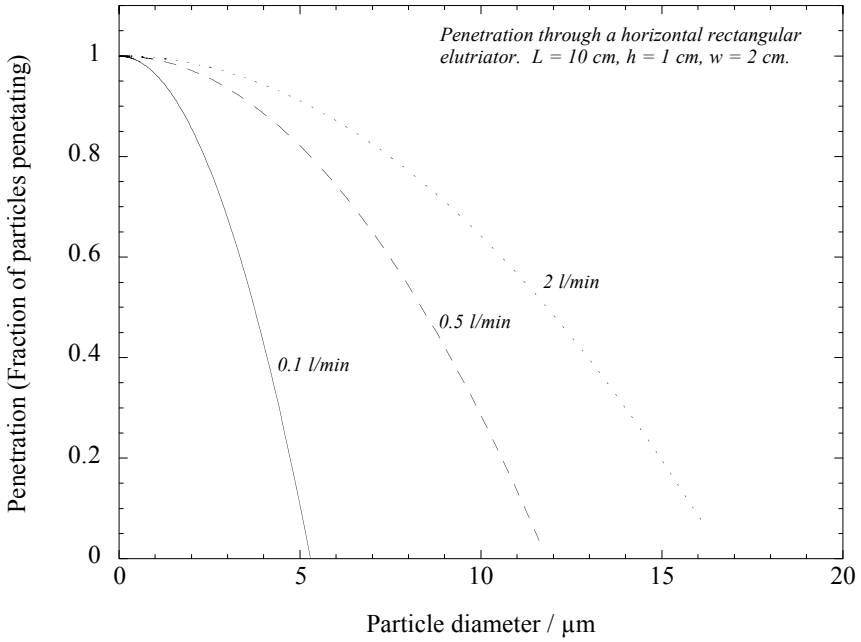

Fig. 6.21. Plotting estimated horizontal elutriator penetration as a function of particle aerodynamic diameter

Aerosol Centrifuge

While gravity provides a convenient force for pre-classifying aerosols, it is somewhat weak, and is dependant on the orientation of the pre-classifier. In many ways centrifugal force is similar to gravity, with the exception that it can be controlled. If an aerosol is passed along a circular path, such as round a coil of tubing, particles will experience a centrifigal force towards the outer surface of the tube. Particle terminal velocity is given by particle mechanical mobility B times the centrifugal force. The expressions above for calculating penetration through horizontal tubes and channels due to gravitational settling can therefore be easily adapted by replacing settling velocity with terminal velocity under the applied force, and length of horizontal tube or channel L with the length of the coiled tube or channel (still L for convenience). For a coil of constant radius R, the channel length is given by

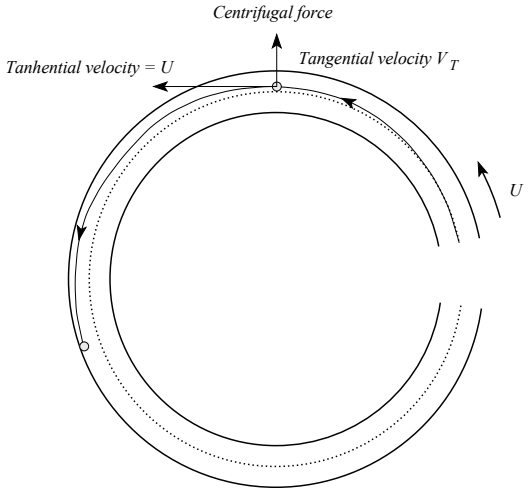

Fig. 6.22. centrifugal aerosol pre-separation

$$L = 2\pi Rn \qquad 6.25$$

where n is the number of revolutions in the coil (n may be a fractional number of revolutions).

Centrifugal force is given by

$$F_c = m\frac{U^2}{R} \qquad 6.26$$

where m is the particle's mass, and U the tangential particle velocity, which in this case is the same as the mean air velocity. Thus in a rectangular channel of width w and height h

that has a constant radius of curvature R and is coiled around n times, penetration may be estimated by

$$P = 1 - \frac{\rho_0 2\pi n U C_s}{18\eta} d_{ae}^2 \qquad 6.27$$

(using equation 6.24. Note that L is replaced with equation 6.25, and g is replaced by the centrifugal acceleration – U^2/R). Note that there is no dependence on the radius of curvature, and that now penetration is proportional to U, whereas for horizontal elutriation it was inversely proportional to U. This expression is only approximate, and depends on the flow Reynolds number being small enough to ensure laminar flow.

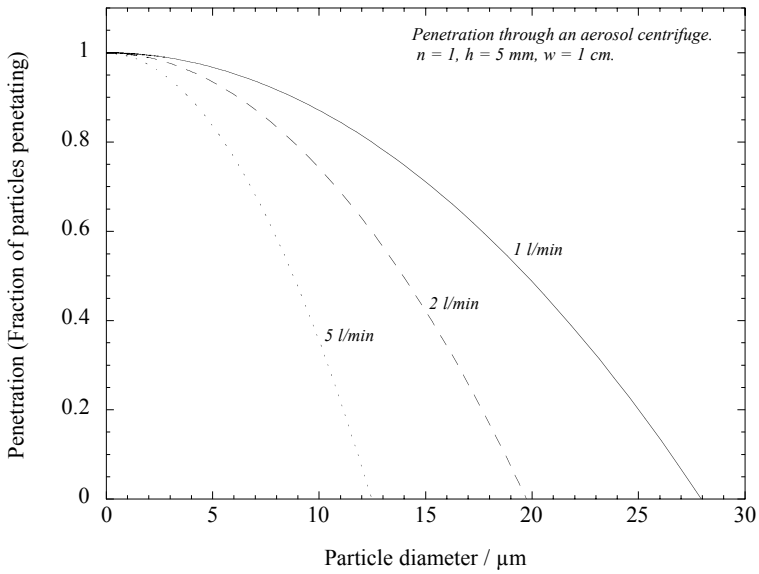

Fig. 6.23. Aerosol centrifuge penetration

Porous Polyurethane Foams

Porous polyurethane foam is finding increasing use as an aerosol pre-classifier within instrumentation, and is worthy of a brief mention here. The foam has an open pore structure allowing air to flow through it. As aerosol particles pass through the convoluted flow-paths between the pores, they deposit out through a

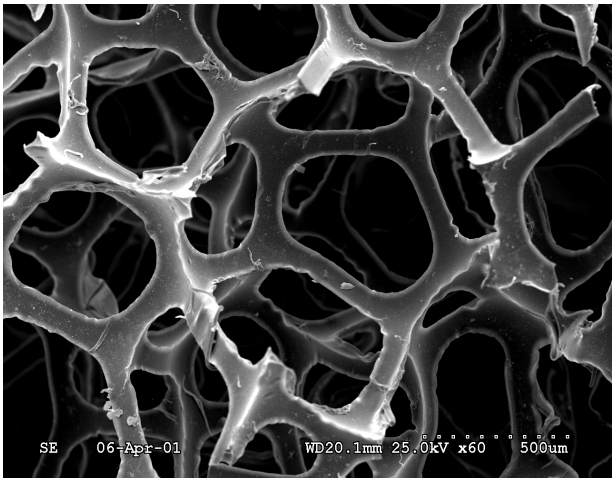

Fig. 6.24. Porous polyurethane foam (PUF)

combination of interception, impaction and gravitational settling – the foam acts as an inefficient filter in effect, capturing particles above a given diameter, and allowing particles smaller than this through. Although the deposition mechanisms are complex, an empirical expression has been developed that relates penetration to foam porosity and thickness, and the flow velocity at the face of a foam plug. The expression predicts that foam plugs of realistic dimensions are useable to separate out health-related particles from an aerosol for collection and analysis (the separated particles are those that penetrate through the foam), and in fact a number of aerosol samplers are now available that rely on porous foam pre-classifiers.

6. Sample Collection

Aerosol collection requires the aerosol particles to be removed from the gas suspension, and deposited onto a suitable substrate or into a suitable media. Whereas up to this point we have been interested in the probability of particles penetrating the sampling system, sample collection is concerned with the probability of particles depositing out of the aerosol – denoted by collection efficiency E. Note that the probability of deposition E is simply $1 - P$. Collection systems need to be matched to the particle sizes of interest – there is little point in using an impactor with a 10 μm cut-point to collect an aerosol sample if it is particles smaller than 5 μm that are of interest. Conversely a collection system capable of collecting particles from 100's of μm in diameter to 10's of nm may be unnecessarily sophisticated if only particles larger than 5 μm are of interest.

A second deciding factor when selecting a collection system is how it interfaces with the sample analysis to be used. Gravimetric analysis (weighing the sample) requires a collection substrate that has a stable weight. Chemical analysis requires a substrate that doesn't interfere with the analysis, and allows complete access to the deposited particles. Microscopy requires the particles to arranged uniformly on the surface of the deposition substrate.

Within these constraints there are many methods of collecting aerosol samples. Examination of a plot of deposition velocities with respect to particle diameter indicates how different deposition mechanisms may be used over different particle size ranges. For the smallest particles, diffusion becomes a dominant mechanism, although it is only effective over a relatively narrow size range. Thermophoresis (deposition in a temperature gradient) leads to an approximately constant deposition velocity below 100 nm in a uniform thermal gradient, and is an effective mechanism for sampling nanometer-diameter particles. Its great strength is that a uniform deposit of particles may be formed on a smooth substrate, making it ideal for collecting samples for electron microscopy. However above 100 nm it introduces too great a dependence on particle diameter for it to be of much use.

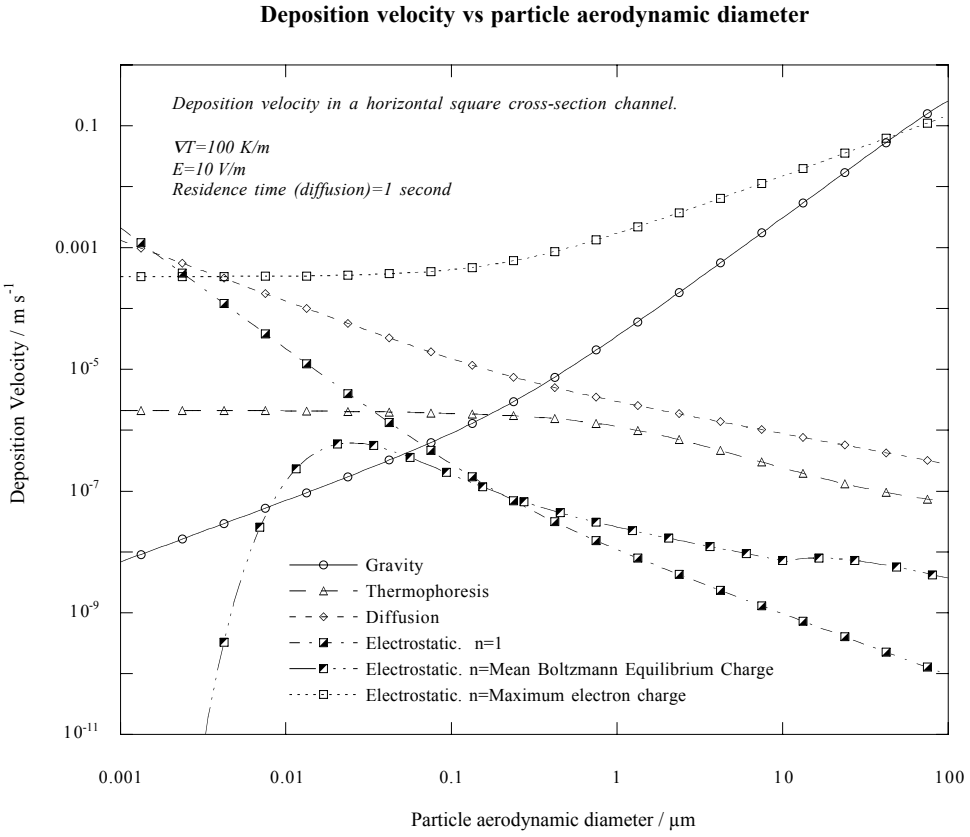

Fig. 6.25. Particle deposition velocity arising from various mechanisms.

Electrostatic precipitation leads to potentially high deposition velocities over a wide range of particle sizes. It is limited in its application to very small particles as below 20 nm it becomes increasingly difficult to charge particles. It is also somewhat difficult to predict deposition velocity (and hence collection efficiency) as a function of diameter, as it depends on how many elementary charges a particle is carrying. However as a sampling method it is effective if the electric field charging mechanism used are sufficient to lead to total deposition of all charged particles within the sampler. Using this approach it is possible to attain a deposition efficiency approaching 100% for particles greater than 20 nm in diameter. If a uniform electrostatic field is used, deposits can be uniform, and lend themselves to particle analysis using optical and electron microscopy. However the collection method is usually considered too cumbersome for sampling where mass-analysis alone is required.

Large particles may be collected effectively using gravitational settling. Using the expressions for penetration through a horizontal tube or channel, it can be seen that complete collection of particles above a critical diameter is possible. The approach is somewhat inconvenient to use in practice however, and is generally not used on a regular basis. An exception is the use of settling plates and receptacles for measuring surface deposits of very large aerosol particles in the environment.

Large particles are also effectively sampled using inertial methods, and we've already seen how inertial impaction may be used to collect particles above a given diameter.

The ideal aerosol sampler would have the ability to collect all particle sizes, from a few nm in diameter to 10's or 100's of μm in diameter. Looking at the plot of deposition velocities, this could only be achieved effectively if the sampler relied on a number of collection mechanisms. For small diameter particles diffusion is one of the most effective collection mechanisms – designing a sampler where the aerosol flowed across a large collection surface would lead to high collection efficiencies at small particle sizes. At large particle sizes inertial collection is highly effective – represented by gravitational settling on the plot. Recall that particles with high inertia can not conform well to flow

streamlines, and so designing a sampler with convoluted flow paths will lead to inertial collection for large particles. Following the argument through, designing a sampler that consisted of the aerosol flowing through narrow convolute channels (or around narrow random obstructions) would provide a high surface area for diffusional deposition, and lead to high particle Stokes numbers for inertial deposition. Such a sampler would be expected to effectively remove a wide range of particle sizes from an aerosol.

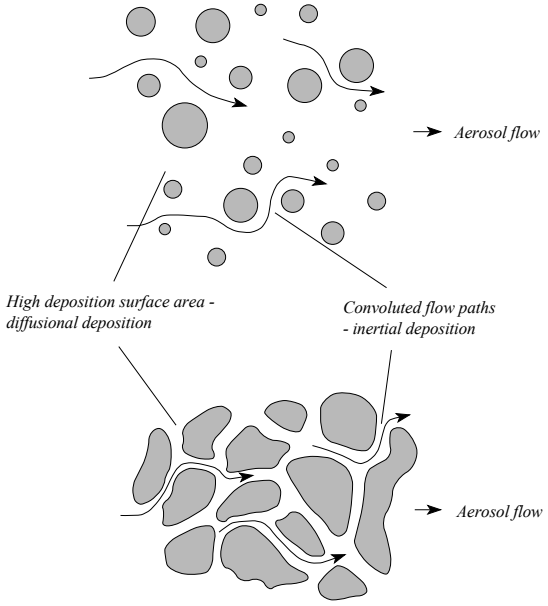

Fig. 6.26. Ideal collection arrangement for maximum collection efficiency

What we have just described is a ***filter*** – one of the most widely used forms of collecting aerosols. Filters are economical and effective for collecting aerosol samples. They are available in a wide range of forms and designs and performance characteristics.

Fibrous filters

Fibrous filters are probably what most people envisage when they think of a filter. The filter is composed of a woven mat of fibers. These may be held together with a binder material which may be as high as 10% of the filter material. However most aerosol sampling is carried out using binder-free filters, as the binder introduces a component that may potentially interfere with subsequent analysis of the aerosol.

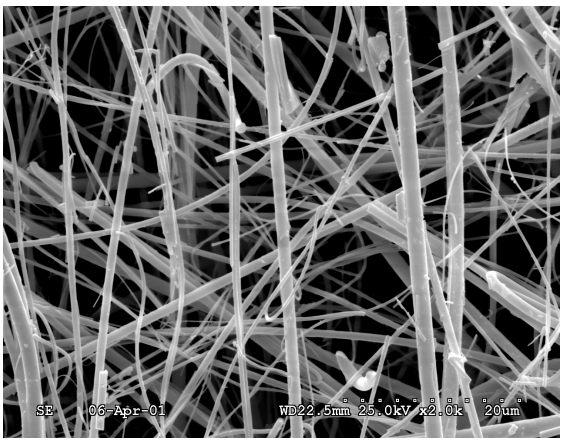

Fig. 6.27. Scanning electron micrograph of a fibrous filter

Fibers of a wide range of diameters are used (ranging from less than 1 μm to over 100 μm) – often in the same filter.

The theoretical sampling efficiency of a fibrous filter is usually approached by looking at the collection efficiency of a single fiber. As an aerosol particle flows around a filter fiber, two mechanisms will dominate its fate. If the particle is small enough to have significant Brownian motion, it stands a significant chance of diffusing to the surface of the fiber, and thus depositing out of the flow. If it has a high Stokes number (given by $\frac{\tau V}{D}$ where V is the particle velocity and D the fiber diameter), it also stands a good chance of impacting onto the surface of the fiber, and depositing out of the flow. Overall filter efficiency may then be estimated by considering the contribution each fiber makes to the sampling efficiency. A qualitative understanding of the resulting collection efficiency can be gained by adding typical deposition efficiency curves for diffusional and inertial deposition over a range of particle diameter. The results are similar to comparing diffusional and inertial deposition velocities. What is found is that while a fibrous filter may be highly efficient at collecting very small and very large particles, there is a region between typically 0.1 μm and 1 μm where collection efficiency is at a minimum. This form of the collection efficiency versus particle diameter is typical of many filter types (not just fibrous filters). The minimum generally falls close to 0.3 μm. It is usual therefore to test filter efficiency with particles of around this diameter (***the most penetrating particle size***), thus giving the minimum collection efficiency of a given filter.

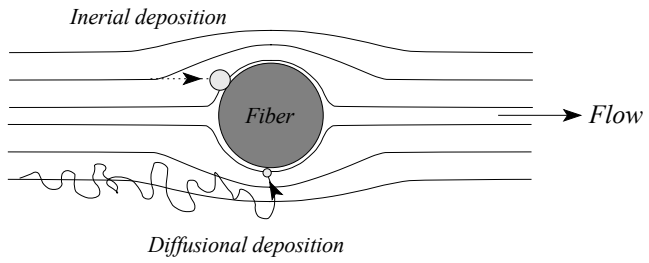

Fig. 6.28. Single fiber collection mechanisms

The qualitative plot of filter efficiency is pretty accurate when compared to real filters. ***Note that it depends only on diffusion and inertia, and NOT the size of the holes in the***

filter. There is a common mis-conception that air filters behave like a sieve, removing particles that are physically unable to pass through the holes. It is interesting to note that given a sufficient depth of filter material, a fibrous filter containing gaps between the fibers of several 100 μm would still exhibit similar characteristics to those plotted.

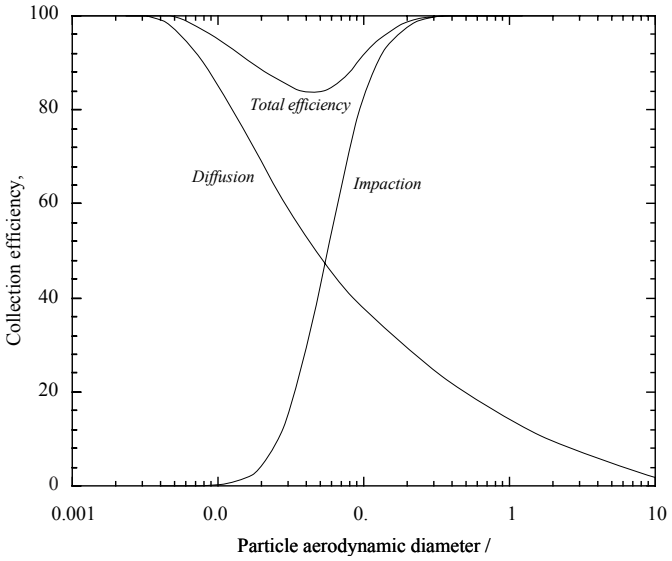

Fig. 6.29. Qualitative plot of filter collection efficiency

Note that fibrous filters are often termed depth filters as particles tend to deposit throughout the volume of the filter.

Membrane filters

Membrane filters are formed from colloidal solutions and have a complex structure that is visually very different from fibrous filters. However the dominant deposition mechanisms resulting from the tortuous path an aerosol has to follow through the membrane are still diffusion and inertial deposition, leading to the collection characteristics being very similar to fibrous filters. A variety of materials are used in their construction, including cellulose esters, polyvinyl chloride, Teflon and sintered

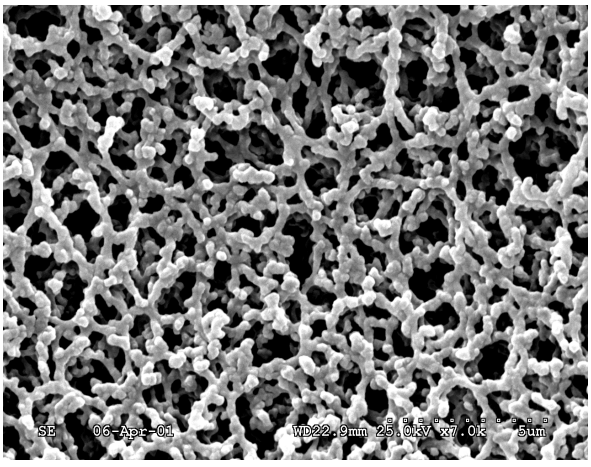

Fig. 6.30. Scanning electron micrograph of a membrane filter (Pore size: 0.3 μm).

metals. The filters are often specified by pore size. However pore size are defined from liquid filtration and often bears little or no resemblance to the size of the physical gaps in the filter structure. As in the case of fibrous filters, particle collection by interception isn't a dominant mechanism, and the mistake of equating pore size with the minimum particle size that will be collected should be avoided!

The dense structure of membrane filters leads to very high collection efficiencies, but also high pressure drops across them (significantly higher than typical fibrous filter pressure drops). Particles tend to be collected preferentially on the leading face of the filter (surface filtration), making them suitable for collecting samples that will be analyzed under the microscope.

Track-etched filters

Track-etched filters are a specialized subset of membrane filters. A non-porous polycarbonate membrane is bombarded with neutrons, and then etched. The etching process preferentially removes the membrane material along the tracks left by the neutrons, leaving an array of cylindrical pores leading through the membrane. Pore density is determined by the irradiation time, and pore diameter by the etching time. Track-etched filters were originally manufactured by the Nucleopore Corporation, and are still frequently referred to as Nucleopore filters.

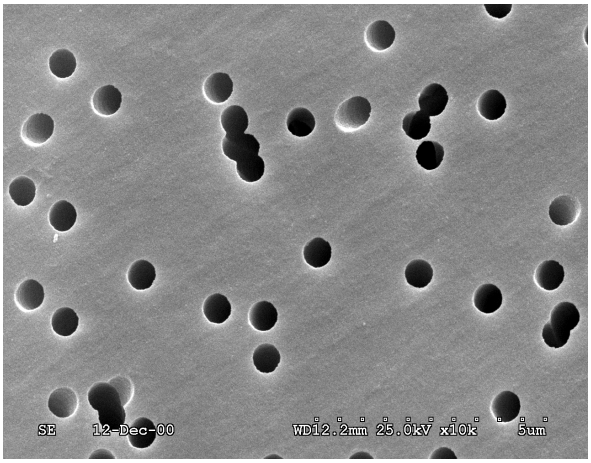

Fig. 6.31. Scanning electron micrograph of a track-etched filter (Pore size: 0.45 μm).

Although diffusion and inertial deposition still dominate collection onto these filters, the simple geometry of the pores leads to their collection characteristics differing somewhat from other filter media. Particles with a large diffusion coefficient will

diffuse to the sides of the pores as they pass through them, and the collection efficiency will depend on filter thickness (track-etched filters are usually only a few μm thick). Particles with high Stokes number with respect to the pore diameter will impact on the surface of the filter. Particles that are physically larger than the pores will also be intercepted, and in this respect track-etched filters come closest to the fallacious analogy with sieves. Track-etched filters therefore tend to have a much more significant region of low sampling efficiency than fibrous and standard membrane filters.

The smooth surface of track-etched filters makes them ideally suited to collecting samples for microscopy analysis, and this is predominantly where they are used. Particles that collect within the pores are lost to analysis in the microscope, and so as a rule of thumb filters with a pore size approaching the smallest particles of interest are selected for use.

7. Sample Analysis

The final step in characterizing an aerosol following sampling is the analyze the collected material. This may take one of two forms: bulk analysis, where all particles undergo the same analysis, and single-particle analysis, where the aerosol is characterized on a particle-by-particle basis.

Bulk analysis.

Once a bulk sample of aerosol particles has been collected, there is a complete battery of analytical procedures that can be applied to determine chemical composition. The majority of these are standard methods that are not specific to aerosols, and thus lie outside the scope of this course.

Where the composition of the aerosol is known prior to sampling (for instance if hardwood dust was being sampled), or is not important, simple gravimetric analysis is used to determine the aerosol mass concentration.

Gravimetric analysis

If an aerosol sampler is operated for time t at a flow rate Q, and an aerosol mass M is collected, the particulate mass per unit volume in the sampled aerosol (m) can be estimated from

$$m = \frac{M}{\text{Volume sampled}} = \frac{M}{Qt} \qquad 6.28$$

If the measured mass is on the stage of a cascade impactor, m refers to the mass concentration of particles *larger* than the impactor stages cut-point, but *smaller* than the cut-point of the preceding stage. Of course m needs to be interpreted in the light of aspiration, pre-classification and sample collection losses. In reality the actual mass concentration as a function of particle diameter is given by

$$m(d) = \frac{M(d)}{QT} \times A(d) \times P_T(d) \times P_c(d) \times E(e) \qquad 6.29$$

where A is aspiration efficiency, P_T is transport penetration efficiency, P_C is pre-classifier penetration efficiency and E is collection efficiency, all as a function of particle diameter d. In the case of filter collection there is no differentiation of M with diameter, and so no correction for these factors can be made. However if sampling is set up to ensure that A, P_T and E are close to 100%, resulting errors will be small. When a pre-classifier is used, the estimated mass concentration m is always referred to in relation to the pre-classification. For instance, *PM10* mass concentration – particulate matter mass concentration below 10 μm, *respirable* mass concentration – mass concentration of particles able to reach the alveolar region of the lungs.

Determining M is not difficult, but requires care. The standard practice is to pre-weigh the collection substrate, and them post-weigh it following collection – the difference in weights giving M. However some substrates, cellulose and cellulose ester filters in particular, are hygroscopic, and change weight with variations in relative humidity. Care

must be taken therefore to ensure that any substrate weight change that isn't associated with the aerosol is accounted for. This is commonly achieved by pre- and post-weighing a number of blank filters, and subtracting the mean weight gain or loss from the aerosol samples. For this approach to be effective, all filters must be in equilibrium with their environment prior to weighing, and it is common to 'condition' them in a temperature and humidity controlled room for up to 24 hours before weighing them.

Single particle analysis

Analyzing collected particles one by one can potentially lead to a wealth of information about the sampled aerosol. Properties such as particle shape, structure and composition are all measurable as a function of particle size, allowing a true multivariate analysis. However this comes at a price – single particle analysis is inordinately time consuming. It therefore tends to be used as more of a research tool where there is something unusual about the aerosol being investigated. The exception is the characterization of airborne fibers, which will be dealt with in a later lecture.

Particle collection. Any form of single particle analysis requires that all particles are discretely deposited and freely accessible to the analysis method without interference from the holding substrate. In practice this means the particles need to be uniformly deposited onto a smooth surface. Thermophoretic deposition, electrostatic precipitation and collection onto membrane filters all fall into this category, and are used according to their suitability to the analysis method. Cellulose ester membrane filters are ideally suited to optical microscopy, as particles are

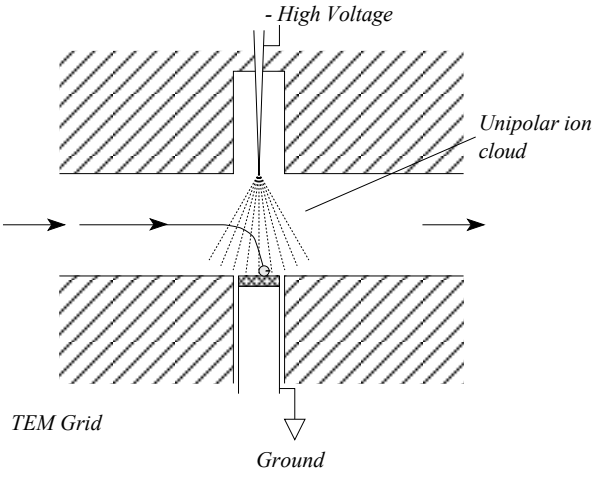

Fig. 6.32. Point to plane electrostatic precipitator. The Particles are charged in the corona-discharge ions, and then deposited in the field between the discharge needle and the electron microscope sample grid.

presented on a relatively smooth surface. Various clearing methods may also be used to render the filters optically transparent. Polycarbonate track-etched filters are commonly used for Scanning Electron Microscope (SEM) samples, presenting a surface enabling aerosol particles to be easily distinguished and characterized. Thermophoresis and electrostatic precipitation are more suited to collecting samples for Transmission Electron Microscopy (TEM). Precipitation is usually onto an electron-transparent carbon support film.

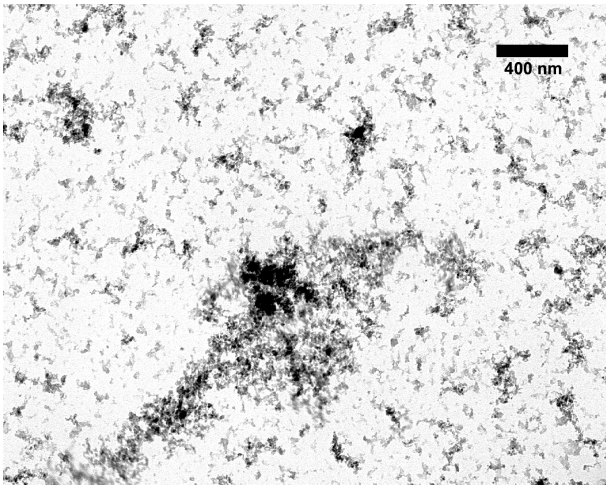

Fig. 6.33. Carbon particles collected in a thermophoretic precipitator

Optical Microscopy. Optical microscopy enables the visual characterization of particles larger than around 0.3 μm in diameter, allowing particle size and shape to be measured (note that a particle needs to absorb approximately 0.3% of the incident light to be visible to the eye). A skilled microscopist can use the physical and optical properties of imaged particles (such as shape, size, surface texture, color, refractive index, crystallographic properties and birefringence) to identify the source of the particle. However quantitative analysis is limited. Spatial resolution is limited by the wavelength of the illuminating light used; a maximum resolution of around 0.25 μm is possible using green light.

Transmission Electron Microscopy (TEM). Electrons traveling in a vacuum behave in a similar manner to visible light – they have a characteristic wavelength, can be focused (using magnetic and electrostatic lenses), and can be used to form images on a phosphorescent screen (or similar). The TEM is a direct analogy of an optical microscope. However the use of electrons instead of visible light leads to a spatial resolution of less than a nm, enabling detailed imaging of the smallest aerosol particles (the actual wavelength of the electrons in the TEM is much smaller than this – resolution in this case is limited by inadequacies in the lens system). Detailed size and shape

analysis is possible on particles up to a few μm in diameter. Above this it becomes impractical to image complete particles. As most particles imaged are electron-opaque, only the outlines of particles are usually seen.

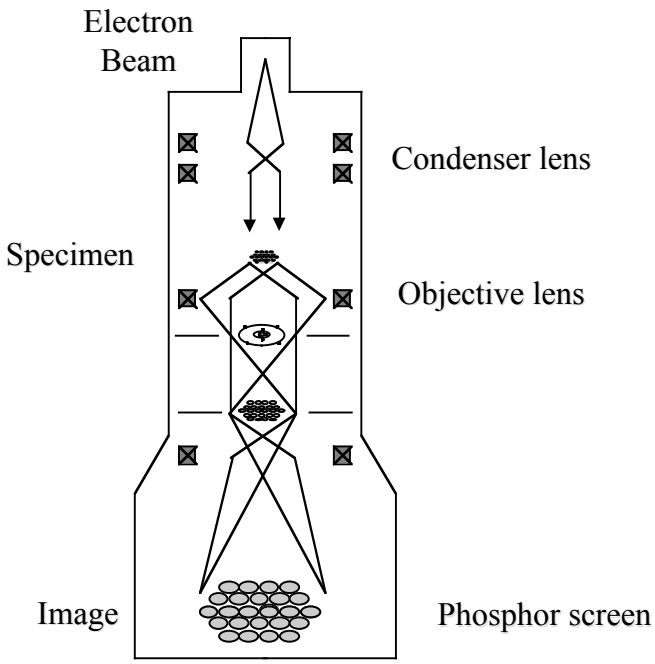

Fig. 6.34. Schematic of a transmission electron microscope

An added advantage of using an electron beam to image particles is that interactions between the beam and the particles lead to secondary signals that may be used for quantitative analysis. Energetic beam electrons are able to excite atomic electrons into higher electron orbits. As these decay, X-rays with discrete energies that are characteristic of the elemental species are emitted. By detecting these X-rays and measuring their energy, it is possible to quantify the elemental composition of particles – the technique is known as Energy Dispersive X-ray analysis, or EDX. Depending on the sophistication of the system, elements from carbon upwards can be quantified, although most systems are limited to elements heavier than silicon.

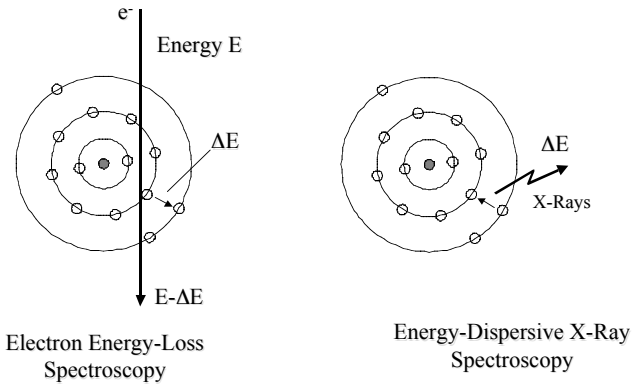

Fig. 6.35. Generation of characteristic X-rays in the

Scanning Electron Microscopy (SEM). Scanning electron microscopy differs from TEM in that secondary signals resulting from electron beam – specimen interactions are used to image the specimen, rather than the electrons forming the beam. The electron beam is focused into a fine point, and scanned in a regular repeating array of lines across the sample surface. At the same time a similar array of lines (a raster) is scanned across a viewing screen (such as a computer monitor). Detectors pick up signals resulting from the electron beam hitting the specimen, and the output from the detectors is used to modulate the intensity of the display raster. Thus an image of the specimen is formed. Magnification is determined by the size of the raster on the specimen, and resolution is governed by the diameter of the electron beam.

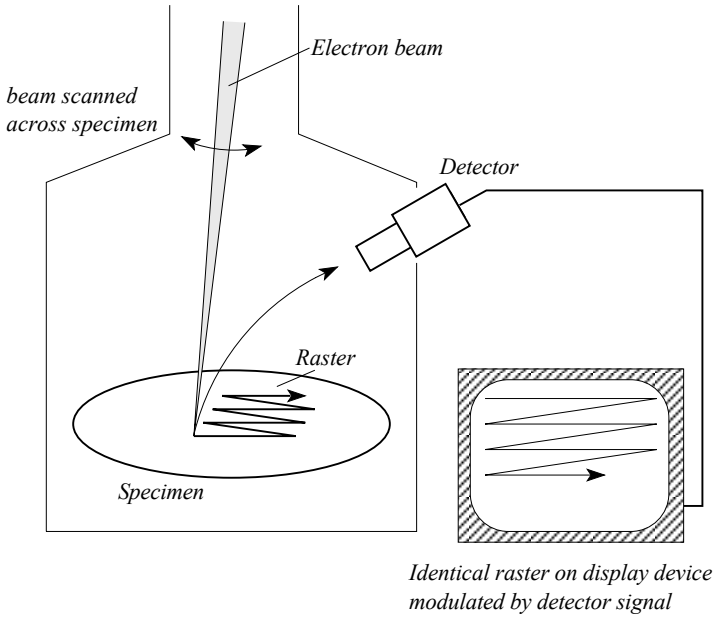

Fig. 6.36. Imaging in a scanning electron microscope

Most SEM images are formed using secondary electrons – low energy electrons knocked out of the specimen by the electron beam. The resulting image maps out the physical surface of the specimen, and is relatively easy to interpret. Characteristic X-rays are also emitted from the specimen, and may be used to quantify the elemental composition of a single part of the specimen, or to image the specimen in terms of elemental dispersion (elemental mapping).

As the electron beam is terminated at the specimen, the means must be provided to remove the electrons and prevent a buildup of charge on the specimen. In practice, this

requires the specimens to be conducting. It is common practice to coat non-conducting specimens with a thin gold film prior to sampling, using sputter coating or vacuum coating.

Spatial resolution of most SEM's is limited to around 50 nm – 100 nm for practical particle analysis, although high resolution research instruments are capable of resolving particles down to 1 nm in diameter.

Environmental SEM. Both TEM and SEM analysis require the sample to be held in a high vacuum. This is OK for robust, solid particles, but is of no use for volatile or semi-volatile particles. Environmental SEM (ESEM) partially overcomes these limitations by allowing imaging under a partial vacuum. Although the use of ESEM's hasn't been widely explored for characterizing aerosol particles, the method does allow the possibility of analyzing some volatile particle species that are unsuitable for conventional SEM or TEM analysis.

Final Word. We have only covered the mainstream single particle analysis approaches here. Be aware that there are many other ways of extracting information from individual particles, including Scanning Probe Microscopy, Raman spectroscopy, Laser Microprobe Mass Spectrometry, Secondary Ion Mass Spectrometry.

PRINCIPLES OF REAL-TIME AEROSOL MEASUREMENT

Suggested reading: [1]Baron and Willeke chapters 13 onwards
[2]Hinds chapters 10, 16
[3]**Vincent, chapter 10**

Material Covered:

- Dynamic aerosol measurement concepts
- Bulk aerosol characterization
  - Mass concentration
  - Number concentration
  - Surface Area Concentration
- Distribution measurement
  - Optical particle sizing
  - Time of flight spectrometry

[1] Aerosol Measurement. Principles, Techniques and Applications. 2nd Ed. Baron, P A and Willeke, K (Eds.). Wiley Interscience, New York. 2001
[2] Aerosol Technology. 2nd Edition. Hinds, W C. Wiley Interscience, New York. 1999.
[3] Aerosol science for Industrial Hygienists. Vincent, J H. Elsevier Science, Bath, UK. 1995.

BACKGROUND NOTES

Background notes include supplemental material that is useful, but not essential, to the course.

1. Introduction

Sampling an aerosol for later analysis is a convenient and proven approach to aerosol measurement. It is also exceedingly time consuming. For instance, to measure the average aerosol mass concentration someone is exposed to in a workplace, you have to pre-condition and pre-weigh the filters, take personal aerosol samples on the person for several hours, then post-condition and post-weigh the loaded filters. The complete process usually takes over three days from start to finish. Another example: say you want to measure the penetration efficiency of a pre-classifier as a function of particle size, and decide to use monodisperse particles and collection on filters. The method is straight forward: for each particle size you're interested in you obtain a sample of monodisperse particles, which you aerosolize and sample through the pre-classifier, at the same time making a reference measurement of aerosol concentration before

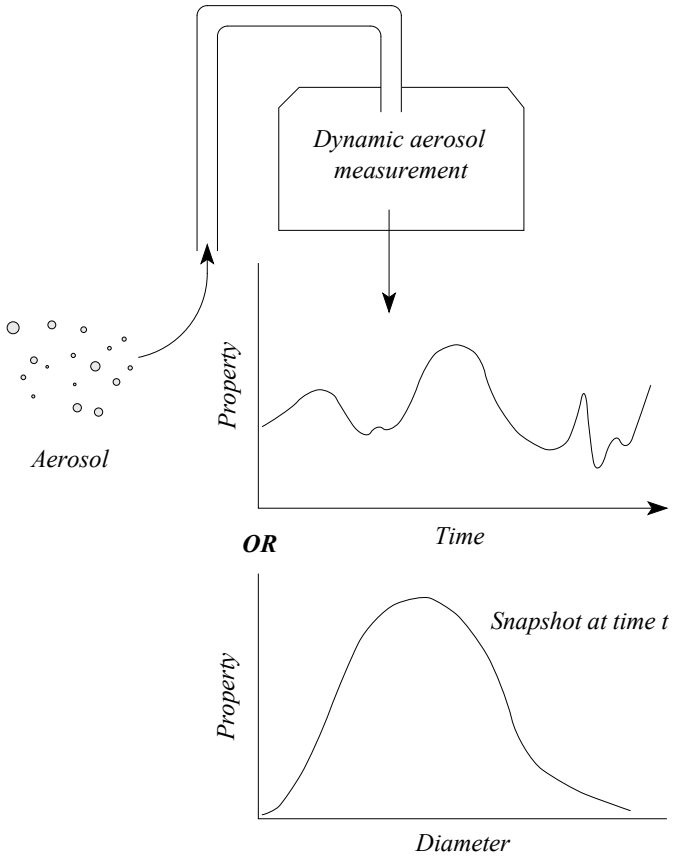

Fig. 8.1. Dynamic aerosol measurement

passing through the pre-classifier. As collection is onto filters, these have to be pre- and post- conditioned, and pre-and post-weighed as above. Thus for each particle size the measurement process may take two to three days. *It is not uncommon for a full instrument characterization along these lines to take over a week.*

The obvious solution to speeding the whole process up would be to measure the various aerosol properties of interest *at the point of sampling*. The process is called ***Dynamic Measurement***.

Dynamic aerosol measurement replaces the collection device at the end of the sampling chain with an instrument capable of giving an instantaneous, or near-instantaneous reading of a chosen aerosol characteristic, such as particle number, mass concentration etc. The measurement instruments are often referred to as *direct-reading instruments*, as they measure the aerosol directly. However this term must be used with caution, as it is open to mis-interpretation, and may lead to confusion. Many instruments measure some property of the aerosol that is relatively easily measured, such as the amount of light scattered by the particles. This is then converted into the property or quantity that is desired, such as particle size, or mass concentration. Strictly speaking, instruments that use this approach are *indirect-reading instruments*, as they measure the quantity of interest indirectly. This isn't so bad if there is a clear physical principle connecting the detected signal to the measured quantity. However where there is no clear connection,

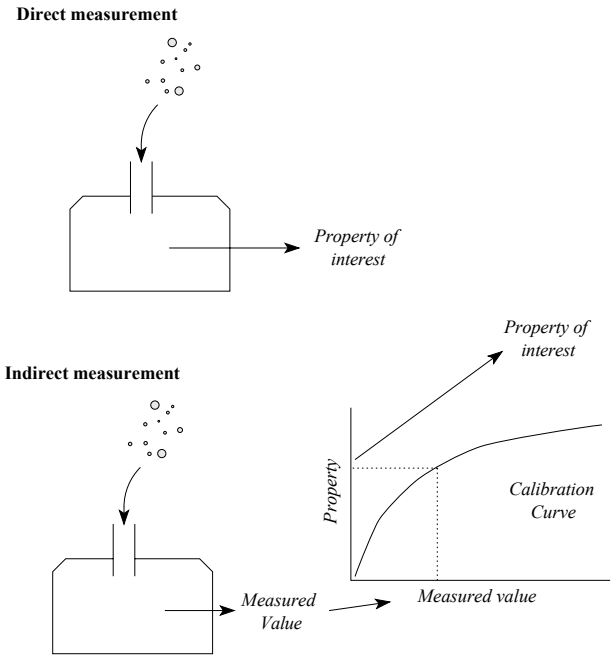

Fig. 8.2. 'Direct' versus 'indirect' dynamic aerosol measurement

empirical calibration curves are required to connect the two, and the term 'direct-reading instrument' is something of a misnomer. To be on the safe side, it's much easier to use the term 'dynamic aerosol measurement'.

As many of these methods measure the quantity of interest indirectly, there are often many factors affecting the accuracy of measurements. If the instrument relies on a calibration curve, accuracy will come down to whether the calibration curve is accurate for the aerosol being sampled. In many cases it is an approximation, as it will vary according to aerosol properties such as size distribution, material and particle shape. The first and foremost thing to remember about most dynamic aerosol measurements therefore is that *while they are often faster and more convenient than sample collection-based methods, they are often not as accurate.* So saying, there are many situations where dynamic measurements are indispensable.

2. Bulk aerosol characterization

2.1 Mass

Aerosol mass concentration is perhaps the most common bulk measurement made. Four approaches to making dynamic mass concentration measurements dominate available instrumentation, and will be discussed here.

β- attenuation

β-particles (energetic electrons emitted from decaying radioactive atoms) are scattered by the massive nuclei of atoms they pass close to them. The more massive the nucleus, the greater the degree of

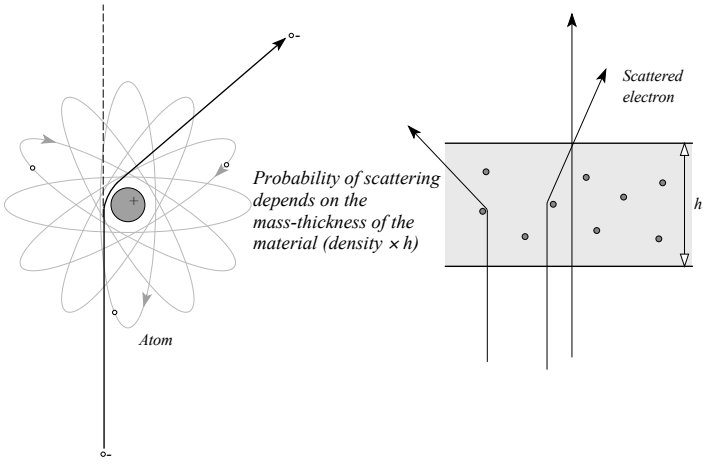

Fig. 8.3. β – attenuation

scattering. This simple principle can be put to use to measure aerosol mass. Aerosol is deposited onto a suitable surface between a β -source and a β -detector. The detector is aligned to only detect non-scattered β -particles. As the mass per unit area of aerosol increases, the number of detected β -particles decreases. The theoretical intensity of the transmitted β-particle flux is given by

$$I = I_0 e^{-\mu x} \qquad 8.1$$

where I_0 is the incident flux, μ is the mass absorption coefficient for beta absorption and x the mass-thickness of the sample (kg/m^2). x is proportional to the deposited aerosol mass ΔM, and so

$$Ln\left(\frac{I}{I_0}\right) = -\mu x = K\Delta M = KQtm \qquad 8.2$$

where K is a constant of proportionality, and depends on the sampling and detection geometry and μ. Q is the sampling flow rate in m^3/s, t is the collection time and m is the aerosol mass concentration.

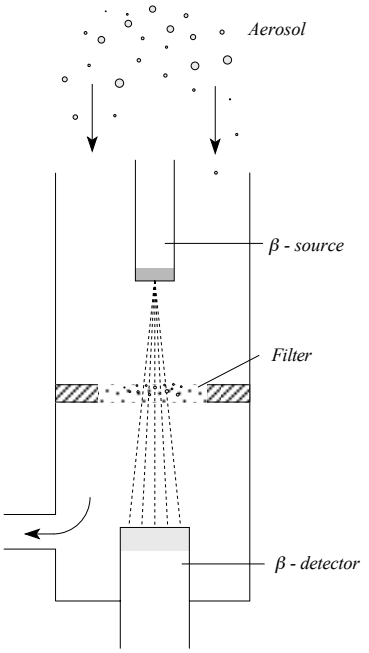

Fig. 8.4. Schematic diagram of a β – gauge for measuring aerosol mass concentration

As the method assumes a homogeneous sample, measurement errors may arise from inhomogeneity in both the sample and the support substrate. In particular, the inclusion of large diameter particles within the sample tends to lead to lead to significant spatial variations in the sample mass-thickness. Correspondingly, it is advisable to either limit sampling to particles smaller than 10 μm in diameter, or to ensure that the average deposit thickness is sufficient for statistically meaningful numbers of particles to be

present.

Errors may also arise from using an inappropriate value of the mass absorption coefficient μ, as it is dependent on atomic number (and therefore the material being sampled).

Piezoelectric mass balance

There are some crystalline materials (such as quartz) that will expand or contract marginally if an electric field is applied along specific crystalline planes - the piezoelectric effect. Applying an oscillating field will lead to physical oscillations in the crystal. When the applied frequency matches a natural resonant frequency of the crystal, very large oscillations may be produced with very little power input – these are the resonant frequencies and are relatively easy to detect. A resonant frequency for a given crystal is *directly dependant* on the mass per unit area of the vibrating crystal planes. Thus by monitoring any change in resonant frequency, changes in mass can be measured directly. Change in frequency Δf is given by

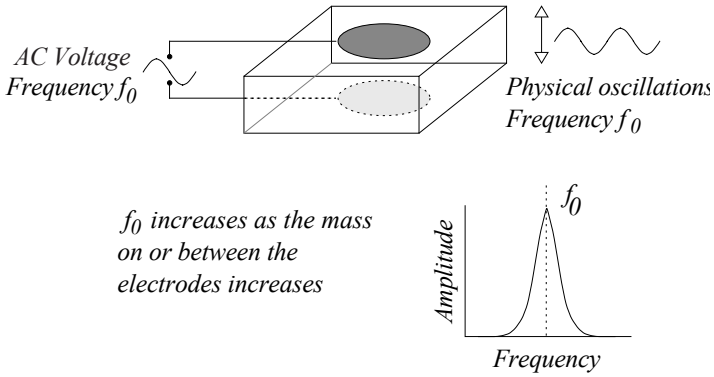

Fig. 8.5. The piezoelectric effect

$$\Delta f = -K_\alpha f_0^2 \frac{\Delta M}{A} \qquad 8.3$$

K_α is a constant, f_0 is the resonant frequency, A is the active area of the crystal and ΔM is the change in mass *on the active area* (equivalent to the area of the electrodes).

The method is potentially very sensitive; in some systems an increase in thickness of just a few atomic layers can be detected.

The technique is used in the piezoelectric aerosol mass balance (usually called the Quartz Crystal Microbalance – QCM) to directly measure aerosol mass. Particles are deposited onto an electrode on one side of a piezoelectric crystal, usually using an impactor or an electrostatic precipitator, and the change in resonant frequency converted into a measure of the deposited mass. Note that the change in mass is given by

$$\Delta M = Qtm \qquad 8.4$$

where Q is the flow rate, t the sampling time and m the aerosol mass concentration (assuming all particles are deposited on the active area of the crystal).

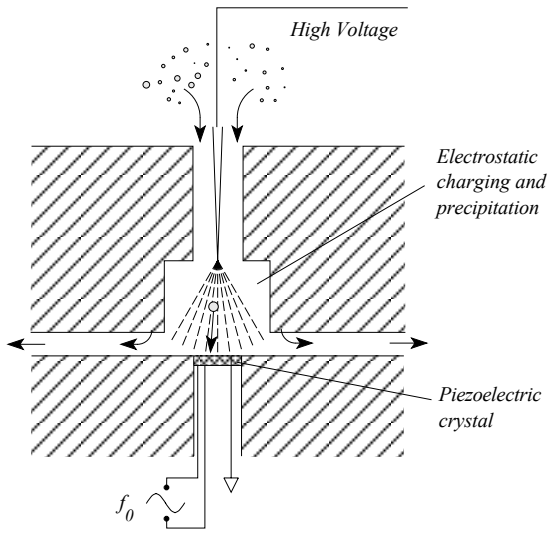

Fig. 8.6. Schematic diagram of a Quartz Crystal Microbalance, using point-to-plane electrostatic

QCM's are limited by the need to deposit aerosol particles onto a hard, solid surface. If there is good adherence between the crystal and the particles, the method is very effective for measuring the mass of deposited aerosol directly. However particle bounce and partial coupling between the particles and the crystal surface can lead to measurement errors. Overloading may also lead to a non-linear response.

Tapered Element Oscillating Microbalance (TEOM)

The TEOM operates using similar physical principles to the piezoelectric mass balance, but with a very different realization. Resonance is a common property of many physical

systems. Where an item is physically oscillating, the resonant frequency is associated with the mass of the item. Thus in principle resonant frequency could be used in many ways to measure deposited aerosol . In practice it is difficult to find an oscillating system that is sensitive to small changes in mass, and has a linear response (or at least a calibrateable response).

One suitable configuration is to suspend a mass at the end of a stiff filament. If a massive object is placed on the end of a light, stiff filament, the resonant frequency of the filament can be related to the mass of the object. This principle is used to great effect in the Tapered Element Oscillating Microbalance (TEOM). The filament is replaced by a stiff, hollow tapered glass element. A filter is placed at the thin end of the element, and aerosol drawn through it. The resonant frequency of the element is inversely proportional to the mass held on the tapered end, and so as aerosol particles collect in the filter, the resonant frequency reduces accordingly. By measuring changes in resonant frequency, a direct measure of deposited aerosol mass may be made. The change in resonant frequency with a change in deposited aerosol mass can be derived from the equations describing simple harmonic motion:

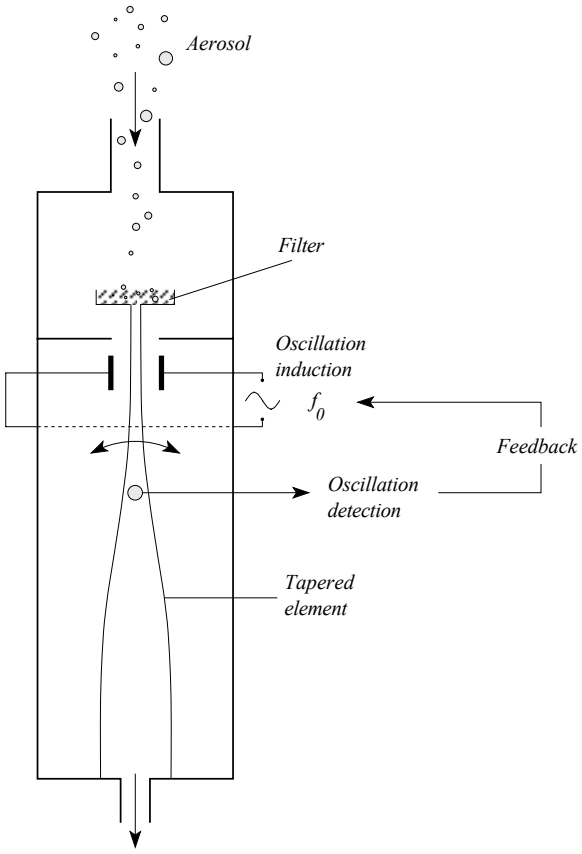

Fig. 8.7. Schematic diagram of the TEOM

$$\Delta M = K_0\left(\frac{1}{f_b^2} - \frac{1}{f_a^2}\right) \qquad 8.5$$

where f_a is the initial resonant frequency before depositing ΔM, and f_b the final resonant frequency. K_0 is a constant that is unique to the tapered element being used. Although the relationship between M and f isn't linear, it is monotonic (each value of M has a single associated value of f), and the dependence on a single calibration constant makes it convenient to use within an instrument. ΔM is related to mass concentration m using equation 8.4.

Potential sources of error are not as numerous as for the QCM. As the aerosol is collected in a filter, particle bounce and re-suspension are not of concern, and particle-collection substrate coupling is usually pretty good. This is helped by the much lower operating frequencies of the TEOM (a few hundred hertz rather than several megahertz). At high mass loadings there is the potential problem of the oscillations being damped sufficiently to affect resonant frequency.

The most significant error source within practical instruments derives from temperature effects. The resonant frequency of the tapered element is somewhat dependent on temperature, and thus in commercial instruments the temperature of the sampled air and the collection and oscillating system are carefully controlled (usually at 50° C). The operating temperature is above typical ambient temperatures to prevent condensation building up in the instrument. However as a result, volatile aerosols have a tendency to evaporate during and after sampling. This may lead to an apparent decrease in collected mass, as deposited volatile particles evaporate, and is a significant source of error where the volume-fraction of volatile components is significant.

TEOM technology currently forms the mainstay of direct-reading environmental aerosol mass measurements. The method is widely used around the world to provide rapid feedback on urban and rural PM10 and PM2.5 aerosol mass concentrations.

Light scattering.

Perhaps the most obvious physical interaction with aerosol particles that leads to their detection is light scattering. For particles much smaller than the wavelength of light the instantaneous electromagnetic field is uniform over the whole particle, leading to charge oscillations within the particle that oscillate in sympathy. These charge oscillations in turn lead to the electromagnetic energy being re-radiated, (scattered) in all directions equally. The intensity of the resulting scattered light at an angle θ to the incident light characterized by the scattering function S, and is proportional to d_p^6, and inversely proportional to λ^4. This intensity and pattern of scattering is known as Rayleigh scattering, and is described in full by

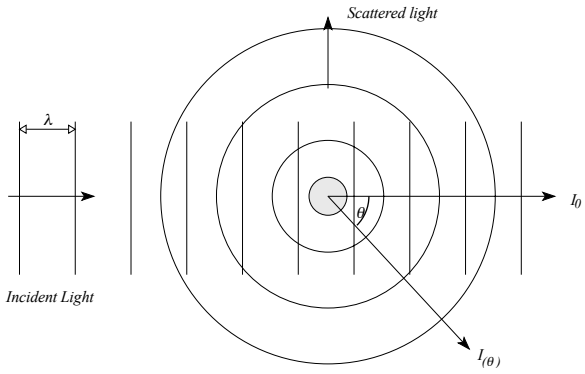

Fig. 8.8. Rayleigh scattering

$$I(\theta) = I_0 \frac{\pi^4 d_p^6}{8R^2\lambda^4}\left(\frac{m^2-1}{m^2+2}\right)\left(1+Cos^2\theta\right) \text{ for } d_p < 0.05\ \mu\text{m} \qquad 8.6$$

$I(\theta)$ is the intensity of light with wavelength λ scattered at an angle θ at a distance R from a particle of diameter d_p with refractive index m. The factor of $(1+\text{Cos}^2\theta)$ accounts for the incident light being at all possible polarizations with respect to the plane of scattering. Plotting this function out with respect to θ shows that the most

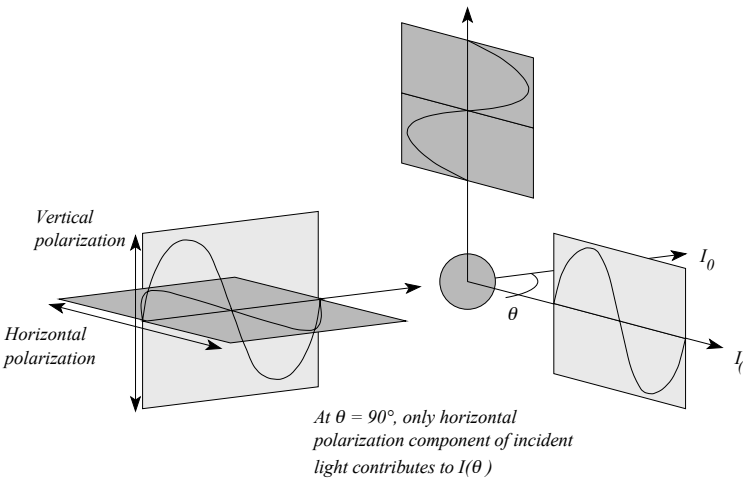

Fig. 8.9. Rayleigh scattering: Scattering direction depends on light polarization

intense scattering occurs in the forward direction (forward scattering) and at 180° (backward scattering).

For large particles, interactions between the light diffracted around the particle, light refracted within the particle and absorbed light become important, leading to the scattered light flux being a function of particle geometry, size and refractive index. Scattering is described in full by Mie theory. A full understanding of Mie theory is beyond this course, but three useful points are worth noting about the resulting scattered light.

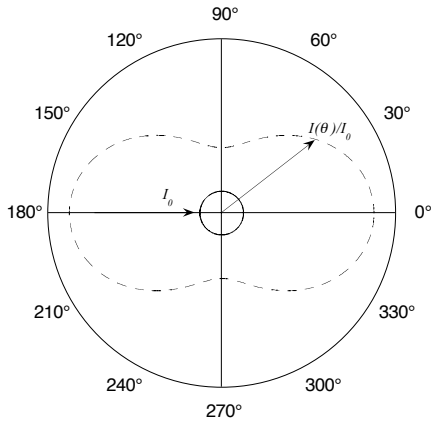

Fig. 8.10. Relative intensity of Rayleigh scattering as a function of scattering angle

- A particle's refractive index and absorption become significant, leading to complex oscillations in scattered light intensity with angle, particle size and particle refractive index.
- These oscillations may be smoothed out if scattered light is averaged over a wide range of angles, and/or polychromatic illumination is used.
- As particle diameter increases, light scattering is increasingly dominated by the particle's projected area, and the scattering function S varies as d_p^2.

There is no direct link between the mass of a particle and the intensity of light it will scatter. However if the density of the particles is known, *mass may be associated with volume, which in turn can be associated with scattering*. Scattering per unit volume S_v for an aerosol is given by the scattering function for particles of diameter d_p (S_d) divided by total particulate volume. For a monodisperse aerosol scattering per unit volume therefore follows the relationship:

$$S_V \propto \frac{6}{\pi d_p^3} S_d \qquad 8.7$$

Thus $S_V \propto d_p^3$ for particles smaller than around 0.5×λ, and $S_V \propto d_p^{-1}$ for particles much larger than λ.

With such a strong dependence on particle size, light scattering is not an obvious choice of method for directly measuring aerosol mass concentration. However for a small region around d_p = l there is a narrow range of particle sizes for which scattering is nearly independent of d_p. Using infrared illumination with λ = 0.94 μm, this region spans from approximately 0.5 μm to 5 μm, making it of some use for health-related aerosol measurement.

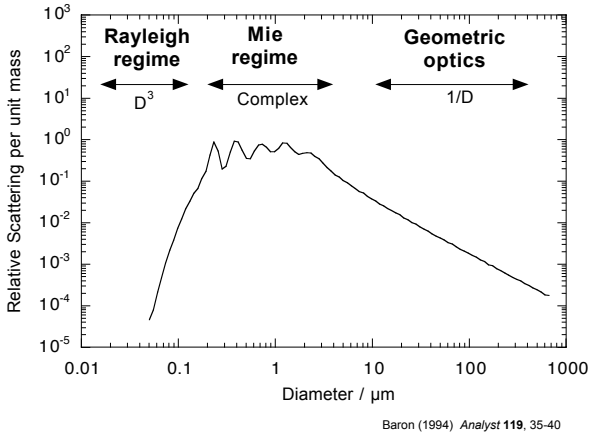

Fig. 8.11. Representation of light scattering as a function of particle diameter

Aerosol photometers use this 'window' to effectively measure aerosol mass concentration from scattered light intensity. The usual configuration is to measure the relative intensity of forward or backward scattering, or light scattered at 90° to the incident beam. Forward scattering photometers are less sensitive to refractive index than those relying on 90° scattering. Aerosol may be drawn past the light source and sensor (active sampling), or be carried into the sensing zone through convection (passive sampling). By using a suitable calibration aerosol the instrument response can be used to estimate the mass concentration of aerosols consisting mainly of particles between 0.5 μm and 5 μm. For more accurate measurements calibration needs to be carried out using an aerosol

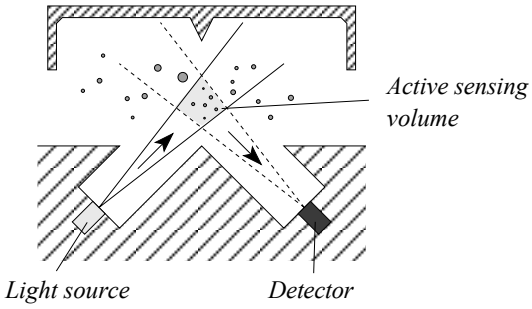

Fig. 8.12. Schematic diagram of a 90° scattering aerosol photometer

identical to that being sampled. The calibration can be extended to larger particle diameters, but only if there is no change in size distribution between the calibration aerosol and the measured aerosol. In general it is unwise to use photometers to measure the mass concentration of aerosols with significant mass distributions above 5 μm.

In principle particle size and refractive index effects could be minimized by detecting light scattered at all angles. This is equivalent to measuring the reduction in transmitted light due to scattering – a much simpler measurement to make – and forms the basis of light extinction measurements. For a parallel beam of light, the ratio of detected to incident light intensity is given by the Lambert-Beer law

$$\frac{I}{I_0} = e^{-\sigma_e L} \qquad 8.8$$

where L is the path length of the beam through the aerosol and σ_e is the aerosol extinction coefficient. σ_e depends on a number of parameters, including particle diameter, and the

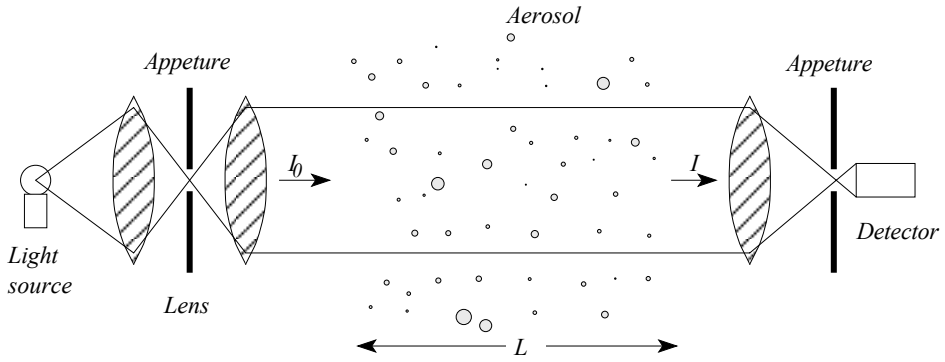

Fig. 8.13. Schematic diagram of aerosol measurement through light extinction

conversion between σ_e and aerosol mass concentration follows a similar relationship with d_p to that discussed for light scattering.

2.2 Number Concentration

Optical particle counters (OPC).

A more direct use for light scattered by aerosols is to detect and count individual particles. If an aerosol is illuminated with a narrow beam of light, particles passing through it will scatter light out of the beam – detecting the scattered light then provides a simple basis for counting the number of particles passing through the beam, and thus measuring particle number concentration. Using a laser for the illumination provides an intense, narrow source of illumination, allowing a wide range of particle sizes to be detected. Detection efficiency falls off rapidly below around 0.3 μm as the intensity of the scattered light drops as d_p^6, and most optical particle counters are unable to detect 100% of particles below 0.1 μm. Sensitivity may be increased by collecting the light scattered over a wide range of angles.

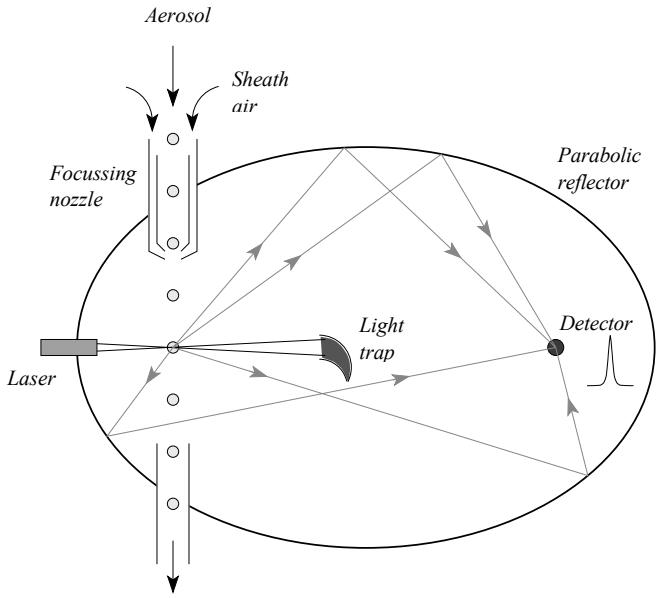

Fig. 8.14. Schematic diagram of an 'ideal' optical particle counter

The counting efficiency of optical particle counters depends on ensuring as many particles as possible pass through the center of the illuminating beam. The usual approach is to restrict the aerosol flow to a narrow region by encasing it in a sheath flow of clean air. A number of devices pass the aerosol through a nozzle arrangement designed to focus the aerosol particles into the center of the flow.

The maximum particle number concentration that optical particle counters can cope with is limited by coincidence errors. When a particle enters the sensing zone, the OPC is unable to detect any other particles until that particle has left the zone, and the sensing electronics 'recovered' (dead time τ). Thus if two or more particles are present in the sensing volume at the same time, they are counted as a single particle. The ratio of the measured particle count N_c to the true count N is given by

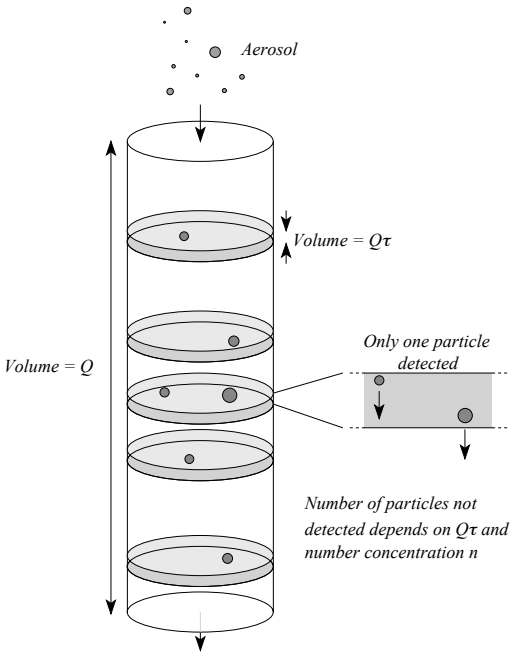

Fig. 8.15. Coincidence in an OPC

$$\frac{N_c}{N} = e^{-nQ\tau} \qquad 8.9$$

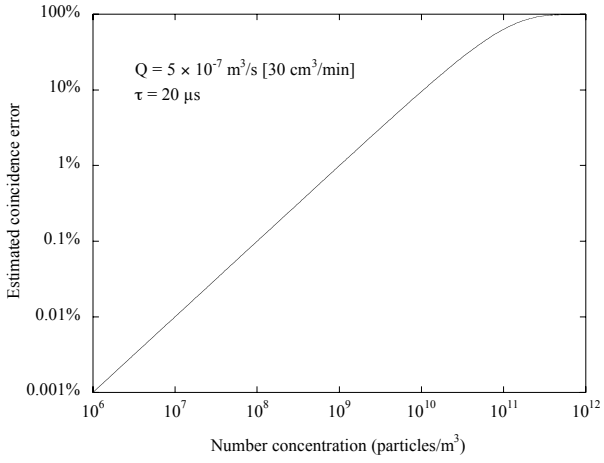

Fig. 8.16. Estimated coincidence error as a function of number concentration for an optical particle counter

Coincidence rate can therefore be reduced by reducing the flow rate through the sensing zone, either by reducing overall flow rate, or decreasing the dimensions of the sensing zone. Most optical particle counters are restricted to measuring concentrations of less than 10^{10} – 10^{12} particles/m^3. Above this, the sampled aerosol needs to be diluted before passing through the counter.

Condensation Particle Counters (CPC)

Although the detection limit of optical particle counters is limited by particle diameter, it may be increased by allowing particles to grow through condensation. If particles are passed through a supersaturated vapor, they act as condensation nuclei and rapidly grow into relatively large droplets which are easily detected using light scattering. Optical Condensation Particle Counters (CPC's) are able to push the detection limit of OPC's down to 3 nm, although a limit of 10 – 20 nm is more usual.

2.3 Surface Area

There has recently been a lot of interest in measurements of aerosol surface area concentration, following research indicating that the toxicity of insoluble particles may be closely associated with surface area. Although off-line measurements of bulk material surface area have been possible for some time using the BET method (Brunaeur, Emmett and Teller), instruments capable of measuring aerosol surface area in the field are not widely available at present. BET has been used with some success for measuring aerosol surface area. The technique relies on adsorbing a monolayer of molecules such as N_2 on the material being tested at low temperatures, then thermally desorbing the molecules. Desorbed molecule concentration is related to the surface area of the analyte. However the collection of relatively large amounts of material is required, and measurements are influenced by particle porosity (which may or may not be important toxicologically) and the collection/support substrate – particularly where the quantity of material analyzed is small. The first instrument designed specifically to measure aerosol surface area was the epiphaniometer. This device measures the surface area of the aerosols by measuring the attachment rate of radioactive ions. The aerosol is exposed to the ions for a short time, while they diffuse to the surface

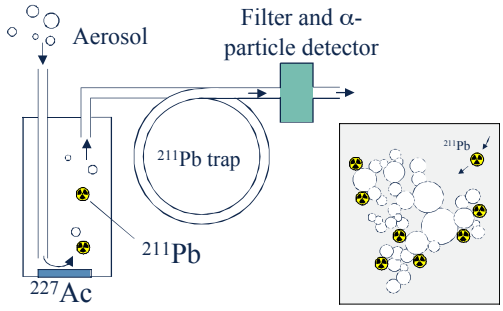

Figure 8.17. Principle of operation of the epiphaniometer

of particles. As the rate of diffusion is dependent on the overall surface area of the aerosol, the resulting radioactivity of the aerosol is directly related to its available surface area – often referred to as the 'active' or Fuchs surface area. As yet, it is unknown how relevant active surface area is to health effects following inhalation exposure. Below approximately 100 nm active surface scales as the square of particle diameter, and thus is probably a good indicator of actual particle surface area for ultrafine particles. However above approximately 1 μm it scales as particle diameter, and so the relationship with actual particle surface area is lost. The epiphaniometer is not well suited to widespread use in the workplace due to the inclusion of a radioactive source.

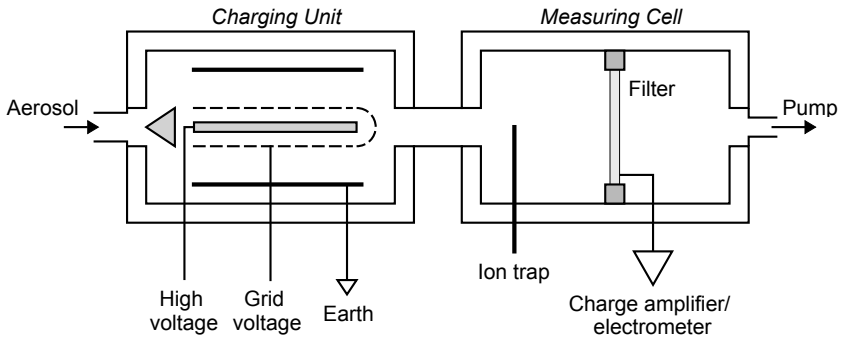

Fig. 8.18. Schematic of the LQ1-DC aerosol surface-area monitor.

The same measurement principle is applied in the aerosol diffusion charger/electrometer. Radioactive ions are replaced by non-radioactive ions, and an electrometer is used to measure the attachment rate of the ions to aerosol particles. The LQ1-DC diffusion charger (Matter Engineering, Switzerland) uses this combination to measure the attachment rate of unipolar ions to particles, and from this the aerosol active surface area is inferred. This instrument is also available in a portable form.

3. Size distribution measurement

So far we have dealt with the dynamic measurement of single aerosol parameters (mass concentration and particle number). A further layer of measurement sophistication is achieved if more information than just count can be derived on a particle-by-particle basis, thus allowing true single particle characterization.

Optical Particle Sizing.

Although we have just considered using scattered light from individual particles to detect their presence so far, it should be obvious that if the relative intensity of the scattered light could be measured accurately, it could be used to provide information on particle size. Although simple in principle, optical particle sizing is dependant on a number of parameters other than particle size that make its use somewhat complex. Particle refractive index, absorption coefficient and shape all contribute to the intensity of the scattered light. Add to this the angular dependency of the scattered light intensity and what should be a relatively easy task of relating intensity to particle diameter becomes rather daunting. However the technique is used to great effect by minimizing the uncertainties associated with various unknown parameters. The effects of particle refractive index and scattering angle, and to a certain extent particle shape, can be reduced by detecting the scattered light over a large solid angle –usually achieved using a parabolic mirror to reflect the scattered light over a wide range of angles onto a detector (see fig. 8.14). Light absorption by particles still causes difficulties, and care must be taken to use appropriate calibration standards. Instrument response is usually calibrated using spherical polystyrene latex spheres, and the response used to map scattered light intensity to particle diameter. The diameter measured by an

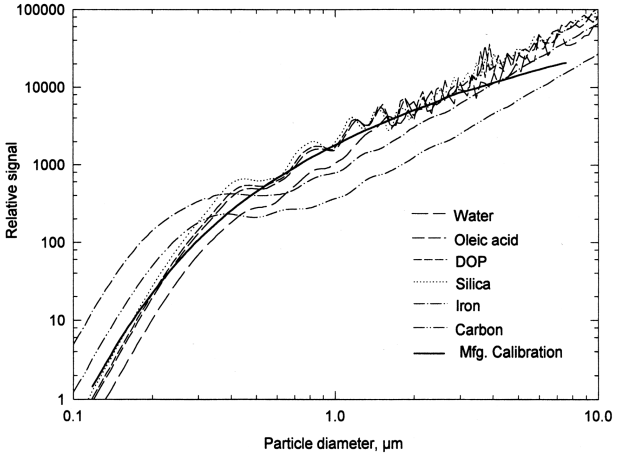

Fig. 8.19. Response curves of a commercial optical particle sizer to different aerosols. From Hinds, p375

optical instrument is therefore the diameter of an equivalent PSL particle that scatters the same relative intensity of light into the detector solid angle. As in the case of aerodynamic diameter, this is an operating definition of particle diameter, *and may not be directly comparable with other measurement methods*.

For each particle detected by an optical particle sizer, an electrical pulse is generated with a height proportional to the detected light intensity. In most processing systems each pulse is associated with a particle diameter using the calibration function, and assigned to a 'bin' that records the number of particles detected between set diameter bounds. The resulting binned particle counts may be used to derive the continuous particle size distribution (lecture 3). Commercial instruments are capable of sizing particles between 0.5 μm and 20 μm.

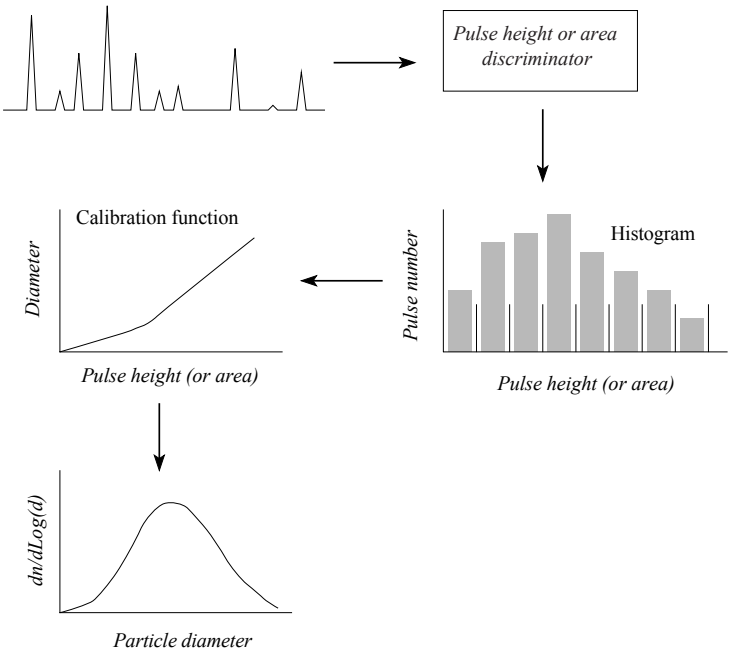

Fig. 8.20. Process of deriving particle size distribution from the output of an optical particle sizer's pulse detector.

Particle time-of-flight sizing

Although measurement of a particle's optical diameter is useful, the behavior of many occupationally and environmentally relevant aerosols is governed by their aerodynamic diameter. Aerodynamic diameter may be estimated in real time using a cascade impactor with piezoelectric mass balances on each stage, although the technique is somewhat insensitive and temperamental. By far the most successful method to be used

commercially has been the aerosol time-of-flight spectrometer (two instruments are available – the TSI 3020 Aerodynamic Particle Sizer (APS) and the TSI Aerosizer).

Recall that particle relaxation time gives an indication of how rapidly a particle will adjust to a new set of flow conditions, based on its inertia. If an aerosol flow is suddenly accelerated, particles with large relaxation times will take some time to adjust to the new conditions, and their velocity will lag behind that of the carrier gas. Particles with smaller relaxation times will adjust more rapidly, and thus the velocity lag will be smaller. Relaxation time, and thus relative velocity, will be a function of aerodynamic diameter. If we could measure the velocity of particles in an accelerating flow with respect to the gas velocity therefore, it should be possible to relate that velocity to particle aerodynamic diameter.

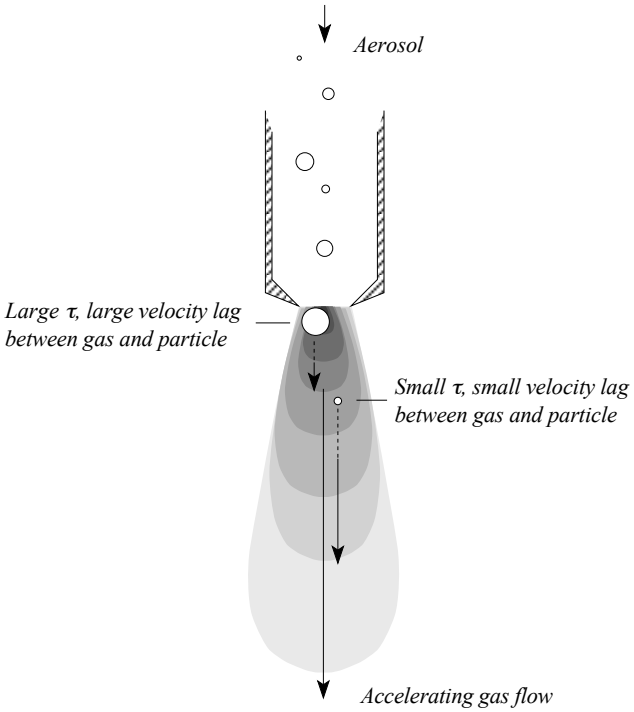

Fig. 8.21. Particle motion in an accelerating gas flow

Time-of-flight instruments such as the TSI APS accelerate the aerosol through a dual nozzle system. Clean air flowing through the outer nozzle serves to control the acceleration, and to confine the aerosol to a narrow flow region. Shortly after the nozzles, while the flow is still accelerating, the particles pass through two laser beams. By detecting pulses from a particle as it passes through both beams, it is possible to measure particle time-of-flight between two set points, and thus particle velocity.

Operation of the APS is sufficiently complex to prevent the simple calculation of a velocity versus particle diameter calibration curve. Calibration is usually carried out by measuring the response to monodisperse polystyrene latex spheres. Measured particle time-of-flight is then related to particle aerodynamic diameter via the calibration curve. As time-of-flight is weakly dependant on particle density, a correction for density also has to be applied to minimize measurement errors.

The current version of the TSI APS (model 3020) will measure aerodynamic diameters between 0.5 μm and 20 μm, and will return a size distribution in terms of particle aerodynamic diameter. However, as with every other aerosol measurement instrument, the measured size distribution needs to be interpreted in terms of sampling losses and instrument response (lecture 4). APS sensitivity drops off close to 0.5 μm. Above 5 μm the particle transport efficiency through the acceleration nozzles also drops rapidly. Thus the shape of measured size distributions close to 0.5 μm and above 5 μm needs to be treated with caution.

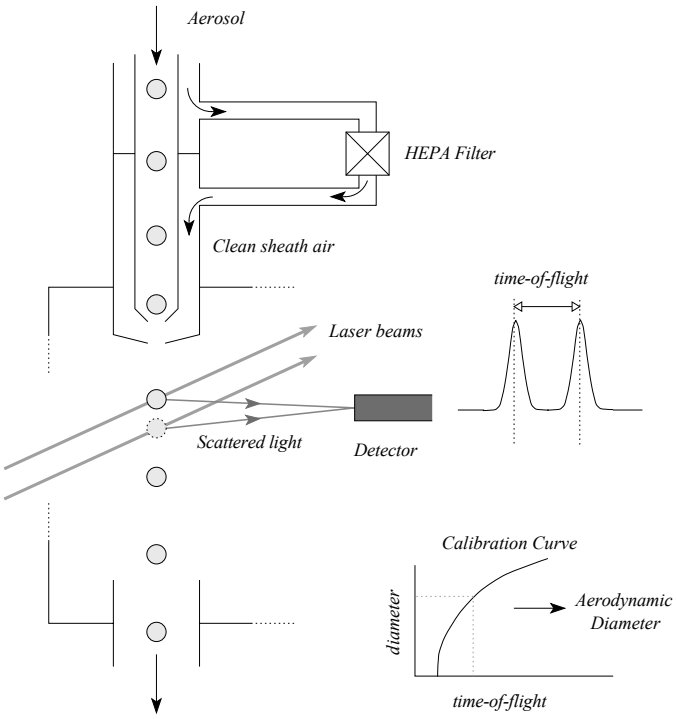

Fig. 8.22. Particle sizing using the Aerodynamic Particle Sizer

Particle time-of-flight instruments suffer from coincidence errors when multiple particles are within the sensing region simultaneously, although the effect on the measured size distribution differs markedly from that seen with optical particle sizers. Particles with diameters close to the limit of detection may produce only one detectable pulse, resulting in a subsequent particle entering the sensing region switching the time-of-flight timer off, and a single 'phantom' particle being measured. If a second particle enters the sensing zone before a first particle has left it, the resulting pulses are interpreted as belonging to two small-diameter particles. The overall result from the two types of coincidence error

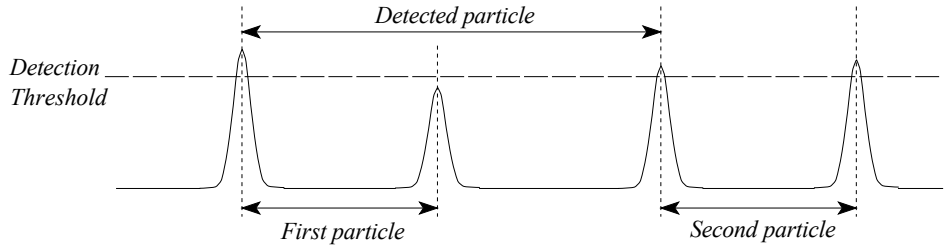

Particles close to the detection threshold - 'Phantom' particles of random sizes detected

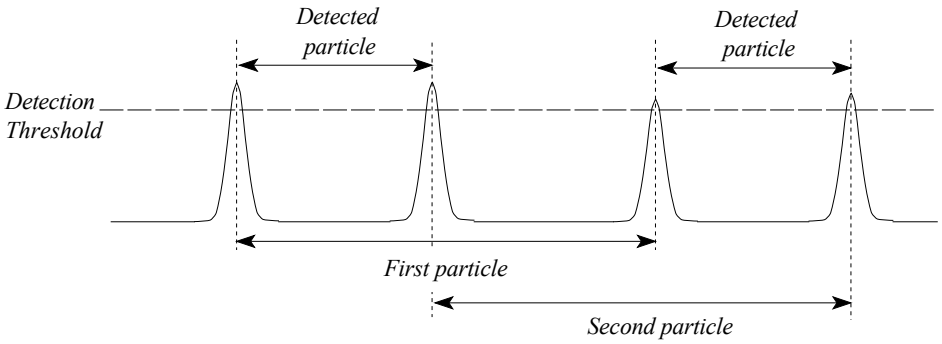

Overlapping particles - two smaller particles detected

Fig. 8.23. Coincidence errors in particle time-of-flight instruments.

is an approximately random background to the measured size distribution. The ratio of the measured particle count to the true particle count is given by equation 8.9.

Electrical mobility analysis

Particle time-of-flight sizing measures particle aerodynamic diameter, and therefore indicates particle behavior under inertial forces. For particles smaller than around 0.5 μm in diameter, where inertial forces become secondary in determining particle behavior, alternative dynamic measurement methods are needed. An approach that has been used for many years is to measure particle electrical mobility, and relate this to an equivalent particle mobility diameter.

Recall that in an electric field E, particle terminal velocity is given by

$$V_{TE} = ZE \qquad 8.10$$

where Z is the particle's electrical mobility. If a charged particle is placed in a uniform electric field between two parallel plates, it will experience a velocity V_{TE} towards the oppositely charged plate, while moving parallel to the plates with the mean flow velocity U. If a negatively charged particle starts off next to the negatively charged plate, it will travel a distance L parallel to the plates before it deposits. If h is the separation between the plates,

$$\frac{h}{V_{TS}} = \frac{L}{U} \text{ and therefore } L = \frac{U}{V_{TE}} h = \frac{U}{ZE} h \qquad 8.11, 8.12$$

The distance L is therefore inversely proportional to electrical mobility Z.

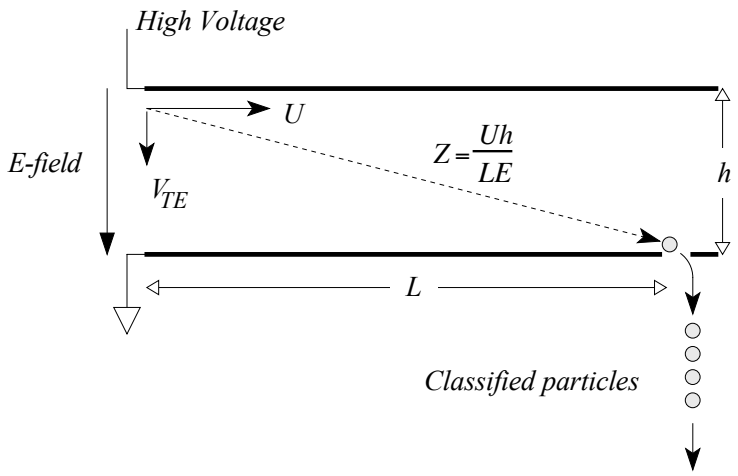

Fig. 8.24. Electrical mobility aerosol classification

Imagine now that at a fixed point L the particles just about to hit the lower plate are removed and counted. All of the particles counted would have the same electrical mobility Z, given by

$$Z = \frac{Uh}{LE} \qquad 8.13$$

By varying E, the electrical mobility of the particles detected is also varied. If E is varied over a range of values, the number of aerosol particles with specific electrical mobilities can be measured. Thus we have the basis of measuring an aerosol size distribution in terms of electrical mobility. The technique is termed ***Differential Mobility Analysis***, as particles with a narrow range of electrical mobilities are detected.

If we can measure Z, it should be possible to derive particle diameter. Z is given by

$$Z = \frac{nEC_s}{3\pi\eta d} \qquad 8.14$$

and so if E and n are known, d can be derived. The real problem comes in determining the number of elementary electrical charges n. Early electrical mobility analyzers took the approach of charging particles, and making assumptions about the relationship between n and d. However problems are encountered when particles acquire *more than one charge*: to a first approximation, the electrical mobility of a particle of diameter d and charge n is the same as that of a particle with diameter $2d$ and $2n$. An alternative approach is to neutralize the aerosol so that the charge distribution on the particles follows the Boltzmann charge distribution.

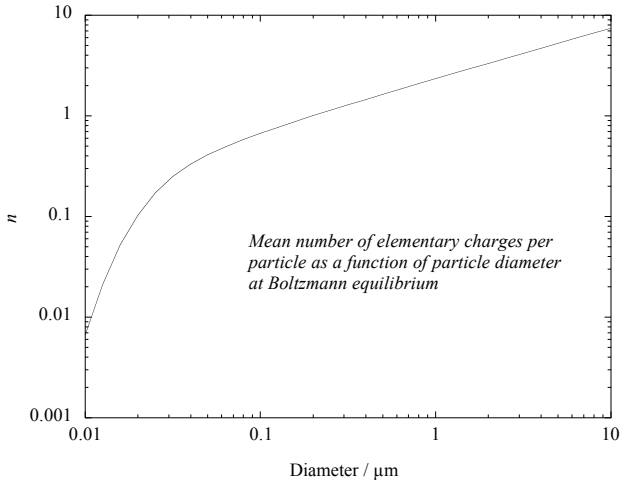

Fig. 8.25. Mean charge n versus diameter at charge equilibrium

Most sub-µm particles will have one or zero charges within the Boltzmann distribution, and corrections can be made for the low probability that a particle within this size range will have more than one charge. However as diameter increases, the probability of multiple charging also increases. Most electrical mobility measurement instruments therefore use an impactor pre-classifier to remove particles larger than 0.5 µm – 1 µm from the aerosol, and therefore are limited to sizing sub-µm particles.

A widely used version of the differential mobility analyzer – the TSI 3080 series of electrostatic classifiers – uses the same approach as described above, but with a cylindrical coaxial electrode geometry. The outer electrode is grounded, and a voltage between 20 and 10,000 volts is applied to the central rod electrode. A clean laminar sheath air flow is passed down between the electrodes, and removed at the base of the instrument. Aerosol is sampled through a pre-classifying impactor, and brought to charge equilibrium using a ^{85}Kr source. The 'neutralized' aerosol is then introduced as an annular flow next to the outer electrode. Charged particles migrate towards the central electrode, and those within a small electrical mobility range (determined by the applied electrode voltage) are removed at the base of the inner electrode. These are subsequently counted using a condensation particle counter.

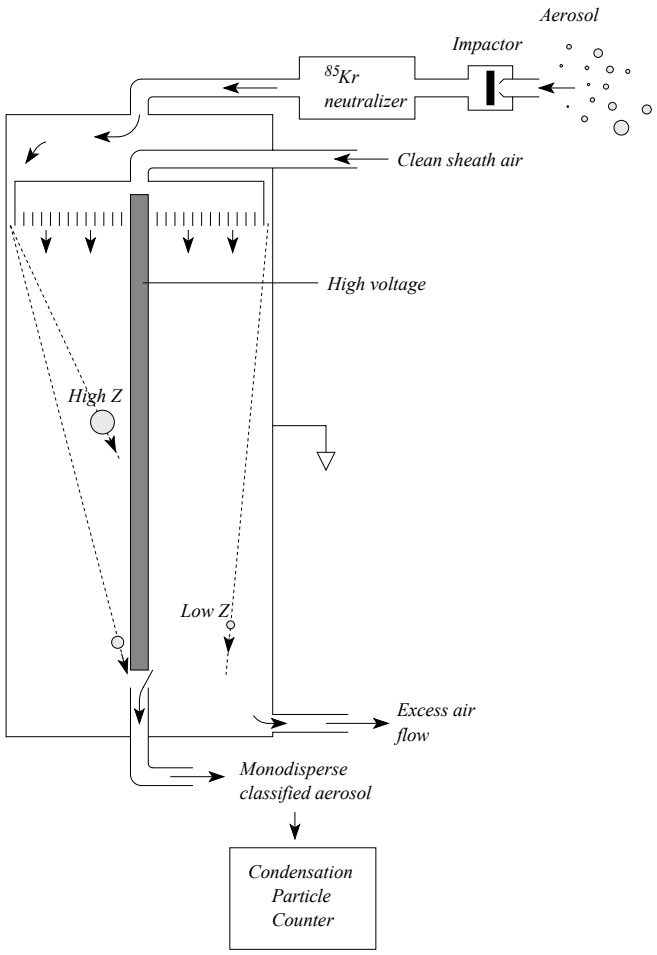

Fig. 8.26. Schematic diagram of a differential mobility analyzer

In its early incarnations, the TSI DMA used to sequentially increment the central electrode voltage, allowing particles within discrete mobility ranges to be counted and binned. A complete size distribution measurement would typically take up to 20 minutes. However more recent models use software routines that enable the mobility distribution to be measured by continuously increasing the electrode voltage (in this configuration the instrument is referred to as the ***Scanning Mobility Particle Sizer, or SMPS***). As a result,

particle size distribution measurements *within* the range 3 nm to 800 nm are possible in less than 60 seconds (although the faster the scan, the lower the resolution and the more limited the size range. Separate DMA'a are needed to cover the full range).

For spherical particles, the measured electrical mobility diameter is closely associated with the particle's physical diameter. For non-spherical particles such as agglomerates interpretation of the measurements isn't so straight forward. However consider that the resistive force leading to V_{TE} is the Stokes drag force, and that at small diameters this is approximately proportional to diameter squared – or the *projected area* of the particles. Thus at a first guess it would be reasonable to assume that the measured particle mobility is associated with projected particle area. This is found to be the case over a wide range of particle sizes and shapes – measured mobility diameter can be approximated by the diameter of a sphere with the same projected area as the particle being measured. Interpreting electrical mobility measurements in this way is useful when dealing with open fractal-like agglomerates, and when comparing DMA measurements to other measurement methods such as optical sizing and aerodynamic particle sizing.

Diffusion batteries

Although sizing sub-µm particles using electrical mobility is very powerful and convenient, it isn't the only mechanism that may be used to measure the diameter of very small particles. Recall that for particles just a few nanometers in diameter diffusion becomes dominant in determining particle behavior. Penetration of particles through a flow

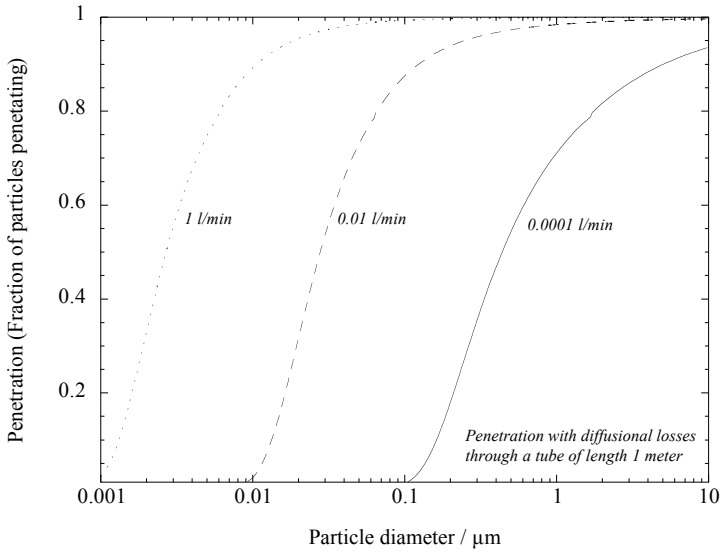

Fig. 8.27. Diffusion-limited penetration through a circular cross-section tube.

channel where diffusive losses dominate is highly dependant on particle diameter and the flow rate through the channel. Going back to diffusion-limited penetration from Notes 4, if penetration is plotted against diameter at different flow rates, penetration curves are predicted with very different cut-points. Now imagine that you could configure a flow system so that the aerosol passed through flow channels with successively lower flow rates, and you were able to measure the particles that penetrated through each successive stage. The particles measured at each point would have diameters smaller than the cut-point of the previous diffusion channels, and thus plotting particle number (or mass) as a function of sampling position would give a cumulative aerosol size distribution.

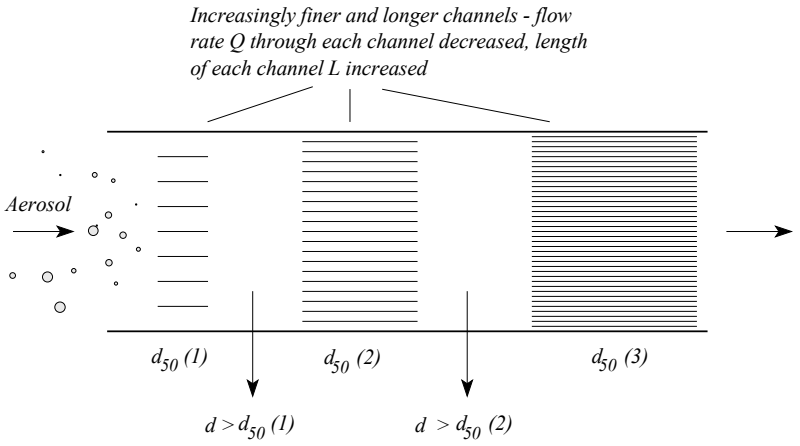

Fig. 8.28. Schematic diagram of particle penetration through a diffusion battery

This basic idea is used within diffusion batteries to measure the size distribution of very small aerosol particles. Within each stage of the diffusion battery banks of diffusion channels are placed in parallel, allowing the flow rate through each channel to be adjusted while keeping the average flow rate constant. The channels may be parallel tubes through which the aerosol flows, or may consist of the holes within a wire mesh (or any other configuration that allows diffusion-

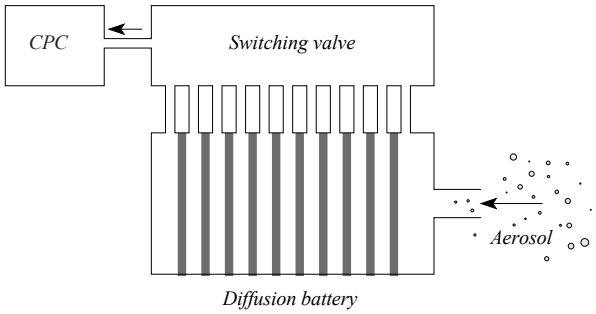

Fig. 8.29. Schematic diagram of a diffusion battery particle sizer.

limited penetration to be controlled). In many cases, particle number concentration between each stage is measured sequentially using a condensation particle counter.

Although diffusion batteries are useful tools for measuring the size distribution of aerosols dominated by nanometer-sized particles, they are frequently limited by the need to measure particle concentration between stages sequentially. However perhaps the greatest limiting factor is associated with the relatively shallow penetration curves of each stage. Unlike a cascade impactor, there is usually a significant probability of a particle penetrating through to one of a number of stages. Thus converting measured particle concentrations into an aerosol size distribution requires a number of assumptions to be made about the initial size distribution. As a result single mode lognormal distributions can be measured reasonably well, bimodal distributions cause difficulties, and for non lognormal or multi-modal distributions there is a significant risk of deriving a size distribution that bears little or no resemblance to reality.

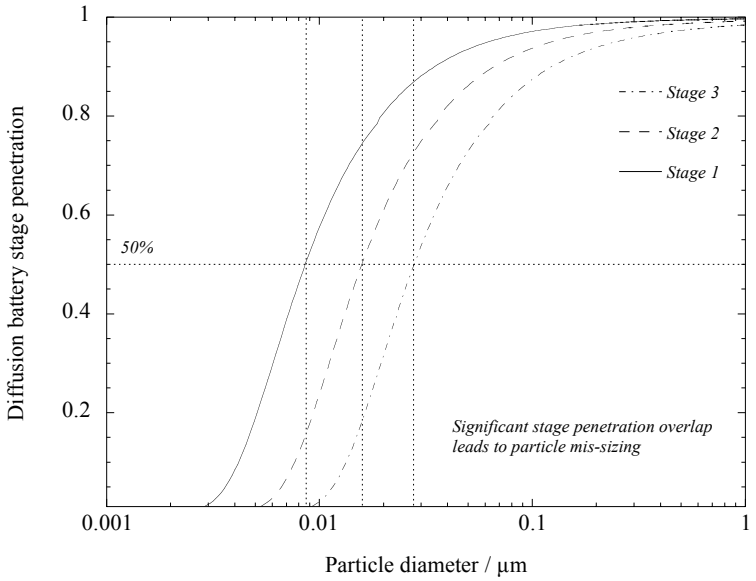

Fig. 30. Indicative penetration through adjacent diffusion battery stages, showing the relatively high probability of a single particle size being associated with a number of stages.

4. Size-resolved chemical speciation

Although in its infancy, no discussion of dynamic aerosol measurement methods would be complete without mentioning size-resolved particle chemical speciation. In the

preceding discussions we have seen that it is possible to measure the size of individual particles (Optical particle sizer, and time-of-flight sizing), and to classify particles according to size (differential mobility analyzer). The obvious next step is to measure other properties of the sized or classified particles, such as chemical composition, allowing these properties to be related to particle diameter.

One method that has been developed over recent years and is now available commercially is Aerodynamic Time Of Flight Mass Spectrometry (ATOFMS). Particles are initially focused into a beam of aerosol particles in a vacuum using a sequence of focusing and acceleration nozzles. As in particle time-of-flight instruments, particle velocity through

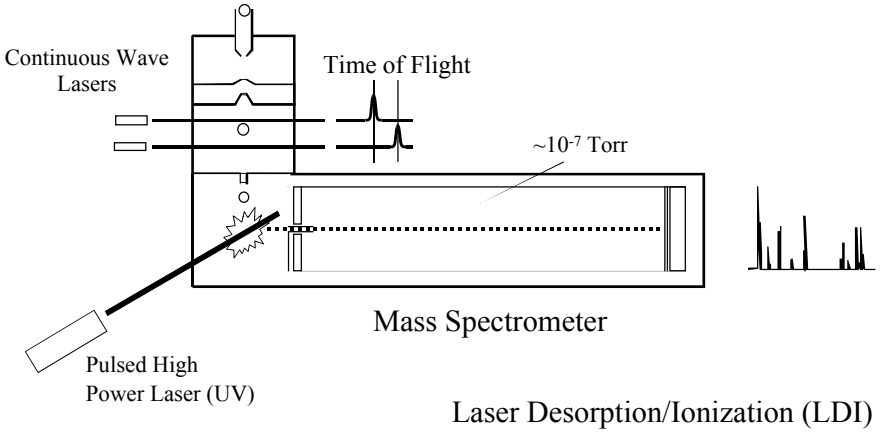

Fig. 31. Schematic diagram of an Aerodynamic Time-Of-Flight Mass-Spectrometer

these acceleration nozzles is a function of aerodynamic diameter, and therefore using time-of-flight measurements within the ATOFMS allows particle aerodynamic diameter to be measured. Each particle within the particle beam is then ablated (usually using an Excimer laser), and the resulting ions analyzed by a mass spectrometer. The measured mass-spec trace can be directly related to the time-of-flight measurement, and thus size-resolved compositional information is available on a particle-by-particle basis. The TSI 3800 ATOFMS is capable of sizing and analyzing particles between approximately 0.3 μm and 3 μm, although research instruments are capable of analyzing particles smaller than 20 nm in diameter.

In its current form, the ATOFMS is just beginning to find applications in the fields of environmental and occupational health. Analysis of environmental aerosols on a particle-by-particle basis is valuable for identifying aerosol sources of aerosol, allowing effective source tracing and control. Similar applications are feasible in the workplace. Other potential uses within the workplace include examining the partitioning of chemical species between different particle size fractions, thus enabling targeted size-selective sampling to be used.

Final Word. We have only covered the mainstream dynamic aerosol measurement approaches here. For complete coverage of available methods, refer to Baron and Willeke.

AEROSOL BEHAVIOR IN THE RESPIRATORY TRACT & HEALTH RELATED SAMPLING STANDARDS – OCCUPATIONAL AEROSOLS

Suggested reading: [1]Baron and Willeke chapter 25
[2]Hinds chapter 11
[3]**Vincent, chapter 6, 8 and 9**

Material Covered:

- Background
- Biologically relevant sampling
    - Concept
    - Respiratory tract aerosol deposition and penetration
- Health-related sampling conventions
- Aerosol sampling in the workplace
    - Size-selective sampling

[1] Aerosol Measurement. Principles, Techniques and Applications. 2nd Ed. Baron, P A and Willeke, K (Eds.). Wiley Interscience, New York. 2001
[2] Aerosol Technology. 2nd Edition. Hinds, W C. Wiley Interscience, New York. 1999.
[3] Aerosol science for Industrial Hygienists. Vincent, J H. Elsevier Science, Bath, UK. 1995.

BACKGROUND NOTES

Background notes include supplemental material that is useful, but not essential, to the course.

1. Background – Occupational aerosol exposure

Aerosol exposure has been associated with occupational illness since the earliest times, and remains a major source of ill health within the workplace to this day. Recognition of the hazard airborne particles present can be traced back to the ancient Greeks and Egyptians. In the 4th century BC, Hippocrates (c. 460 – 370 BCE) recorded details of occupational diseases associated with aerosols, including lead poisoning. Plinius Secundus (Pliny the Elder, 23 – 79) is recorded as recognizing the harmfulness of inhaling dust in the 1st century AD, noting the use of loose bladders wrapped round refiners' faces to prevent inhalation of 'fatal dust'. However, it wasn't until the 15th and 16th centuries that a clear understanding began to emerge between aerosol and occupational health. Around this time, technical and economic developments in Europe led to an increased demand for gold and lead. As mines became deeper, so the injuries and poor health associated with mining became more obvious. The writings of the founders of modern occupational hygiene such as Paracelsus (1493 – 1541), Agricola (1495 – 1555) and Ramazzini (1633 – 1714) are clearly influenced by the incidence of ill health and death associated with mining at the time. However, they also extend to many other industries. Without exception, aerosols are acknowledged by these authors as presenting a major health hazard to workers in industrial environments. Ramazzini in particular documents many occupations where inhalation of "…very fine particles inimical to human beings…" is a problem, including the inhalation of metal particles, gypsum, flour, stone dust and tobacco dust.

The industrial revolution of the late 19th and early 20th centuries introduced new and greater exposures to aerosols, and increasing awareness of the associated hazards. Mining was undertaken with increased intensity – particularly for coal – and exposure to

soot, metal fumes and aerosols such as cotton dust increased markedly. Alice Hamilton carried out seminal research in the early 1900's into the health of workers in America, and readily understood the close association between aerosol exposure and ill health: Her work laid the foundation for occupational hygiene in the USA. At the same time, researchers such as Tyndall, Aitken and Rayleigh were laying the foundations for modern aerosol science that would provide the means to understand and control occupational aerosols.

An understanding of aerosol toxicity and how to measure and control exposure developed rapidly over the 20th century, and much of the research from this period defines how we now approach occupational aerosols. Although the current understanding of occupational hygiene has expanded significantly from previous centuries, aerosols are still perceived as one of the highest profile health hazards. Numerous aerosols are widely understood to be harmful to heath if inhaled, including lead particles, asbestos, diesel smoke, crystalline silica, radon progeny, viruses, fungal spores, endotoxins and so forth. Unlike gases or vapors, aerosols pose a particularly complex hazard, as probable dose and toxicity are associated with particle size, shape and chemical structure, as well as composition. For example, SiO_2 presents a relatively low risk when present in its amorphous form, while the crystalline form is highly toxic. However, particles of crystalline silica larger than a few micrometers in diameter present a low health risk as they have a low probability of entering the lower lungs when inhaled (depositing instead in the upper airways, where they are relatively innocuous).

Many chronic respiratory diseases result in pneumoconiosis – a broad term from the Greek meaning "dust in lungs". Severe forms of pneumoconiosis are associated with fibrotic lung change. The current definition of the disorder refers to an accumulation of dust in the lungs, and the tissue reaction to its presence – essentially associating it with solid, relatively insoluble particles that are respirable (i.e. are capable of penetrating to the terminal bronchioles and beyond). Most insoluble dusts are associated with pneumoconiosis at sufficient sustained exposure levels. The least harmful of these dusts have little biological interaction with the lungs, and are generally classified as nuicance

dusts or Particles Not Otherwise Classified (PNOCs). However, a number of dusts do interact with the respiratory system to a significant degree, leading to specific forms of pneumoconiosis, including asbestosis (asbestos inhalation), silicosis (crystalline silica inhalation), siderosis (iron particle or fume inhalation) and chronic beryllium disease (from inhaling beryllium compounds).

Asbestosis and silicosis are associated with a wide range of occupations, and deserve further mention. SiO_2 is the most abundant mineral on earth, with much of it being present in a free (i.e. unattached to another mineral) crystalline form. Thus, any occupation that leads to dust being formed from rock, stone, or natural mineral products such as bricks and mortar has an associated risk of crystalline silica exposure. While amorphous silica is classified as a nuisance dust, the crystalline form is highly toxic in the lungs, leading to silicosis. The disease was known to the Greeks and Egyptians, and in modern times it peaked in the late 19^{th} and early 20^{th} centuries, coinciding with the industrial revolution. Current work practices have lowered the incidence of silicosis significantly, although the prevalence of crystalline silica still results in exposures leading to the disease. Classic silicosis results from low to moderate exposure over 20 years or more, and primarily leads to an increased disposition to micobacterial infections and progressive massive fibrosis. Accelerated silicosis results from higher exposures over 5 – 10 years, and progressive respiratory illness is virtually certain, even following cessation of exposure. Very high exposures over as little as a year can lead to acute silicosis, resulting in progressive respiratory illness in a matter of years following exposure.

The term asbestos covers a group of fibrous hydrated silicates (fibrous polymorphs of chrysotile, amosite, crocidolite, fibrous tremolite, fibrous anthophyllite and fibrous actinolite). All these materials are asbestiform – that is, they are capable of shedding increasingly fine fibers down to the fibrils that form the mineral, allowing a single inhaled fiber to divide into many thin fibers in the lungs. Fibers may be relatively straight, as in the case of crocidolite and other amphiboles, or curved, as is found with chrysotile. Asbestos can be used to form materials that are excellent insulators against heat, cold and noise, have good dielectric properties, great tensile strength, are flexible

and resist corrosion by alkalis and most acids. Correspondingly the material has been used since ancient times, and is currently associated with over 3000 commercial applications. Recognition of the extreme toxicity of inhaled asbestos fibers in the latter part of the 20th century has led to a great reduction in its use. Today, the majority of potential exposures arise during asbestos abatement, although it is still mined, and used in applications such as break linings. As well as being associated with asbestosis (fibrosis of the lungs), exposure can also lead to malignant mesothelioma, and all types of lung cancer. Toxicity is associated with the shape of the fibers, leading to exposure controls based on the number and shape of particles inhaled. Other minerals exist and are in use that show similar properties to asbestos, but are not formally classified as such. These include vermiculite – a group of silicate materials that expand on heating and can be contaminated with asbestiform minerals, and zeolite – hydrated aluminum silicates that may occur in a fibrous form. Both materials are associated with lung disease, lung cancer and mesothelioma.

Man Made Vitreous Fibers (MMVF) provide a fabricated non-asbestiform substitute for asbestos, particularly for thermal and acoustic insulation. While MMVF fibers can have similar sizes and aspect ratios to asbestos fibers, they are relatively soluble by comparison, leading to reduced lung residence times. By nature they are not crystalline and do not shed smaller fibers, and generally appear to be less toxic than asbestos.

Unlike the dusts associated with pneumoconiosis, soluble particles and droplets are relatively short lived in the lungs, and tend to lead to material-specific reactions that are less well associated with the physical nature of the particles. These may range from pulmonary irritation to systemic toxicity. Inhalation of isocyanates for instance may lead to a response ranging from transient irritation to chronic sensitization and reduced lung function. Lead on the other hand is a systemic poison, and toxicity is associated with the transport of material from the respiratory system to specific target organs.

A number of aerosols lead to short term flu-like symptoms following inhalation, which are usually classified under the umbrella term of Inhalation Fever. Symptoms are self-

limiting, but can be temporarily debilitating. Agents include endotoxins, metal and metal oxide fumes (in particular zinc oxide fume, leading to metal fume fever), pyrolysis products of polytetrafluoroethylene (PTFE) and moldy grain dust. Workers usually build up tolerance to the exposure, although symptoms can recur following an absence of exposure, such as a weekend or short break away from work. Inhalation fever is usually distinguished from acute lung injury, although a number of the agents associated with it can lead to acute injury following sufficiently high or prolonged exposures. Exposure to cotton dust is a case in point, with prolonged and excessive exposure leading to byssinosis. As with inhalation fever, symptoms occur a few hours following exposure, and are more acute after a period of non-exposure (leading to the colloquial term *Monday Morning Asthma*). Permanent dyspnea may develop following several years of exposure.

Inhalation of fungal spores can also lead to an acute response following high temporal exposures, and presents a particular hazard when the rapid spread of fungal growth in buildings occurs. Biological aerosols are also widely associated with the airborne transmission of infections. The risk of infection following inhalation is associated with the number of viable organisms entering the respiratory system, leading to methods of measuring exposure geared to identifying inhaled organisms capable of reproducing. However, the biological material associated with the organisms may also elicit a toxic response in its own right, requiring much broader classification of inhaled bioaerosols. Polymerase Chain Reaction (PCR) assays are finding increasing use to identify biological material based on DNA profiles.

In recent years, interest has been shown in a group of aerosols characterized by low solubility particles smaller than 100 nm in diameter (often termed ultrafine particles). Laboratory based research has shown that on a mass for mass basis, chemically inert materials such as TiO_2 increase in toxicity with decreasing particle size. There are indications that the toxicity of similar low-solubility materials is associated with the surface area of the particles. However, there are as yet few indications that ultafine particles pose a specific threat in the workplace.

Traditionally, workplace and ambient aerosols have been categorized as fumes (fine particles and agglomerates generated through combustion and vapor condensation), smokes (solid and liquid particles arising from incomplete combustion), dusts (solid particles generated through mechanical means), sprays (liquid aerosols with relatively large particle sizes, usually produced through mechanical means) and mists (liquid aerosols with finer particles, generally produced through condensation or atomization). These definitions tend to be used as descriptors rather than discrete classifications, and when considering sampling and health effects their use can be somewhat misleading (for example, a size selective sampler will not differentiate between a fume, smoke or mist, and the distinction between health effects arising from a fume and a sub-micron dust can be somewhat blurred). While philosophies and approaches may differ, there is a great deal of commonality between methods used to characterize occupational aerosols, and those used in other areas of aerosol measurement. In this lecture the emphasis is therefore on the basic sampling philosophies and methods used on a day to day basis in the workplace and general environment.

2. Health Related Aerosol Exposure Measurement

The are four primary reasons for measuring occupational aerosols – 1. Measurement of exposure or dose. 2. Assessment of compliance with an emission or exposure standard. 3. Enhancing understanding of processes leading to aerosol formation, and the impact of the aerosol on the environment/personnel. 4. Apportioning aerosol sources to the aerosol present at a given exposure point. Of these we will focus on number 1 – assessment of compliance with emission or exposure standards.

Note on terminology: Traditionally, workplace and ambient aerosols have been categorized as the following:

> **Fumes:** fine particles and agglomerates generated through combustion and vapor condensation.

Smokes: solid and liquid particles arising from incomplete combustion.

Dusts: solid particles generated through mechanical means.

Sprays: liquid aerosols with relatively large particle sizes, usually produced through mechanical means.

Mists: liquid aerosols with finer particles, generally produced through condensation or atomization.

These definitions tend to be used as descriptors rather than discrete classifications, and when considering sampling and health effects their use can be somewhat misleading (for example, a size selective sampler will not differentiate between a fume, smoke or mist, and the distinction between health effects arising from a fume and a sub-micron dust can be somewhat blurred).

Biologically Relevant Sampling

Health related aerosol sampling is ultimately concerned with measuring that aspect of the aerosol that leads to specific health effects. Thus, the method and metric used aim to provide biologically relevant information. The biological effects resulting from deposition of an aerosol in the *respiratory tract* will depend on the dose received, and the body's response to the deposited particles. Physiological response to an aerosol is dependent on the chemical and physical nature of the particles and the location of the interaction (i.e. deposition region). The ultimate goal of health related aerosol measurement is therefore to ascertain the dose of aerosol delivered to the body and to

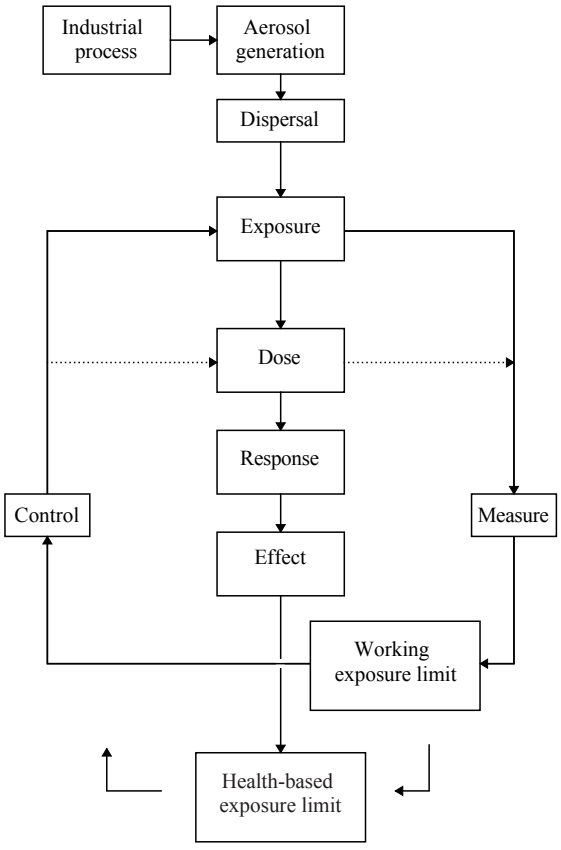

Fig. 9.1. Framework for an integrated approach to occupational aerosol sampling (adapted from Vincent, 1995)

evaluate whether the dose or potential dose is sufficient to cause adverse health effects.

Deposition region is primarily governed by particle size and shape. Response may be a function of mass, chemical composition or morphology, and possibly particle size and surface chemistry. Ideally dose should be expressed in terms of the most appropriate metric. However additional restraining factors on health-related aerosol measurements include the practical and economic application of measurement methods. In practice, it is often simpler to measure penetration to the relevant areas of the respiratory system rather than dose, thus giving a measure of the ***potential dose***. Mass and bulk chemical composition are easier to measure than parameters such as particle shape and surface area, and correlation between health effects and concentration indicates mass to be a suitable metric in many cases. Asbestiform fibers present an exceptional case where dose is best represented by particle number and shape, and accordingly a number and morphology-based metric is used.

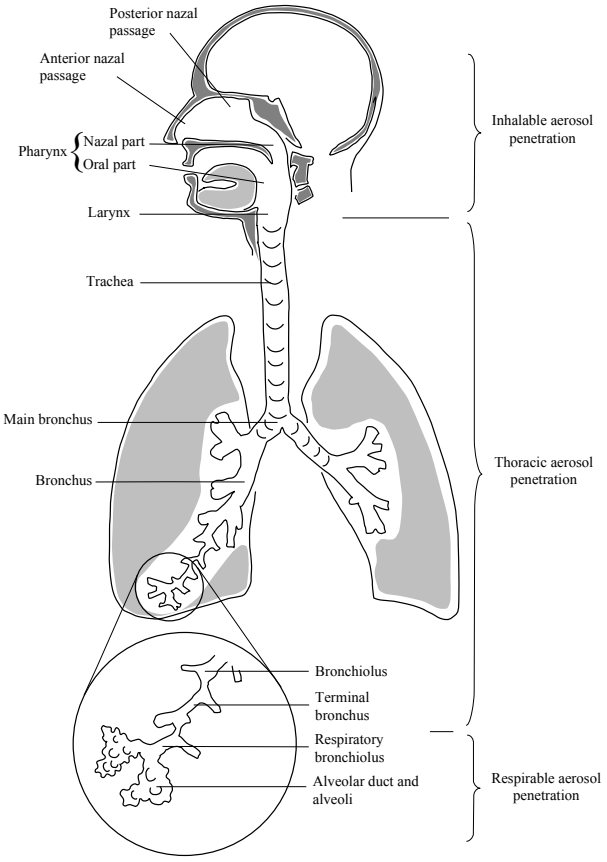

Fig. 9.2. Schematic diagram of lung deposition regions

Deposition regions

The respiratory system is an effective size-selective aerosol sampler not all airborne particles will have the same probability of entering it. Large particles are excluded from entering the nose and mouth (the nasopharyngeal region) through inertial separation.

Aspiration efficiency is a function of a number of parameters, including particle size, external air speed, orientation to the prevailing air movement direction and breathing rate and volume. However for external wind speeds of a few m/s and lower the probability of a particle entering the mouth or nose (termed ***inhalable particles***) may be generalized as being around 100% for particles with aerodynamic diameters of a few micrometers and below, reducing to around 50% at 100 μm aerodynamic diameter.

Aerosol deposition in the nasopharyngeal region is dominated by inertial impaction, although interception and (for particles in the nanometer size range) diffusion also contribute. Further inertial separation and interception occurs as the particles pass into the trachea and the upper lungs (tracheobronchial region). Although variations between individuals are high, penetration into the tracheobronchial region may be typified by particles smaller than approximately 10 μm aerodynamic diameter. As the airways bifurcate to ever finer branches towards the alveolar region, aerosol particles are predominantly removed from the flow through a combination of impaction, interception, charge effects and diffusion. Unlike the preceding regions where deposited particles are cleared through the action of cilia transporting them to the upper airways, particles depositing in the alveolar region are cleared through the action of alveolar macrophages engulfing them, and transporting them to ciliated airways (phagocytosis). Particle deposition is through impaction and diffusion, and penetration to the region is restricted to particles around 4 μm and less aerodynamic diameter. The clearance mechanism employed in the alveolar region, together with the close proximity of the bloodstream, leads to a number of health effects specific to particle deposition within this region.

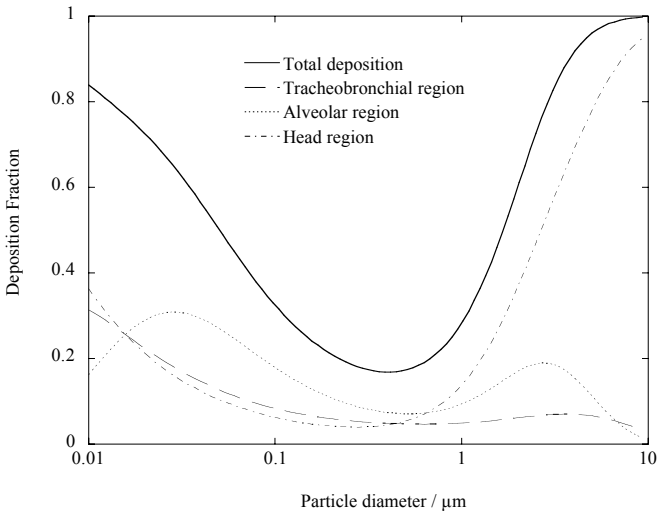

Fig. 9.3. Modeled lung deposition as a function of particle size and deposition region (nose breathing only)

Particle Characteristics and Biological Response

Although particle aerodynamic diameter dominates deposition within the respiratory tract, the subsequent effect on health is a combination of physical particle characteristics and biological response. On deposition, the body may react to the chemical substances contained within the particle, interact with the particle surface, or be influenced by physical parameters such as size and morphology.

Highly soluble particles and droplets will be rapidly assimilated by the body; particularly in the alveolar region. Local effects such as irritation and inflammation, and systemic responses, may become manifest over very short time periods. The gradual release of agents from low solubility particles will have a much longer response time. However low solubility particles may also act as vectors for the transport of high solubility solids, liquids and gases present as fine surface layers, thus leading to a response not indicated by the bulk aerosol particle properties alone. For example, adsorption of nitrogen oxides and sulfur dioxide onto particles can lead to health effects at levels normally considered safe.

Very low solubility particles are more likely to have health effects associated with their physical characteristics. Lung overload phenomena are associated with the physical limitations of the lungs' clearance mechanisms as opposed to chemical interactions with the deposited particles. Particle shape is a factor for fibrous aerosols. It also influences available surface area, which may be related to toxicity through surface interactions or increased solubility. Where open agglomerates of particles exist, such as those resulting from combustion (such as diesel exhaust particulates), metal processing, welding or fine powder production, the aerosol may have a very high specific surface area, and be formed from particles able to penetrate to the alveolar region. In some fine powders, including ultrafine titanium dioxide, carbon blacks and fumed silicas, specific surface areas in excess of 200 m^2/g are achieved amongst particles with aerodynamic diameters less than 4 μm (In comparison, an aerosol of spherical particles 4 μm in diameter and with unit density would have a specific surface area of 1.5 m^2/g). There is evidence that for some

low solubility materials, toxic response may be associated with surface area or even particle number. However little is known of the role of what may be termed available surface area, which will be influenced by particle surface structure, and biological mechanisms.

Some of the responses observed on inhaling aerosols are reversible; some may be chronic. Some effects are cumulative; others are not. For some substances, there may be an exposure level below which no effects are observed (a 'no-effect' level). For others, notably carcinogens, there may be no identifiable 'no-effect' level. For a class of substances known as sensitizers, relatively high exposure levels may be experienced without obvious effect until a person becomes 'sensitized' to the substance. Following sensitization, exposure to very low levels may result in a significant biological response.

Biologically relevant exposure monitoring requires the range of interactions and responses, together with aerosol dose and particle form, to be taken into account. It can be seen that in principle there are a number of particle characteristics that will influence the toxicity of inhaled particles. Although characteristics such as size, morphology, surface area and structure may be influential, current technology lacks the means to characterize workplace aerosols as completely as may be desirable. Fortunately, the specificity of many workplace aerosols enables successful exposure monitoring to be carried out by linking a related metric (such as mass concentration) to empirical dose-response data. The extent to which this approach is tenable where toxicity data are sparse is questionable however.

Sampling Conventions

The accurate measurement of aerosol exposure via inhalation ***requires sampling devices that match particle deposition to the relevant areas of the respiratory system***. However, aerosol deposition is highly dependent on the individual, and not trivial to replicate in a sampling device. Two different approaches to the problem exist:

1. Instrument-based standards. A reference instrument is developed that follows the desired particle selection characteristics. The performance of this instrument then forms the basis for subsequent aerosol measurement standards. All measurements are made with the reference instrument, allowing good comparability between samples. The downside of this approach is that the choice of instruments is very restrictive, and the reference instrument may not suit every sampling situation. There is also only a limited attempt to match samples with a biologically meaningful measure of aerosol exposure. This approach is used in US ambient aerosol monitoring, and still dominates US occupational aerosol exposure monitoring.

2. Performance based standards. A reference function describing particle separation characteristics is developed, based on particle behavior in the respiratory system. Any instrument that is subsequently designed and shown to follow this function is then considered an acceptable device for sampling with respect to the standard. This approach is advantageous in that a wide variety of sampling devices are potentially available, enabling suitable samplers to be chosen for a wide variety of situations. However, it is often difficult to get a sampling device to agree perfectly with a performance based standard, and as a result there are always inherent errors when comparing the results of a performance based sample to what the 'ideal' sampler would have measured. This is the approach taken for workplace sampling in Europe, and is gaining ground in the US.

Broad standards have been developed describing representative penetration characteristics of aerosol particles through the respiratory system as a function of aerodynamic diameter. These provide a basis for estimating the aerosol concentration potentially available to cause harm within specific areas of the respiratory system, and underlie many industrial hygiene aerosol sampling methods.

Early estimates of penetration into what was considered the most vulnerable part of the system – the alveolar region – were proposed in the 1950's and 1960's, resulting in the British Mines Research Council (BMRC) and the American Conference of Government Industrial Hygienists' (ACGIH) conventions describing respirable aerosols. More

recently, the International Standards Organization (ISO) and the ACGIH arrived at convergent conventions describing the probability of particles penetrating to the nasopharyngeal, tracheobronchial and alveolar regions. However, it wasn't until the early 1990's that international consensus was reached on particle penetration standards between ISO, ACGIH and the European Committee for Standardization (CEN). The resulting conventions describe penetration as a function of particle aerodynamic diameter into the respiratory system (***inhalable aerosol***), into the tracheobronchial region (***thoracic aerosol***) and into the alveolar region (***respirable aerosol***), with thoracic and respirable aerosol as sub-fractions of the inhalable aerosol. These are now widely used as the standards to which industrial hygiene aerosol samplers should conform.

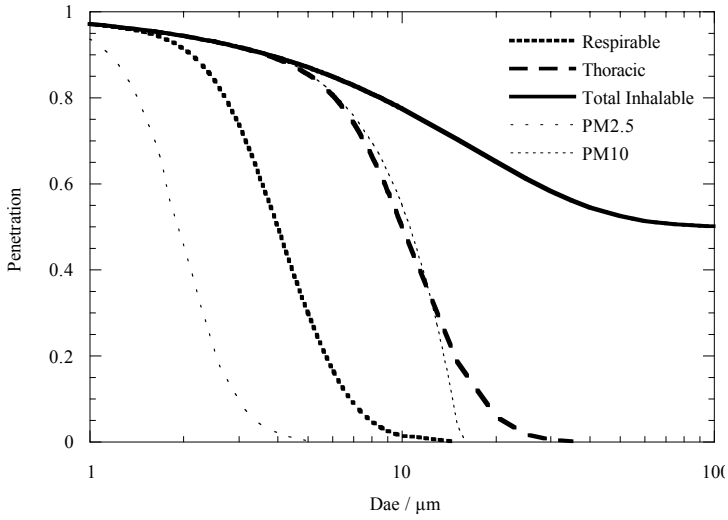

Fig. 9.4. International aerosol workplace sampling conventions (shown against US ambient sampling curves)

The Inhalable convention is based on particle penetration through the mouth and nose of a breathing manikin over a range of wind speeds and orientations with respect to the wind, and is defined as

$$SI\left(d_{ae}\right) = 0.5 \times \left(1 + e^{-0.06 d_{ae}}\right) \qquad 9.1$$

for $0 < d_{ae} < 100$ µm. $SI(d_{ae})$ is the fraction of particle entering the system as a function of aerodynamic diameter d_{ae}.

Both the thoracic and respirable conventions are expressed as sub-fractions of the inhalable convention, and are based on lung penetration measurements. The thoracic convention is given as

$$ST(d_{ae}) = SI(d_{ae}) \times (1 - F(x))$$

$$x = \frac{\ln(d_{ae} / \Gamma)}{\ln(\Sigma)} \qquad 9.2$$

$ST(d_{ae})$ is the fraction of particles penetrating beyond the larynx as a function of aerodynamic diameter. $F(x)$ is a cumulative log-normal distribution, with a Mass Median Aerodynamic Diameter Γ of 11.64 μm and a Geometric Standard Deviation Σ of 1.5.

The respirable convention $SI(d_{ae})$ is similarly given as

$$SR(d_{ae}) = SI(d_{ae}) \times (1 - F(x))$$

$$x = \frac{\ln(d_{ae} / \Gamma)}{\ln(\Sigma)} \qquad 9.3$$

where the cumulative log-normal distribution has a Mass Median Aerodynamic Diameter Γ of 4.25 μm, and a Geometric Standard Deviation Σ of 1.5. A respirable convention for susceptible groups is also defined, with Γ = 2.5 μm, although this hasn't been implemented in any exposure standards as yet. Standards relating to penetration to the *tracheobronchial* and *extrathoracic* regions are defined by the difference between the respirable and thoracic conventions (tracheobronchial), and the thoracic and inhalable conventions (extrathoracic). Note that the resulting diameters for 50% penetration for the respirable and thoracic standards are 4 μm and 10 μm respectively.

Ambient aerosol exposure standards are based on much more pragmatic guidelines. In 1987 EPA set a national Ambient Air Quality Standard (NAAQS) for particulate matter called PM-10 – particles smaller than 10 μm in diameter. the Federal Reference Method

(FRM) defining the penetration of a PM-10 sampler is based on the performance of a specific sampler, and closely matches the thoracic sampling convention for industrial aerosols. In contrast the PM-2.5 FRM is designed to distinguish between different aerosol sources rather than relate to aerosol dose/exposure in a specific part of the respiratory tract. The standard, loosely defined as particles smaller than 2.5 μm aerodynamic diameter, is designed to differentiate between particles making up the accumulation mode (assumed to derive from combustion and nucleation processes) and those in the coarse mode (assumed to derive from mechanical processes). There has been some evidence of a greater correlation between PM-2.5 levels and health effects in the general population compared to the correlation with PM-10, which goes some way to justifying this choice of standard.

Indoor Air Quality (IAQ) exposure monitoring is usually carried out using the EPA PM-2.5 and PM-10 standards. However as the FRM's for PM-10 and PM-2.5 are too cumbersome for IAQ measurements (especially personal exposure measurements) a number of personal sampling devices matching the EPA sampling standards are used.

3. Exposure Standards and Limits

Occupational Exposure Limits

Health-based aerosol exposure limits follow country-specific systems, but in the majority of cases follow a similar philosophy. In the United States, the primary sources of occupational exposure limits for the workplace are: (1) National Institute for Occupational Safety and Health (NIOSH) Recommended Exposure Limits (REL's); (2) the US Department of Labor (OSHA and MSHA) Permissible Exposure Limits (PEL's) and (3) the American Conference of Government Industrial Hygienists' (ACGIH) Threshold Limit Values® (TLVs®). NIOSH RELs are Time-Weighted Average (TWA) concentrations for up to a 10 h workday during a 40 h workweek. OSHA PELs are TWA concentrations that must not be exceeded during any 8 h work shift of a 40 h workweek. The ACGIH TLVs are 8 h TWA concentrations for a normal 8 h workday and a 40 h

workweek, to which nearly all workers may be exposed, day after day, without adverse effects. In the UK a two tier system of Occupational Exposure Standards (OES) and Maximum Exposure Limits (MELs) is employed. Each represents an 8 h TWA exposure limit. An OES is set where a no-effect level can be identified for a substance, thus giving an exposure limit below which adverse effects aren't expected (as for the ACGIH TLVs®). MELs are employed where there is no clear no-effect level. As there will be a degree of resultant health effects manifest whatever exposure limit is chosen (above zero), the choice of limit is in essence a political decision. Reflecting the nature of substances having MELs, there is an obligation on UK industries to keep exposures as low as reasonably practicable, even when this results in a target exposure significantly below the limit.

Even below these various exposure limits, a small percentage of workers may experience adverse health effects due to individual susceptibility, a pre-existing medical condition and/or a hypersensitivity (allergy). In addition, some materials may act in synergy with other substances to produce undesirable health effects, even if the occupational exposures to individual contaminants are controlled at the level set by the evaluation criteria. For example, gases such as oxides of nitrogen and sulfur dioxide may adsorb on dust particles and produce health effects at levels normally considered safe. Furthermore, some substances are absorbed by direct contact with the skin and mucous membranes and thus, potentially increase the overall exposure.

For substances that may potentially lead to health effects following short exposures, or high peak exposures, short term exposure limits (STELs) are generally set to complement the 8 – 10 TWA limits. These are generally sampled against over shorter time periods – typically 15 minutes – and are collected during periods when the concentration of contaminant is likely to be highest.

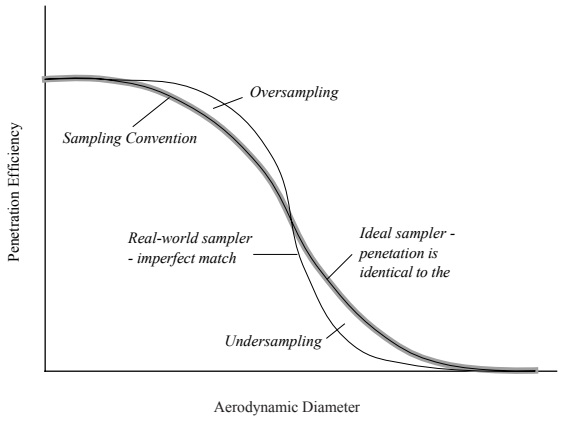

Fig. 9.5. Sampling with respect to a standards-based sampling convention

Sampling against exposure conventions

The accuracy and relevance of aerosol samples taken within the workplace predominantly rely on selection of an appropriate sampling device. Filter selection, pump selection and use, sampling strategy and sample handling also play a role in determining the accuracy and suitability of samples.

Matching the sampler to sampling requirements

A number of the industrial hygiene aerosol samplers introduced to the market in recent years have been developed and tested against International sampling conventions. However, many devices are still available that were brought into use prior to acceptance of the current conventions. Some of these agree reasonably well with the relevant convention and others have been brought into line by altering the sampling flow rate. Others, such as the closed face 37 mm filter cassette, show poor agreement with the current conventions.

Fig. 9.6. IOM inhalable sampler

The analytical development of inhalable samplers has been hampered by the complexities of how external conditions affect aspiration, together with the difficulties of making penetration measurements with particles up to 100 µm aerodynamic diameter. The IOM personal inhalable sampler was the first sampler built to match the inhalable convention, and was developed following aspiration measurements with a breathing mannequin. Although the sampler has shortcomings (for instance it is very accessible to sample tampering, and there is evidence for significant projectile entry in some environments) it

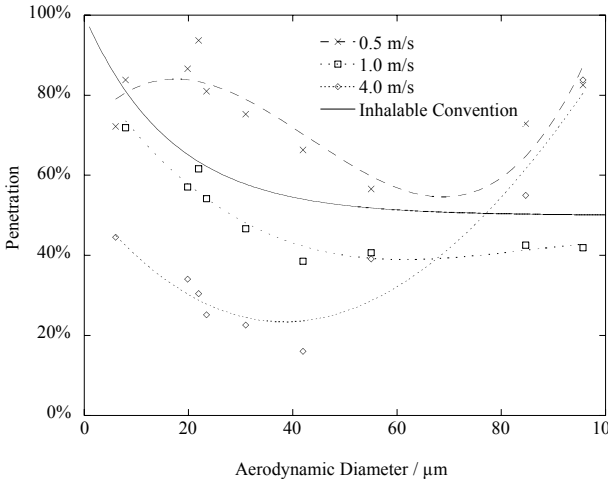

Fig. 9.7. Measured IOM sampler performance

is still regarded as a benchmark sampler. More recent samplers such as the CIP10-I address some of the problems inherent in the IOM inhalable sampler, but still fall short of the ideal. Samplers such as the button sampler (SKC) have been developed specifically to reduce inter-sampler variability and wind speed-dependence common to a number of inhalable samplers. Samplers following the thoracic and respirable conventions have been easier to engineer. The development of an empirical understanding of particle penetration through cyclones and polyurethane foams in particular has led to sampling devices that match the respirable and thoracic conventions reasonably well.

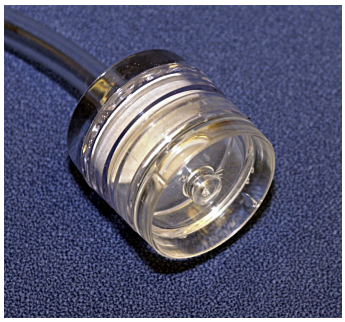

Fig. 9.8. Closed face 37 mm cassette

From the available samplers that lie within acceptable performance criteria, the choice of device will depend largely on the sampling requirements. Static and personal samplers should not be interchanged, except where otherwise indicated. High flow rate samplers should be used to increase the aerosol detection limit, for instance during short term sampling or when the sampled material has a low exposure limit (although the detection limit will also be dependent on the filter used and the analysis method applied). Where high air movements are expected, samplers with a sampling efficiency that aren't so prone to wind speed should be selected. Other considerations should include whether the aerosol charge is likely to affect sampling, whether projectiles are likely to enter the sampling orifice and be included in the sample, and whether there is a possibility of significant sample loss during transport. Table 9.1 summarizes the majority of workplace sampling devices currently available or in use, and gives some indication as to their application.

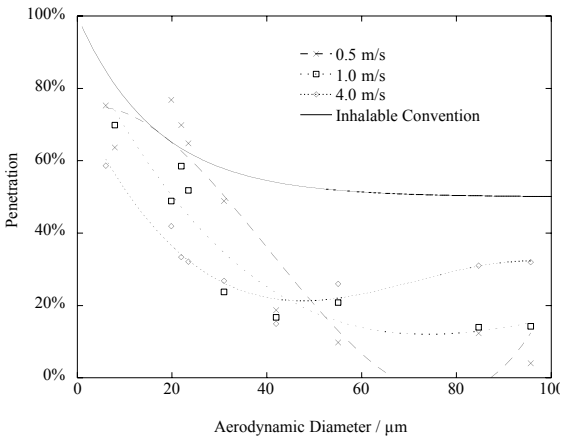

Fig. 9.9. Measured 37 mm (closed face) sampler performance

Filter and substrate selection

Industrial hygiene aerosol samples are generally collected onto a filter, within a polyurethane foam, or onto an impenetrable impaction substrate such as mylar (which is usually coated with a layer of grease or oil to prevent particle bounce). Filters may be held in a cartridge within the sampler, as is the case with the IOM inhalable sampler, or may be mounted directly into the sampling head. Selection of a suitable substrate is governed by the sampling equipment used and the subsequent sample analysis. Low-power lightweight pumps require filters with relatively low pressure drops at the operating flow rate. Gravimetric analysis requires a high degree of weight stability in changing environmental conditions. Chemical analysis requires that the collected material can be released from the substrate and/or background levels of the analyte are low. Sample analysis by microscopy requires deposited particles to lie on the surface of the substrate. Table 2 summarizes the properties of filters, collection substrates and filter holders commonly used within the workplace.

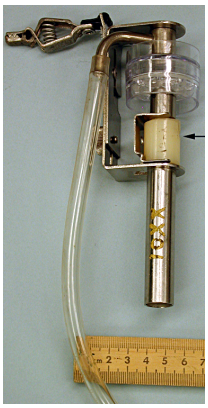

Fig. 9.10. Dorr-Oliver respirable cyclone

The accuracy of gravimetric samples may be affected by water adsorption onto substrates and filter holders, and by losses or gains in material during transit. In particular, cellulose ester membrane filters, polyurethane foams and conducting plastic filter cassettes are particularly prone to weight changes following water uptake. To combat bias from such sources, it is common practice to weigh a number of control, or blank filters with each set of sample filters (typically one blank per 10 samples, with a minimum of three blanks). It is advisable to condition filters in the weighing area (preferably a temperature and humidity controlled environment) for up to 24 hours before weighing to allow them to reach an equilibrium weight. It is generally not advisable to desiccate the filters prior to weighing, as weight changes after removal of the filter can be sufficiently rapid to lead to significant

Fig. 9.11. GK2.69 cyclone. May be used as a thoracic or respirable sampler

weight change during weighing. Where possible, blank filters should be transported with the sample substrates and exposed to the same conditions, to minimize bias resulting from handling, transport and changes in environment.

Other sources of bias include electrostatic attraction where substrates are highly charged, and buoyancy effects. Electrostatic charge build-up may be significant for substrate materials such as PVC and PTFE, particularly when working at low relative humidities. In all instances samples should be neutralized using a source of bipolar ions. A common approach is to place samples close to a radioactive anti-static source prior to weighing. Buoyancy changes only become necessary when the volume of the sample exceeds around 0.1 cm^3. For most substrates this isn't a problem, although it may be significant when using large integral filter holders or substrate supports.

Sampling Strategy

While 'static' or 'area' sampling with fixed point samplers is still used in many situations, it is now widely accepted that representative aerosol sampling in the workplace should be carried out in the breathing zone – frequently defined as a region of the body not more than 0.3 m from the mouth and nose. However placement of sampling devices in this region does not guarantee representative sampling, and large variations in sampled aerosol concentration can be seen across the front of the body, depending on worker orientation, placement of the aerosol source and local air movements.

As a matter of convention, exposure measurements for chronic hazards are usually taken for the duration of a single work shift. An 8-hour TWA mass concentration (c_m) relates to the process whereby exposure occurring within a 24 hour period is treated as being equivalent to a single uniform exposure over 8 hours. A TWA mass concentration can be determined from a single full-shift sample, or it can be calculated from a series of consecutive samples. Where sampling gaps occur over a shift, exposures during these periods should be estimated from adjacent measurements, or from additional information

(See example 1). The TWA for a given time period (e.g. 8 hours, or 15 minutes for a STEL) is calculated by:

$$c_m = \frac{\sum_{i=1}^{n} c_{mi} \times t_i}{T}, \qquad \sum_{i=1}^{n} t_i = \text{full shift duration} \tag{6.4}$$

where T is the given reference period (in minutes), t_i is the duration of sample i in minutes and c_{mi} is the mass concentration of sample i.

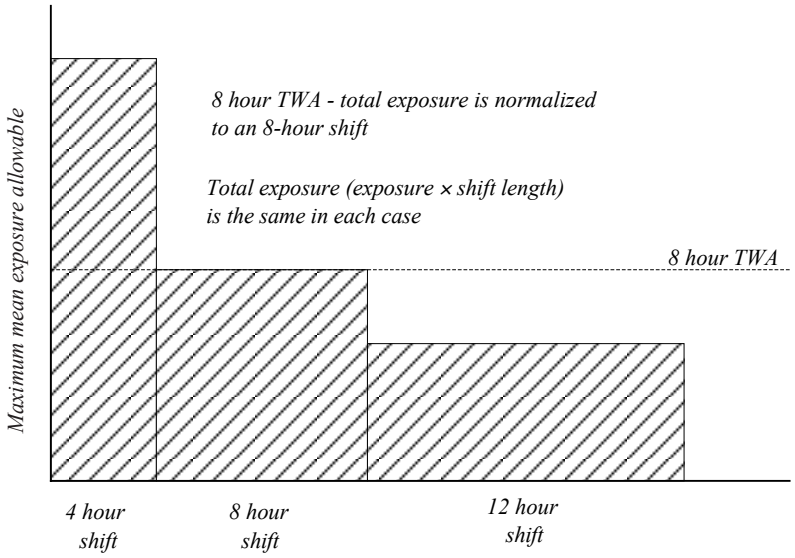

Fig. 12. Representation of aerosol exposure as a Time Weighted Average

For purposes of determination of compliance with occupational exposure limits, it is generally desirable to sample the workers assumed to be at maximum risk. Where the maximum-risk employees cannot be ascertained, employees should be selected at random. Calculating the 95% one-sided lower confidence limit (LCL) and the 95% one-sided upper confidence limit (UCL) is recommended. These are calculated as follows:

$$LCL(95\%) = \chi - t_\alpha \times CV_T$$
$$UCL(95\%) = \chi + t_\alpha \times CV_T \qquad 6.5$$
$$\chi = \frac{c_m}{OEL}$$

where t_α = 1.645 when α = 0.95, CV_T is the coefficient of variation for the sampling/analytical method and OEL is the exposure limit. If LCL and χ are above unity, then the exposure is classified as non-compliant. If UCL and χ are below unity, then the exposure is classified as compliant. Finally, if unity lies between LCL and χ, or between UCL and χ, the exposure is classified as possible over-exposure.

Measurement of size distribution

Full characterization of the size distribution of an aerosol may be carried out during non-routine investigations using a range of available methods described previously. Although many instrument types have been used in the workplace, cascade impactors are often the instrument of choice, giving an indication of the mass-weighted size distribution of an aerosol. Impactors are generally capable of giving the size distribution of an aerosol between around 0.1 μm and 15 μm aerodynamic diameter and above. Static cascade impactors such as the Anderson eight stage impactor and the Micro Orifice Uniform Deposit Impactor (MOUDI) have found relatively widespread use in the workplace. The Anderson consists of eight multi-orifice stages with cut points between 10 μm and 0.4 μm when operated at 28.3 l/min. Collection is usually onto aluminum foils, although other substrates are available. The use of multi-orifices in the Anderson impactor allows deposits to be distributed with relative evenness onto substrates. This is taken further within the MOUDI, where many orifices per stage, together with rotating substrates, lead to highly uniform deposits. The MOUDI is available in an 8 stage or 10 stage version, and is capable of making aerosol size distribution measurements down to 0.056 μm at 30 l/min.

Aerosol size distributions within the breathing zone are generally of greater relevance to health than static samples, and two cascade impactors have been developed to enable personal aerosol size distribution measurements to be made. The Marple personal cascade impactor is configurable with up to eight stages, and will provide information on particle size distribution down to 0.5 µm at a flow rate of 2 l/min. The Personal Inhalable Dust Spectrometer is similar in concept to the Marple impactor, although the slot shaped impactor jets of the Marple device are replaced by circular jets. Cut points in the 8 stages of the PIDS range from 0.9 µm to 19 µm at 2 l/min.

Cascade impactors are of limited use for measuring aerosol size distributions up to the limit of the inhalable convention (100 µm aerodynamic diameter), due to the relatively low cut point of the upper stage in most cases. Extrapolation of measured size distributions above this cut point is dependent on assumptions about the sampled aerosol

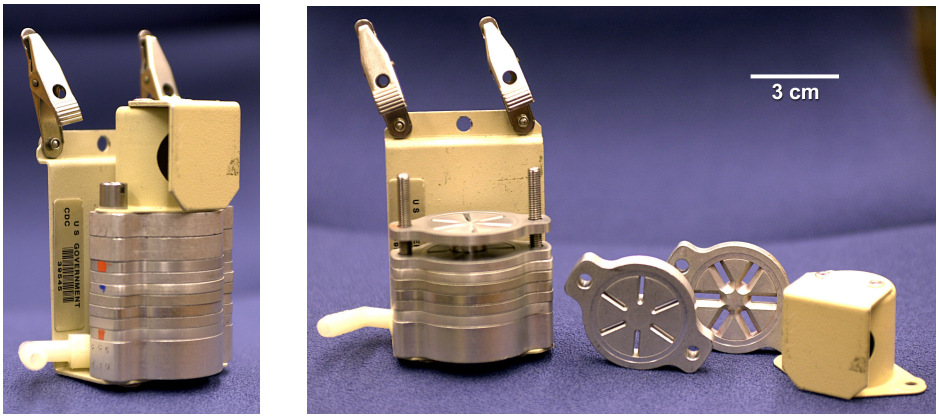

Fig. 9.13. Marple Personal Cascade Impactor

and the aspiration efficiency of the device, and is generally not reliable. However the PIDS was designed with an inlet designed to follow the inhalable convention. It may be assumed that summing all deposits within the PIDS impactor gives a measure of the inhalable aerosol mass, and subsequent analysis of the deposits gives the size distribution as a function of the inhalable aerosol. Such an approach is advantageous to Industrial Hygiene measurements, where ultimately measurements need to be related to the mass of particles inhaled.

In cases where the specific health-related fractions of the aerosol are of more concern than a detailed analysis of particle size distribution, a number of samplers allow simultaneous measurement of all three fractions. The IOM personal multi-fraction sampler uses aerosol separation within polyurethane foams to achieve this. Aerosol is sampled through a 15 mm diameter inhalable inlet at 2 l/min. Two polyurethane foam selectors of different grades placed in series then separate the thoracic and respirable sub-fractions. The sampler enables the inhalable fraction to be measured by weighing deposits in both foams and the backing filter. The combined deposits on the filter and adjacent foam give the thoracic fraction, and the filter alone gives the respirable aerosol fraction. A similar approach using polyurethane foams has been developed for use with the conventional IOM inhalable sampling head. An alternative approach is used by the Personal Spectrometer (PERSPEC). The inhalable aerosol fraction is introduced to a highly divergent flow of clean air, and deposited onto a 47 mm filter. Deposition position is dependent on particle size, thus by weighing the complete filter the inhalable fraction can be determined, or by weighing specific areas of the filter (after cutting them out) different sub-fractions can be measured. The Respicon sampler (TSI) achieves separation of the three aerosol size fractions using a series of virtual impactors. A modified version has been developed (Respicon TM) that allows real-time monitoring of each fraction using light scattering.

Use of dynamic measurement (direct reading) instruments

Dynamic measurement instruments (commonly referred to as real-time measurement instruments) are widely used in the workplace. For routine measurements, aerosol photometers are widely used, and available from an increasing number of manufacturers. Their use covers checking short term, task-specific or instantaneous exposure levels, and identifying exposure hot spots. Systems have also been developed that combine photometer measurements with simultaneous video filming of workers, allowing direct comparison between work tasks and exposure levels. The implementation of the measurement method has various guises, from passive instruments relying on convection to bring particles into the sensing zone (as with the Mini-RAM, and the later personal

Data-RAM), to pumped devices such as the Microdust Pro (Casella), to instruments incorporating data loggers (e.g. the DustTrak (TSI) and Data-RAM (MIE)). Most devices are compact, with the majority being portable, and a number of them being suitable for personal sampling.

Over a relatively narrow size range (approximating to the upper end of respirable size fraction) the light scattered from an aerosol is roughly proportional to the scattering volume. Thus after correcting for density, scattered light may be used as an indirect measure of mass concentration. The method is relatively good for measuring respirable aerosol concentration, but becomes tenuous when used for the thoracic sub-fraction, and potentially misleading when used to measure the inhalable aerosol mass concentration (the sensitivity to equivalent aerosol masses represented by 20 μm particles is approximately a factor of 10^2 lower than the sensitivity to 2 μm particles). Instruments such as the Respicon TM go some way to overcoming this size dependence of photometry by selectively concentrating larger particles through the use of virtual impaction. In some situations it is feasible to calibrate a photometer to the inhalable mass concentration, but only when the fine particles detected form a constant fraction of the inhalable aerosol. Optical single particle detection and sizing instruments such as the Grimm 'Work-check' range of particle counters/sizers overcome some of the limitations of photometers, but their sensitivity is still restricted to a similar range of particle sizes.

In all cases it is advisable to calibrate photometers before using them with different aerosols, as particle size distribution, shape and refractive index will affect measurements. Calibration is usually performed by carrying out parallel gravimetric sampling, and applying an adjustment factor to the photometer to ensure results agree. Many photometers have the facility to collect aerosol passing through the sensing zone on a filter, thus simplifying calibration. Zero offset checks are also recommended before use by placing the photometer in a clean environment: deposits on the optics and surfaces of the sensing zone can lead to the instrument calibration being offset.

Recent developments in Condensation Particle Counter (CPC) technology have led to a commercially available portable device with logging capabilities, suitable for semi-quantitative particle number measurements. The P-Trak (TSI) is designed to provide near-instantaneous measurements of particle concentration between 20 nm and approximately 1 μm. Although it is primarily aimed at investigating aerosol number concentration levels and variations, and tracking contamination sources in indoor environments, it is also being applied to measuring real-time particle number concentration measurements in the workplace.

4. Fibrous Aerosols

Many aerosol particles experienced in the workplace or environment are compact, or behave in a similar manner to spherical particles. However fibers represent an extreme of particle shape, and because of their shape they tend to behave somewhat differently from compact or spherical particles. A number of fibrous materials also have unique physical properties, leading to them being in widespread use. Asbestos, for example, includes six commercial materials that have high tensile strength and chemical resistance, together with very good thermal and acoustic insulation properties. A variety of other widely encountered materials are used in a fibrous form, including glass, ceramics and carbon. Organic fibers such as cotton, wood and other cellulose-based material are also widely used. All of these materials are capable of shedding airborne fibers which may, depending on their size and chemistry, be harmful.

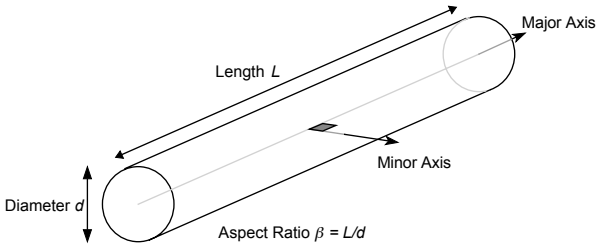

Fig. 9.14. Schematic of a fiber.

Asbestos fiber has been associated with fibrosis of the lung (asbestosis), lung cancer and cancer of the lining around the lung (mesothelioma) for many years. Much of the toxicity of asbestos is thought to be associated with the chemistry, low solubility, length and diameter of the fibers. Where other airborne fibers have similar properties to asbestos,

similar health concerns exist (for instance, exposure to thin ceramic and glass fibers is of concern, although generally such fibers dissolve in the lungs more rapidly than mineral fibers, and are not considered as high a health hazard). Asbestos fibers are composed of thin fibrils which may be as narrow as 0.025 μm in diameter. Airborne fibers can be individual fibrils, or bundles of fibrils with lengths from less than 0.5 μm to several hundred μm. As the toxicity of materials such as asbestos is associated with particle shape, exposure characterization and monitoring methods differ markedly from other aerosols.

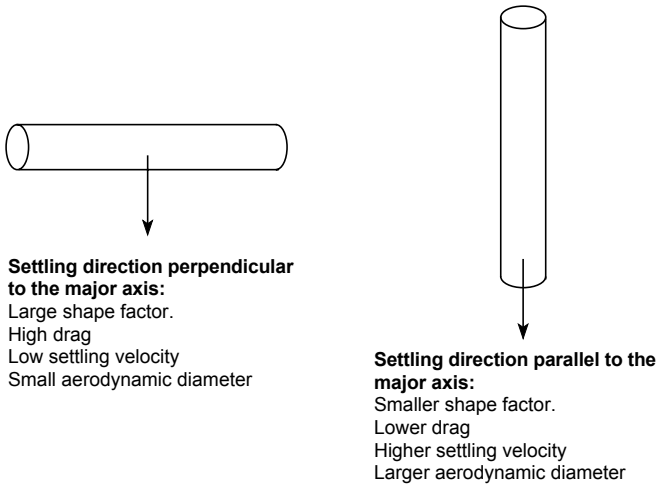

Fig. 9.15. Fiber settling

The shape of fibrous particles has a profound effect on their aerodynamic properties. Aerodynamic diameter depends on the orientation of the fiber to the direction of motion. If a settling fiber is aligned parallel to the direction of motion, it presents little air resistance (low drag) resulting in a high settling velocity, and has a large aerodynamic diameter. On the other hand, if it is aligned perpendicular to the direction of motion, the drag is greater, leading to a low settling velocity, and the fiber behaves aerodynamically like a smaller particle. the difference in drag between the two orientations is typically between 15% to 30%. Settling fibers will tend to align in the maximum drag orientation – i.e. with their major axis perpendicular to the direction of motion.

As a rule of thumb, the aerodynamic diameter of a fiber is strongly influenced by its physical diameter, and as a rough estimate tends to be between 3 and 5 times the physical fiber diameter. Fibers will deposit under the same mechanisms as compact particles. However because of their relatively small aerodynamic diameter compared to their length, it is possible to get very long fibers into the lungs that severely challenge the

lung's defense mechanisms. One theory as to why fibers are so toxic is that macrophages are unable to remove fibers longer than 15 – 20 μm or so from the lungs that deposit as a result of having aerodynamic diameters of less than 5 μm. Furthermore, it seems that macrophages are killed in the process of attempting to remove fibers, leading to localized inflammation.

Because fiber shape is so important, exposure assessment is carried out in terms of particle shape and number, rather than bulk mass concentration. There are a number of exposure standards and measurement methodologies implemented internationally. In the States OSHA regulations require that workers are not exposed to more than 0.1 fibers per cm^3 averaged over 8 hours, while MSHA (Mine Safety and Health Administration) sets the 8 hour time weighted average limit at 2 fibers/cm^3. Fibrous aerosol sampling is carried out using a 25 mm diameter sampler with a 50 mm long conductive cowl to prevent direct deposition or contamination of the filter surface. Fiber detection and analysis following collection is carried out using either Phase Contrast Microscopy (PCM), Polarized Light Microscopy (PLM), Scanning Electron Microscopy (SEM) or Transmission Electron Microscopy (TEM) depending on what information is required from the sample. PCM is most frequently used to measure airborne concentrations of fibers as it is relatively fast and inexpensive. To image fibers in a light microscope they are collected on cellulose ester filters which are chemically cleared on a glass slide to make them transparent, and to provide contrast when imaging the fibers (usually a liquid or resin with a refractive index close to that of the filter is used to impregnate the sample and fill the gap between the sample and the cover slip). One of the most commonly used methods is the acetone-triacetin method, which provides samples lasting between 6 and 24 months. The use of PCM allows fibers thicker than around 0.25 μm to be detected, and enables the number of fibers collected to be estimated. The exact definition of fibers in the context of exposure standards varies with the standard used, but generally covers all particles with an aspect ratio greater than 3:1 and a length greater than 5 μm. It is also common to rule that fibers larger than 3 μm in diameter are not counted, and fibers attached to other particles greater than 3 μm in diameter are not counted.

There are a number of error sources encountered in fiber counting, including sampling error, non-uniformity on collection filters and human counting error. As a result the errors associated with measuring airborne fiber concentration can be relatively high. To minimize errors a number of inter-laboratory proficiency schemes exist to ensure analytical labs. are operating within acceptable accuracy limits (e.g. RICE (the UK Regular Inter-Laboratory Counting Exchange), AFRICA (the international Asbestos Fiber Regular Interchange Counting Arrangement) and PAT (AIHA's Proficiency Analytical Testing) programs). One of the limitations of PCM is that fibers around 0.25 μm in diameter are hard to detect with 100% efficiency. In principle fiber couning using TEM or SEM overcomes this limitation, allowing fibers with diameters down to nanometer widths to be detected and counted. However somewhat inexplicably inter-laboratory comparisons with TEM analysis have shown poorer accuracy over PCM.

One of the advantages of SEM and TEM analysis is that analytical systems such as X-ray Energy Dispersive Spectroscopy (EDS or EDX) allows elemental analysis of fibers, and thus identification of fiber type/source. Optical PLM can also be used to identify asbestos fibers from non-asbestos fibers (asbestos fibers appear bright under cross polarization), and go some way towards identifying asbestos types.

There has been some work on developing dynamic fiber detection systems. The Fibrous Aerosol Monitor (FAM) is perhaps the most successful. Fibers are aligned in an electric field, and caused to oscillate at a set frequency within the field. They are illuminated with light polarized perpendicular to their major axis, and scattered light detected at 90° in the plane perpendicular to the major axis.

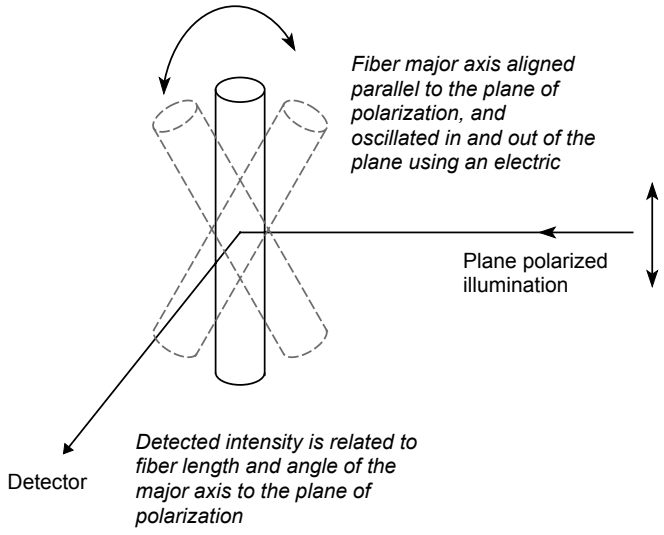

Fig. 9.16. Principle of operation of the Fibrous Aerosol Monitor (FAM)

As the fibers oscillate, the detected scattered light intensity oscillates at the same frequency. No oscillation occurs for compact particles, enabling the instrument to differentiate between fibrous and compact particles. Other attempts have been made to detect fibers in real time: all rely on aligning the fibers, and detecting scattered light that is dependent on fiber shape.

5. Future Trends

Perhaps the most significant change in industrial hygiene aerosol measurement over the past two decades has been the development and gradual adoption of size selective sampling conventions. These now enable measurements that have greater biological relevance to be made in the workplace. Although the next few years are likely to see the current position being consolidated, there is scope for the present sampling conventions to be revised. The inhalable convention is limited in its scope and applicability. Its abrupt termination at 100 μm brings into question whether the ingression of large particles and projectiles into more open samplers is acceptable, or leads to inaccurate measures of aerosol concentration. In addition the inability to develop inhalable samplers thus far that follow the convention over a wide range of wind speeds raises the question of whether the standard is unattainable, or inappropriate.

At the other end of the size spectrum, toxicological information on responses to nanometer-sized low solubility particles are challenging the applicability of current sampling conventions and philosophies. Recent toxicology on low toxicity insoluble materials such as titanium dioxide has indicated that a more appropriate dose metric for depositing in the alveolar region may be particle number, or surface area. These studies appear to support some epidemiology investigations of the general population, indicating correlation between inhalation of fine particles and health effects. The extent to which such findings are applicable to exposure within the workplace is not apparent at present. However to begin to understand the relevance of exposure to very fine particles, and the appropriate metric to use for dose, developments in the measurement of exposure in

terms of particle number, surface area are necessary. As the debate on the appropriate dose and exposure metric develops, there will no doubt be further extensions to the manner in which aerosol exposure in the workplace is measured in the sub-respirable size range.

Current trends in workplace sampling practice indicate a desire within the industrial hygiene community to adopt methods that provide measurements with greater rapidity and with less effort. In particular there is a growing interest in relating exposure to specific tasks and operations, thus requiring highly sensitive or rapid-response aerosol measurement methods. Such trends are perhaps most obvious in the increased use (and abuse) of direct-reading photometer-based instruments. These provide a rapid indication of exposure, both allowing a more rapid response to problem situations than filter collection and analysis allows, together with a means of avoiding the expense of sample collection and analysis where it isn't necessary. However, their attraction has seen their increasing but erroneous use to estimate exposure to inhalable aerosol. This clear need for direct reading instruments that extend to the inhalable fraction is likely to lead to the development of new devices. Although it is not at all clear at present whether workable technologies will present themselves, there are a number of possible contenders: The application of optical methods may be further increased to large particle sizes through the size selective concentration of particles and the detection of individual large particles. The development of handheld oscillating microbalance methods is underway, although it is unclear whether there will be collection and sensing problems associated with particles approaching 100 μm in diameter. Aerosol mass sensing methods based on filter pressure drop are being developed for fine particles. At present the indications are that size-dependent effects will hinder their extension to 100 μm, although size-selective concentration and aerosol-specific calibration may lead to successful applications.

Passive samplers provide another route to simplified exposure measurement, and have been under development for some time. They offer the simplicity of a discrete lightweight badge-type sampler with no need for a sampling pump. The passive sampler developed by Brown et al. relies on electrostatic deposition onto an pre-prepared electret

material. Aerosol is carried to the deposition zone through convection, thus no pump is required. Although the device is not designed along size-selective lines, good correlation has been seen with size selective samplers in some cases, and it is likely that such samplers could be developed into indicative screening devices.

A different approach to making size-selective sampling more accessible and less expensive is seen in the increasing utilization of porous foam pre-separators. The use of foam allows relatively inexpensive size separation devices to be constructed, and provides the possibility of modifying existing samplers to different applications. At the same time, new methods of creating size-selective samplers that are better suited to occupational aerosol sampling (for instance by operating at higher flow rates, giving better agreement with the sampling conventions, providing a more compact, lighter sampler and operating at lower pressure drops) are under constant development. Recent work includes the investigation of virtual, axial-flow and tangential-flow cyclones, the development of centrifugal personal samplers and the development of inhalable samplers with inlet screens, reducing the adverse effects of wind speed and large particle projectiles on samples.

The desire for simplification also extends to standards against which exposure is measured. While the current emphasis is on monitoring worker exposure, the concept of controlling emissions at the source is gaining ground. The application of such thinking to the workplace will possibly result in the use of exposure modeling to estimate exposure risk, accounting for materials used, generation processes involved, emission control measures applied and dispersion in the workplace. The logical endpoint is the estimation of exposures from materials and processes within the workplace, and the relegation of aerosol exposure measurement to a supportive role. However sufficient questions surround the classification of materials in terms of their ability to form an aerosol during specific processes, together with the containment or release and transport of generated aerosols, to ensure that developments in aerosol measurement methods in the workplace will continue for a number of years to come.

Useful References

ACGIH (1968). *Threshold Limit Values of airborne contaminants*, Cincinnati, OH, American Conference of Government Industrial Hygienists.

ACGIH (1995). *Air sampling instruments, 8th Edition*, ACGIH.

ACGIH (1998). *Particle size-selective sampling for particulate air contaminants*. Cincinnati, OH, American Conderence of Government Industrial Hygienists.

ISO (1995). Air Quality - Particle size fraction definitions for health-related sampling. Geneva, International Standards Organisation**: ISO Standard 7708**.

OSHA (1998). Respiratory Protection Standard 29CFR1910.134.

ANNEX A – GENERAL RESOURCES

- Aerosol Terminology
- Comparison of sizes and size ranges
- Range of aerosol mass concentrations
- Nomenclature
- Properties of airborne particles

Aerosol Terminology

Aerosols are traditionally subdivided into categories according to their physical form. Although not a scientific classification (and certainly not a rigid classification), these following definitions are in common usage:

Aerosol: A suspension of solid or liquid particles in a gas. Aerosols are usually stable for a few seconds. The term aerosol refers to both the gas and the suspended particles, which may vary in size from less than a nanometer to 100's of μm. At high concentrations, typically when the density of the aerosol is greater than 1% of the gas density alone, the particles and gas are closely coupled, and the suspension has bulk properties that differ from a more dilute aerosol. Aerosol particles may be liquid or solid.

Aggregate: In the context of aerosols, the term usually refers to a heterogeneous particle in which the various components are not easily broken up. Sometimes used interchangeably with agglomerate (esp. When discussing powders).

Agglomerate: A group of particles held together by van der Waals forces or surface tension. The term tends to be used loosely, and often refers to small primary particles sintered together for form a larger particle with an open structure.

Bioaerosol: An aerosol of biological material and of biological origin. Bioaerosols include viruses, bacteria, spores and pollen.

Cloud: A visible aerosol with clear, defined boundaries. Also used to refer to a dense aerosol where the particulate mass influences the bulk aerosol properties significantly.

Droplet: Airborne liquid-based particle. In the context of aerosols, droplets are usually considered to be relatively large, and typically 100 μm – tens of mm in diameter.

Dust: A solid-particle aerosol formed through the mechanical breakage of a bulk material, usually through crushing or grinding. Particles typically range in size from the sub-μm to 100's of μm, and are usually irregularly shaped.

Flocculate: A group of particles very loosely held together.

Fume: A solid-particle aerosol produced by the condensation of vapor or gaseous combustion products. They often take the form of fractal-like clusters (agglomerates) of very small primary particles, which are typically of the order of 10 – 30 nm in diameter.

Haze: An atmospheric aerosol that affects visibility.

Mist and Fog: Liquid-particle aerosols formed through condensation or atomization. Particles are spherical with diameters ranging from less than a μm to 100's of μm.

Nanoparticle: Typically particles smaller than 100 nm in diameter. The term nanoparticle is often used in the context of intentionally-produced particles, but not always.

Particle: A small, discrete object.

Particulate: A particle. Also used as an adjective to indicate the particle-like properties of a material.

Primary particle: A particle introduced to the air as a solid or liquid particle. The smallest particles making up an agglomerate.

Secondary particle: Usually used to refer to particles formed in the air through gas-to-particle conversion. Sometimes used to refer to agglomerates or re-suspended particles.

Smog: An aerosol consisting of solid and liquid particles. Photochemical Smog: An aerosol formed in the atmosphere by the action of sunlight on hydrocarbons and nitrogen oxides. Particles are generally smatter than 1 – 2 μm.

Smoke: A solid or liquid aerosol arising from incomplete combustion, or vapor condensation. Particles are typically sub-μm in diameter.

Ultrafine particle: Typically particles smaller than 100 nm in diameter. Ultrafine particles historically referred to ant airborne particles in this size range, irrespective of source.

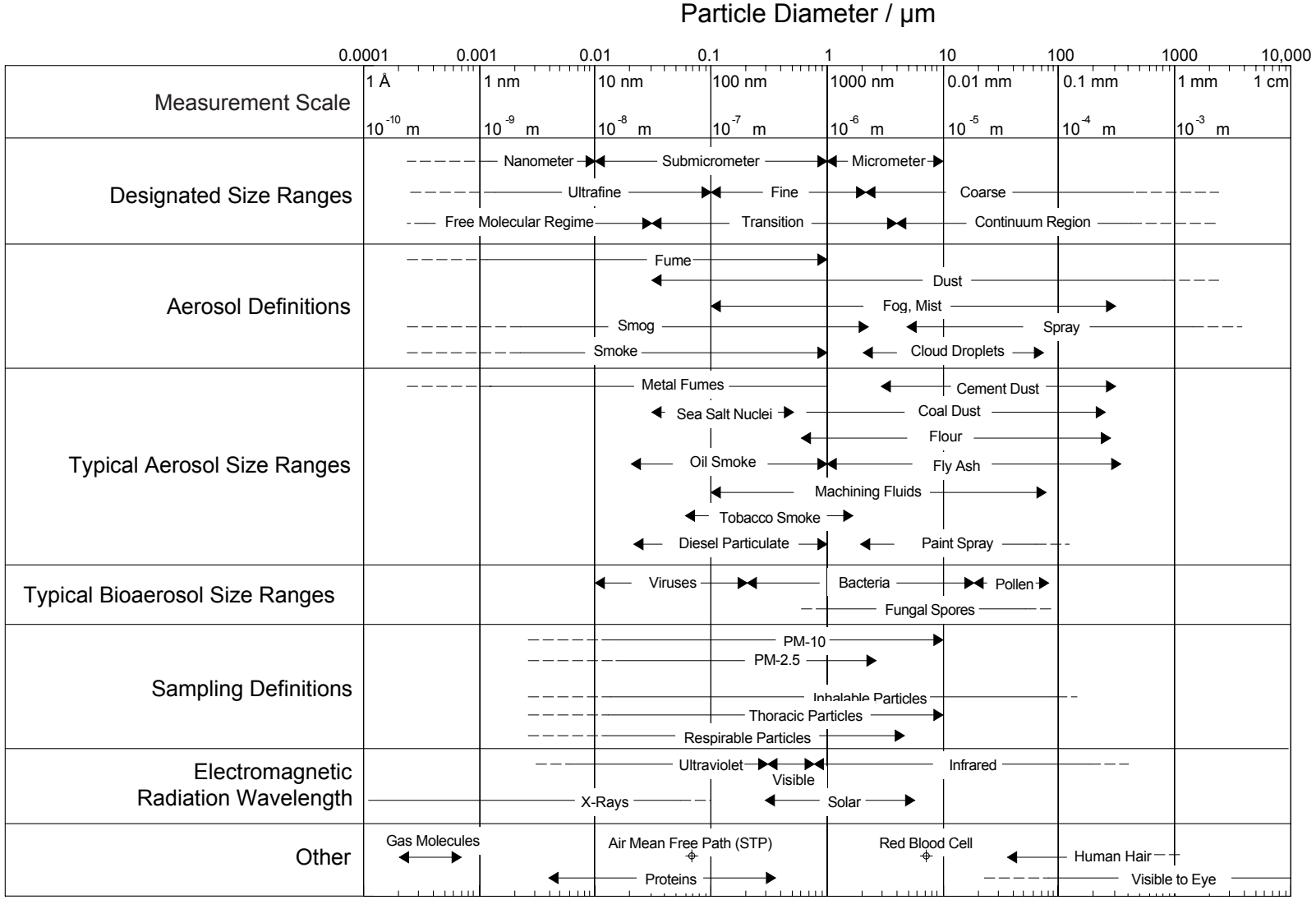

Adapted from Hinds, W. *'Aerosol Technology'*. John Wiley & Sons Inc. New York, 1999

Comparison of sizes and size ranges

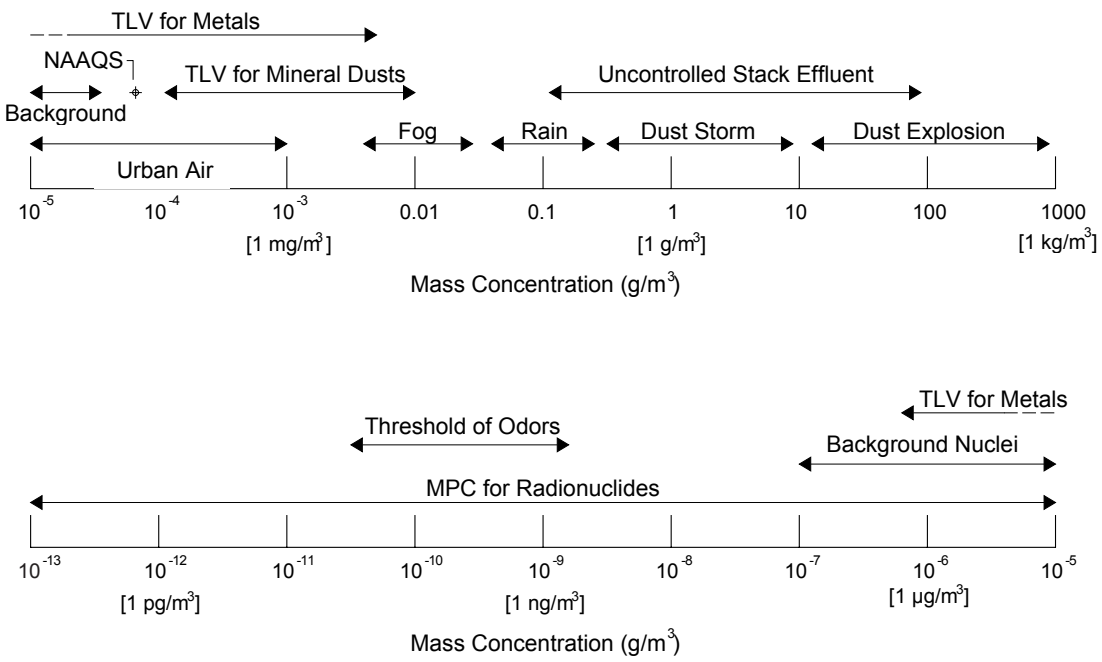

Adapted from Hinds, W. *'Aerosol Technology'*. John Wiley & Sons Inc. New York, 1999

Range of aerosol mass concentrations

Nomenclature

Note that in some cases a symbol may be used to denote different values in different contexts. All equations listed should be evaluated using SI units (kg, m, s) – SI units for the values below are listed where appropriate.

B	Particle mechanical mobility [m N^{-1} s^{-1}]
c	Velocity, usually gas molecule velocity [m]
c	Velocity, usually gas molecule velocity [m]
c_x	Velocity in the x-direction [m]
c_{rms}	Root mean square velocity [m/s]
$\bar{c}$	Mean velocity [m/s]
C	Concentration (e.g. gas concentration). [Concentration units/m^3]
C_D	Drag coefficient [dimensionless]
C_c	Cunningham slip correction
C_s	Slip Correction [dimensionless]
D	Diffusion coefficient [m^2/s]
	Characteristic length [m]
d	Particle diameter [m]
d_p	Particle diameter [m]
d_{ae}	Aerodynamic diameter [m]
d_e	Equivalent diameter (diameter of sphere with same volume) [m]
d_s	Stokes Diameter [m]
D	Diffusion constant [m^3 s^{-1}]
F	Force [kg m/s^2 or N]
F_D	Drag Force [kg m/s^2 or N]
F_E	Electric force [N]
F_{th}	Thermophoretic force [N]
g	Gravity [9.81 m/s^2]
J	Flux. Particles: [#/m^2/s]
k	Boltzmann constant [1.38×10^{-23} J/K]
K	Coagulation coefficient [m^3/s]
KE	Electrostatic constant [9×10^9 N m^2 C^{-2}]
m	Mass. Often of a single particle or molecule. [kg]
	Mass concentration. [Kg/m^3]
n	Number of moles of gas (gas kinetics) [mol]
	Number of molecules per unit volume (gas kinetics) [#/m^3]
	Particle number concentration [#/m^3]
n_c	Molecule collisions per second [#/s]
N_a	Avogadros Number [6.022×10^{23} mol^{-1}]
N_i	Ion number concentration [#/m^3]
P	Pressure [N/m^2 or Pa]
Q	Flow rate [m^3/s]
R	Gas constant [8.31 Pa m^3/K mol]
Re	Reynolds number. [Dimensionless]
S	Stopping distance [m]
Stk	Stokes number [dimensionless]
t	Time [s]
T	Temperature [K]
U	Velocity. Usually free stream gas velocity. [m/s]
V	Volume [m^3]
	Velocity [m/s]
V_T	Terminal velocity [m/s]
V_{TS}	Settling velocity [m/s]
V_{th}	Thermophoretic deposition velocity [m]
Z	Electrical mobility [m^2 V^{-1} s^{-1}]
η	Viscosity [kg m^{-1} s^{-1}]
λ	Mean free path [m]
λ_p	Particle mean free path [m]
λ_g	Gas mean free path [m]
ρ	Density [kg/m^3]

ρ_g Gas density [kg/m^3]

ρ_p Particle density [kg/m^3]

ρ_0 'Unit' density [1000 kg/m^3]

τ Relaxation time [s]

χ Shape factor. [dimensionless]

∇T Temperature gradient [K/m]

Temperature:	293	K	Boltzmann Constant (k)	1.38×10^{-23}	J/K
Pressure:	101.3	Pa	Air Viscosity	1.831×10^{-05}	Kg/(m s)
Particle Density	1000	kg/m^3	Air Mean Free Path	6.6489×10^{-08}	m

Diameter d	Slip Correction C_s	Settling Velocity V_{TS}	Relaxation Time τ	Mechanical Mobility B	Diffusion Coefficient D	Particle mean velocity $\bar{c}$	Particle mean free path λ	Coagulation Coefficient K
μm		m/s	s	m/(N.s)	m^2/s	m/s	m	m^3/s
0.001	225.989	6.73E-09	6.86E-10	1.31E+15	5.30E-06	140.231	9.62E-08	3.12E-16
0.002	113.292	1.35E-08	1.38E-09	3.28E+14	1.33E-06	49.579	6.82E-08	4.40E-16
0.003	75.727	2.03E-08	2.07E-09	1.46E+14	5.92E-07	26.987	5.58E-08	5.39E-16
0.004	56.945	2.71E-08	2.76E-09	8.25E+13	3.34E-07	17.529	4.85E-08	6.22E-16
0.005	45.676	3.40E-08	3.47E-09	5.29E+13	2.14E-07	12.543	4.35E-08	6.94E-16
0.006	38.164	4.09E-08	4.17E-09	3.69E+13	1.49E-07	9.542	3.98E-08	7.58E-16
0.007	32.798	4.78E-08	4.88E-09	2.72E+13	1.10E-07	7.572	3.69E-08	8.15E-16
0.008	28.775	5.48E-08	5.59E-09	2.08E+13	8.43E-08	6.197	3.46E-08	8.67E-16
0.009	25.645	6.18E-08	6.30E-09	1.65E+13	6.68E-08	5.194	3.27E-08	9.14E-16
0.01	23.142	6.89E-08	7.02E-09	1.34E+13	5.42E-08	4.434	3.11E-08	9.56E-16
0.02	11.883	1.42E-07	1.44E-08	3.44E+12	1.39E-08	1.568	2.26E-08	1.18E-15
0.03	8.138	2.18E-07	2.22E-08	1.57E+12	6.36E-09	0.853	1.90E-08	1.18E-15
0.04	6.270	2.99E-07	3.04E-08	9.08E+11	3.67E-09	0.554	1.69E-08	1.11E-15
0.05	5.153	3.84E-07	3.91E-08	5.97E+11	2.42E-09	0.397	1.55E-08	1.02E-15
0.06	4.411	4.73E-07	4.82E-08	4.26E+11	1.72E-09	0.302	1.45E-08	9.45E-16
0.07	3.884	5.67E-07	5.78E-08	3.22E+11	1.30E-09	0.239	1.38E-08	8.78E-16
0.08	3.491	6.65E-07	6.78E-08	2.53E+11	1.02E-09	0.196	1.33E-08	8.20E-16
0.09	3.186	7.68E-07	7.83E-08	2.05E+11	8.30E-10	0.164	1.29E-08	7.70E-16
0.1	2.944	8.76E-07	8.93E-08	1.71E+11	6.90E-10	1.40E-01	1.25E-08	7.28E-16
0.2	1.886	2.25E-06	2.29E-07	5.47E+10	2.21E-10	4.96E-02	1.14E-08	5.11E-16
0.3	1.559	4.18E-06	4.26E-07	3.01E+10	1.22E-10	2.70E-02	1.15E-08	4.34E-16
0.4	1.406	6.70E-06	6.83E-07	2.04E+10	8.24E-11	1.75E-02	1.20E-08	3.96E-16
0.5	1.319	9.81E-06	1.00E-06	1.53E+10	6.18E-11	1.25E-02	1.25E-08	3.74E-16
0.6	1.263	1.35E-05	1.38E-06	1.22E+10	4.93E-11	9.54E-03	1.32E-08	3.60E-16
0.7	1.224	1.79E-05	1.82E-06	1.01E+10	4.10E-11	7.57E-03	1.38E-08	3.50E-16
0.8	1.195	2.28E-05	2.32E-06	8.66E+09	3.50E-11	6.20E-03	1.44E-08	3.43E-16
0.9	1.173	2.83E-05	2.88E-06	7.56E+09	3.06E-11	5.19E-03	1.50E-08	3.37E-16
1	1.156	3.44E-05	3.51E-06	6.70E+09	2.71E-11	4.43E-03	1.56E-08	3.33E-16
2	1.078	1.28E-04	1.31E-05	3.12E+09	1.26E-11	1.57E-03	2.05E-08	3.13E-16
3	1.052	2.82E-04	2.87E-05	2.03E+09	8.22E-12	8.53E-04	2.45E-08	3.06E-16
4	1.039	4.95E-04	5.04E-05	1.51E+09	6.09E-12	5.54E-04	2.80E-08	3.03E-16
5	1.031	7.67E-04	7.82E-05	1.20E+09	4.83E-12	3.97E-04	3.10E-08	3.01E-16
6	1.026	1.10E-03	1.12E-04	9.91E+08	4.01E-12	3.02E-04	3.38E-08	3.00E-16
7	1.022	1.49E-03	1.52E-04	8.46E+08	3.42E-12	2.39E-04	3.64E-08	2.99E-16
8	1.019	1.94E-03	1.98E-04	7.39E+08	2.99E-12	1.96E-04	3.88E-08	2.98E-16
9	1.017	2.45E-03	2.50E-04	6.55E+08	2.65E-12	1.64E-04	4.11E-08	2.98E-16
10	1.016	3.02E-03	3.08E-04	5.89E+08	2.38E-12	1.40E-04	4.32E-08	2.97E-16
20	1.008	1.20E-02	1.22E-03	2.92E+08	1.18E-12	4.96E-05	6.07E-08	2.95E-16
30	1.005	2.69E-02	2.75E-03	1.94E+08	7.85E-13	2.70E-05	7.41E-08	2.95E-16
40	1.004	4.73E-02	4.82E-03	1.45E+08	5.88E-13	1.75E-05	8.45E-08	2.95E-16
50	1.003	7.30E-02	7.44E-03	1.16E+08	4.70E-13	1.25E-05	9.34E-08	2.95E-16
60	1.003	1.04E-01	1.06E-02	9.68E+07	3.92E-13	9.54E-06	1.01E-07	2.95E-16
70	1.002	1.38E-01	1.41E-02	8.30E+07	3.36E-13	7.57E-06	1.07E-07	2.94E-16
80	1.002	1.76E-01	1.79E-02	7.26E+07	2.94E-13	6.20E-06	1.11E-07	2.94E-16
90	1.002	2.16E-01	2.20E-02	6.45E+07	2.61E-13	5.19E-06	1.14E-07	2.94E-16
100	1.002	2.58E-01	2.63E-02	5.80E+07	2.35E-13	4.43E-06	1.16E-07	2.94E-16

Properties of Airborne Particles